Optical Waveguides (OPT568)

Govind P. Agrawal

Institute of Optics
University of Rochester
Rochester, NY 14627

Introduction

- Optical waveguides confine light inside them.
- Two types of waveguides exist:
  - ⋆ Metallic waveguides (coaxial cables, useful for microwaves).
  - ⋆ Dielectric waveguides (optical fibers).
- This course focuses on dielectric waveguides and optoelectronic devices made with them.
- Physical Mechanism: Total Internal Reflection.

Total Internal Reflection

- Refraction of light at a dielectric interface is governed by Snell's law: $n_1 \sin\theta_i = n_2 \sin\theta_t$ (around 1620).
- When $n_1 > n_2$, light bends away from the normal $(\theta_t > \theta_i)$.
- At a critical angle $\theta_i = \theta_c$, θ_t becomes 90° (parallel to interface).
- Total internal reflection occurs for $\theta_i > \theta_c$.

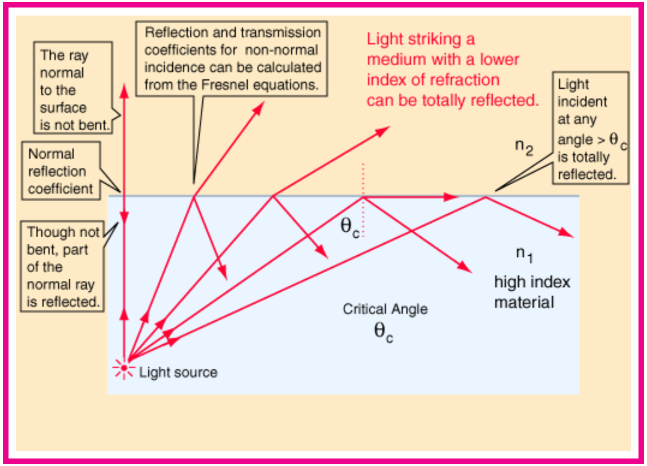

Historical Details

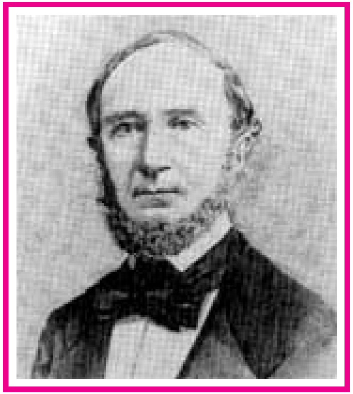

Daniel Colladon

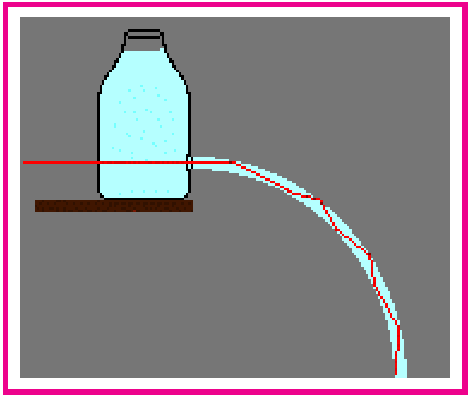

Experimental Setup

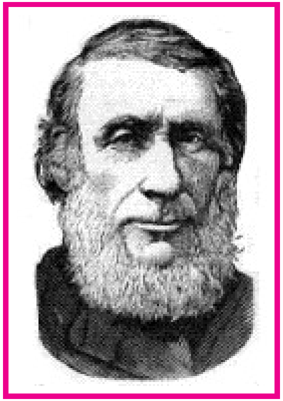

John Tyndall

- TIR is attributed toJohn Tyndall (1854 experiment in London).
- Book City of Light (Jeff Hecht, 1999) traces history of TIR.
- First demonstration in Geneva in 1841 by Daniel Colladon (Comptes Rendus, vol. 15, pp. 800-802, Oct. 24, 1842).
- Light remained confined to a falling stream of water.

Back
Close

Historical Details

- Tyndall repeated the experiment in a 1854 lecture at the suggestion of Faraday (but Faraday could not recall the original name).
- Tyndall's name got attached to TIR because he described the experiment in his popular book Light and Electricity (around 1860).
- Colladon published an article The Colladon Fountain in 1884 to claim credit but it didn't work (La Nature, Scientific American).

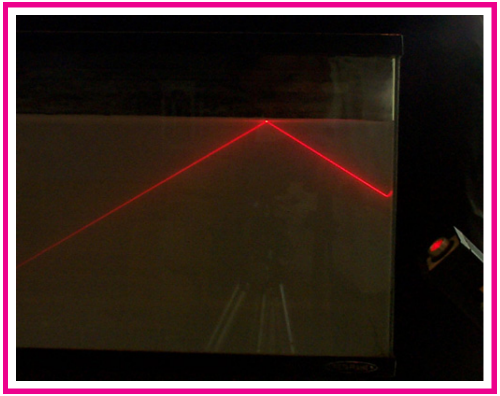

A fish tank and a laser pointer can be used to demonstrate the phenomenon of total internal reflection.

Dielectric Waveguides

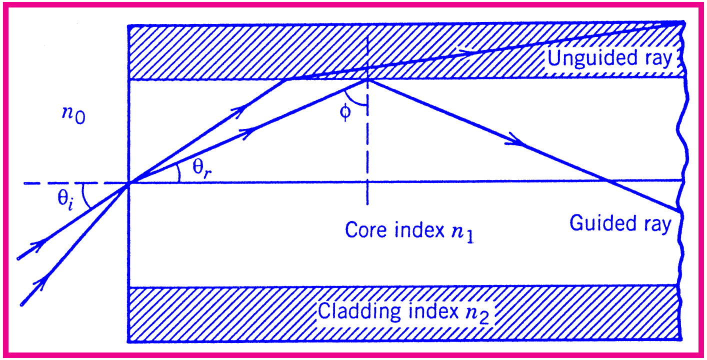

- A thin layer of high-index material is sandwiched between two layers.
- Light ray hits the interface at an angle $\phi = \pi/2 - \theta_r$ such that $n_0 \sin\theta_i = n_1 \sin\theta_r$.
- Total internal reflection occurs if $\phi > \phi_c = \sin^{-1}(n_2/n_1)$.
- Numerical aperture is related to maximum angle of incidence as

$$\mathrm{NA} = n_0 \sin\theta_i^{\max} = n_1 \sin(\pi/2 - \phi_c) = \sqrt{n_1^2 - n_2^2}.$$

Geometrical-Optics Description

- Ray picture valid only within geometrical-optics approximation.
- Useful for a physical understanding of waveguiding mechanism.
- It can be used to show that light remains confined to a waveguide for only a few specific incident angles angles if one takes into account the Goos–Hänchen shift (extra phase shift at the interface).
- The angles corresponds to waveguide modes in wave optics.
- For thin waveguides, only a single mode exists.
- One must resort to wave-optics description for thin waveguides (thickness $d \sim \lambda$).

Maxwell's Equations

$$\nabla \times \mathbf{E} = -\frac{\partial \mathbf{B}}{\partial t}$$

$$\nabla \times \mathbf{H} = \frac{\partial \mathbf{D}}{\partial t}$$

$$\nabla \cdot \mathbf{D} = 0$$

$$\nabla \cdot \mathbf{B} = 0$$

Constitutive Relations

$$\mathbf{D} = \varepsilon_0 \mathbf{E} + \mathbf{P}$$

$$\mathbf{B} = \mu_0 \mathbf{H} + \mathbf{M}$$

Linear Susceptibility

$$\mathbf{P}(\mathbf{r},t) = \varepsilon_0 \int_{-\infty}^{\infty} \chi(\mathbf{r},t-t')\mathbf{E}(\mathbf{r},t')\,dt'$$

Nonmagnetic Dielectric Materials

- $\mathbf{M} = 0$, and thus $\mathbf{B} = \mu_0 \mathbf{H}$.
- Linear susceptibility in the Fourier domain: $\tilde{\mathbf{P}}(\omega) = \varepsilon_0 \chi(\omega) \tilde{\mathbf{E}}(\omega)$.
- Constitutive Relation: $\tilde{\mathbf{D}} = \varepsilon_0 [1 + \chi(\omega)] \tilde{\mathbf{E}} \equiv \varepsilon_0 \varepsilon(\omega) \tilde{\mathbf{E}}$.
- Dielectric constant: $\varepsilon(\omega) = 1 + \chi(\omega)$.
- If we use the relation $\varepsilon = (n + i\alpha c/2\omega)^2$,

$$n = (1 + \mathrm{Re}\,\chi)^{1/2}, \qquad \alpha = (\omega/nc)\,\mathrm{Im}\,\chi.$$

- Frequency-Domain Maxwell Equations:

$$\begin{aligned} \nabla \times \tilde{\mathbf{E}} &= i\omega\mu_0 \tilde{\mathbf{H}}, \qquad \nabla \cdot (\varepsilon \tilde{\mathbf{E}}) = 0 \\ \nabla \times \tilde{\mathbf{H}} &= -i\omega\varepsilon_0 \varepsilon \tilde{\mathbf{E}}, \qquad \nabla \cdot \tilde{\mathbf{H}} = 0 \end{aligned}$$

Back
Close

Helmholtz Equation

- If losses are small, $\varepsilon \approx n^2$.
- Eliminate $\mathbf{H}$ from the two curl equations:

$$\nabla \times \nabla \times \tilde{\mathbf{E}} = \mu_0 \varepsilon_0 \omega^2 n^2(\omega) \tilde{\mathbf{E}} = \frac{\omega^2}{c^2} n^2(\omega) \tilde{\mathbf{E}} = k_0^2 n^2(\omega) \tilde{\mathbf{E}}.$$

- Now use the identity

$$\nabla \times \nabla \times \tilde{\mathbf{E}} \equiv \nabla(\nabla \cdot \tilde{\mathbf{E}}) - \nabla^2 \tilde{\mathbf{E}} = -\nabla^2 \tilde{\mathbf{E}}$$

- $\nabla \cdot \tilde{\mathbf{E}} = 0$ only if n is independent of $\mathbf{r}$ (homogeneous medium).
- We then obtain the Helmholtz equation:

$$\nabla^2 \tilde{\mathbf{E}} + n^2(\omega) k_0^2 \tilde{\mathbf{E}} = 0.$$

Back
Close

Planar Waveguides

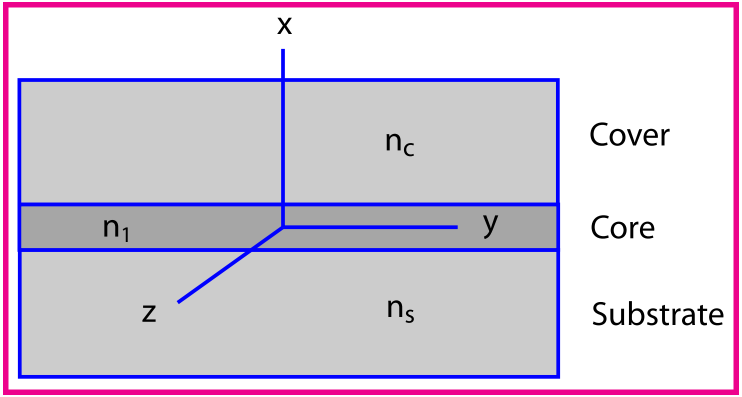

- Core film sandwiched between two layers of lower refractive index.
- Bottom layer is often a substrate with $n = n_s$.
- Top layer is called the cover layer ($n_c \neq n_s$).
- Air can also acts as a cover ($n_c = 1$).
- $n_c = n_s$ in symmetric waveguides.

Modes of Planar Waveguides

- An optical mode is solution of Maxwell's equations satisfying all boundary conditions.
- Its spatial distribution does not change with propagation.
- Modes are obtained by solving the curl equations

$$\nabla \times \mathbf{E} = i\omega\mu_0\mathbf{H}, \qquad \nabla \times \mathbf{H} = -i\omega\varepsilon_0 n^2\mathbf{E}$$

- These six equations solved in each layer of the waveguide.
- Boundary condition: Tangential component of $\mathbf{E}$ and $\mathbf{H}$ be continuous across both interfaces.
- Waveguide modes are obtained by imposing the boundary conditions.

Modes of Planar Waveguides

$$\frac{\partial E_z}{\partial y} - \frac{\partial E_y}{\partial z} = i\omega\mu_0 H_x, \qquad \frac{\partial H_z}{\partial y} - \frac{\partial H_y}{\partial z} = i\omega\epsilon_0 n^2 E_x$$

$$\frac{\partial E_x}{\partial z} - \frac{\partial E_z}{\partial x} = i\omega\mu_0 H_y, \qquad \frac{\partial H_x}{\partial z} - \frac{\partial H_z}{\partial x} = i\omega\epsilon_0 n^2 E_y$$

$$\frac{\partial E_y}{\partial x} - \frac{\partial E_x}{\partial y} = i\omega\mu_0 H_z, \qquad \frac{\partial H_y}{\partial x} - \frac{\partial H_x}{\partial y} = i\omega\epsilon_0 n^2 E_z$$

- Assume waveguide is infinitely wide along the y axis.
- $\mathbf{E}$ and $\mathbf{H}$ are then y-independent.
- For any mode, all filed components vary with z as $\exp(i\beta z)$. Thus,

$$\frac{\partial \mathbf{E}}{\partial y} = 0, \quad \frac{\partial \mathbf{H}}{\partial y} = 0, \quad \frac{\partial \mathbf{E}}{\partial z} = i\beta\mathbf{E}, \quad \frac{\partial \mathbf{H}}{\partial z} = i\beta\mathbf{H}.$$

TE and TM Modes

- These equations have two distinct sets of linearly polarized solutions.
- For Transverse-Electric (TE) modes, $E_z = 0$ and $E_x = 0$.
- TE modes are obtained by solving

$$\frac{d^2E_y}{dx^2} + (n^2k_0^2 - \beta^2)E_y = 0, \qquad k_0 = \omega\sqrt{\varepsilon_0\mu_0} = \omega/c.$$

- Magnetic field components are related to E_y as

$$H_x = -\frac{\beta}{\omega\mu_0}E_y, \qquad H_y = 0, \qquad H_z = -\frac{i}{\omega\mu_0}\frac{dE_y}{dx}.$$

- For transverse magnetic (TM) modes, $H_z = 0$ and $H_x = 0$.
- Electric filed components are now related to H_y as

$$E_x = \frac{\beta}{\omega\varepsilon_0 n^2}H_y, \qquad E_y = 0, \qquad E_z = \frac{i}{\omega\varepsilon_0 n^2}\frac{dH_y}{dx}.$$

Solution for TE Modes

$$\frac{d^2E_y}{dx^2} + (n^2k_0^2 - \beta^2)E_y = 0.$$

- We solve this equation in each layer separately using $n = n_c,\ n_1$, and n_s.

$$E_y(x) = \begin{cases} B_c \exp[-q_1(x-d)]; & x > d, \\ A\cos(px - \phi) \quad ; & |x| \le d \\ B_s \exp[q_2(x+d)] \quad ; & x < -d, \end{cases}$$

- Constants p, q_1, and q_2 are defined as

$$p^2 = n_1^2k_0^2 - \beta^2, \quad q_1^2 = \beta^2 - n_c^2k_0^2, \quad q_2^2 = \beta^2 - n_s^2k_0^2.$$

- Constants B_c, B_s, A, and ϕ are determined from the boundary conditions at the two interfaces.

Boundary Conditions

- Tangential components of **E** and **H** continuous across any interface with index discontinuity.
- Mathematically, E_y and H_z should be continuous at $x = \pm d$.
- E_y is continuous at $x = \pm d$ if

$$B_c = A\cos(pd - \phi); \qquad B_s = A\cos(pd + \phi).$$

- Since $H_z \propto dE_y/dx$, dE_y/dx should also be continuous at $x = \pm d$:

$$pA\sin(pd - \phi) = q_1 B_c, \qquad pA\sin(pd + \phi) = q_2 B_s.$$

- Eliminating A, B_c, B_s from these equations, ϕ must satisfy

$$\tan(pd - \phi) = q_1/p, \qquad \tan(pd + \phi) = q_2/p$$

The Institute of OPTICS

UNIVERSITY of ROCHESTER

TE Modes

- Boundary conditions are satisfied when

$$pd - \phi = \tan^{-1}(q_1/p) + m_1\pi, \qquad pd + \phi = \tan^{-1}(q_2/p) + m_2\pi$$

- Adding and subtracting these equations, we obtain

$$2\phi = m\pi - \tan^{-1}(q_1/p) + \tan^{-1}(q_2/p)$$

$$2pd = m\pi + \tan^{-1}(q_1/p) + \tan^{-1}(q_2/p)$$

- The last equation is called the eigenvalue equation.
- Multiple solutions for $m = 0, 1, 2, \ldots$ are denoted by TE_m.
- Effective index of each TE mode is $\bar{n} = \beta/k_0$.

TM Modes

- Same procedure is used to obtain TM modes.
- Solution for H_y has the same form in three layers.
- Continuity of E_z requires that $n^{-2}(dH_y/dx)$ be continuous at $x = \pm d$.
- Since n is different on the two sides of each interface, eigenvalue equation is modified to become

$$2pd = m\pi + \tan^{-1}\left(\frac{n_1^2 q_1}{n_c^2 p}\right) + \tan^{-1}\left(\frac{n_1^2 q_2}{n_s^2 p}\right).$$

- Multiple solutions for different values of m.
- These are labelled as TM_m modes.

TE Modes of Symmetric Waveguides

- For symmetric waveguides $n_c = n_s$.
- Using $q_1 = q_2 \equiv q$, TE modes satisfy

$$q = p\tan(pd - m\pi/2).$$

- Define a dimensionless parameter

$$V = d\sqrt{p^2+q^2} = k_0 d\sqrt{n_1^2 - n_s^2},$$

- If we use $u = pd$, the eigenvalue equation can be written as

$$\sqrt{V^2-u^2} = u\tan(u - m\pi/2).$$

- For given values of V and m, this equation is solved to find $p = u/d$.

TE Modes of Symmetric Waveguides

- Effective index $\bar{n} = \beta/k_0 = (n_1^2 - p^2/k_0^2)^{1/2}$.
- Using $2\phi = m\pi - \tan^{-1}(q_1/p) + \tan^{-1}(q_2/p)$ with $q_1 = q_2$, phase $\phi = m\pi/2$.
- Spatial distribution of modes is found to be

$$E_y(x) = \begin{cases} B_\pm \exp[-q(|x| - d)]; & |x| > d, \\ A\cos(px - m\pi/2) \;\; ; & |x| \le d, \end{cases}$$

  where $B_\pm = A\cos(pd \mp m\pi/2)$ and the lower sign is chosen for $x < 0$.

- Modes with even values of m are symmetric around $x = 0$ (even modes).
- Modes with odd values of m are antisymmetric around $x = 0$ (odd modes).

TM Modes of Symmetric Waveguides

- We can follow the same procedure for TM modes.
- Eigenvalue equation for TM modes:

$$(n_1/n_s)^2 q = p \tan(pd - m\pi/2).$$

- TM modes can also be divided into even and odd modes.

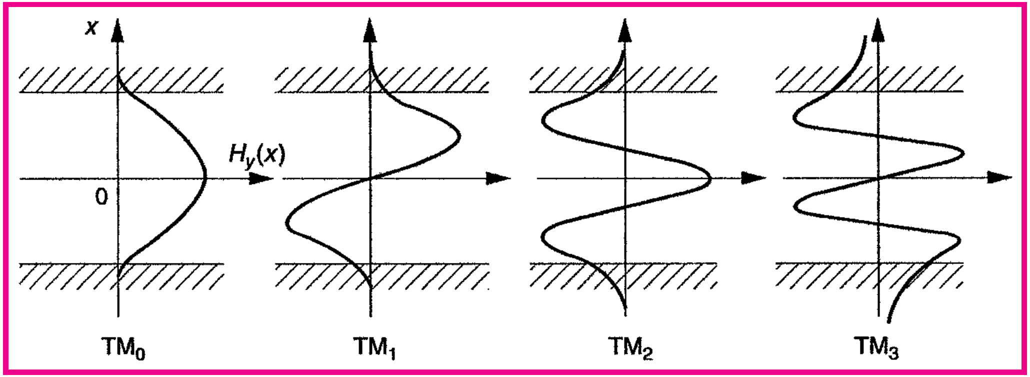

Symmetric Waveguides

- TE_0 and TM_0 modes have no nodes within the core.
- They are called the fundamental modes of a planar waveguide.
- Number of modes supported by a waveguide depends on the V parameter.
- A mode ceases to exist when $q = 0$ (no longer confined to the core).
- This occurs for both TE and TM modes when $V = V_m = m\pi/2$.
- Number of modes = Largest value of m for which $V_m > V$.
- A waveguide with $V = 10$ supports 7 TE and 7 TM modes ($V_6 = 9.42$ but V_7 exceeds 10).
- A waveguide supports a single TE and a single TM mode when $V < \pi/2$ (single-mode condition).

Modes of Asymmetric Waveguides

- We can follow the same procedure for $n_c \neq n_s$.
- Eigenvalue equation for TE modes:

$$2pd = m\pi + \tan^{-1}(q_1/p) + \tan^{-1}(q_2/p)$$

- Eigenvalue equation for TM modes:

$$2pd = m\pi + \tan^{-1}\left(\frac{n_1^2 q_1}{n_c^2 p}\right) + \tan^{-1}\left(\frac{n_1^2 q_2}{n_s^2 p}\right)$$

- Constants p, q_1, and q_2 are defined as

$$p^2 = n_1^2 k_0^2 - \beta^2, \quad q_1^2 = \beta^2 - n_c^2 k_0^2, \quad q_2^2 = \beta^2 - n_s^2 k_0^2.$$

- Each solution for β corresponds to a mode with effective index $\bar{n} = \beta / k_0$.
- If $n_1 > n_s > n_c$, guided modes exist as long as $n_1 > \bar{n} > n_s$.

Modes of Asymmetric Waveguides

- Useful to introduce two normalized parameters as

$$b = \frac{\bar{n}^2 - n_s^2}{n_1^2 - n_s^2}, \qquad \delta = \frac{n_s^2 - n_c^2}{n_1^2 - n_s^2}.$$

- b is a normalized propagation constant $(0 < b < 1)$.
- Parameter δ provides a measure of waveguide asymmetry.
- Eigenvalue equation for TE modes in terms V, b, δ:

$$2V\sqrt{1-b} = m\pi + \tan^{-1}\sqrt{\frac{b}{1-b}} + \tan^{-1}\sqrt{\frac{b+\delta}{1-b}}.$$

- Its solutions provide **universal** dispersion curves.

Modes of Asymmetric Waveguides

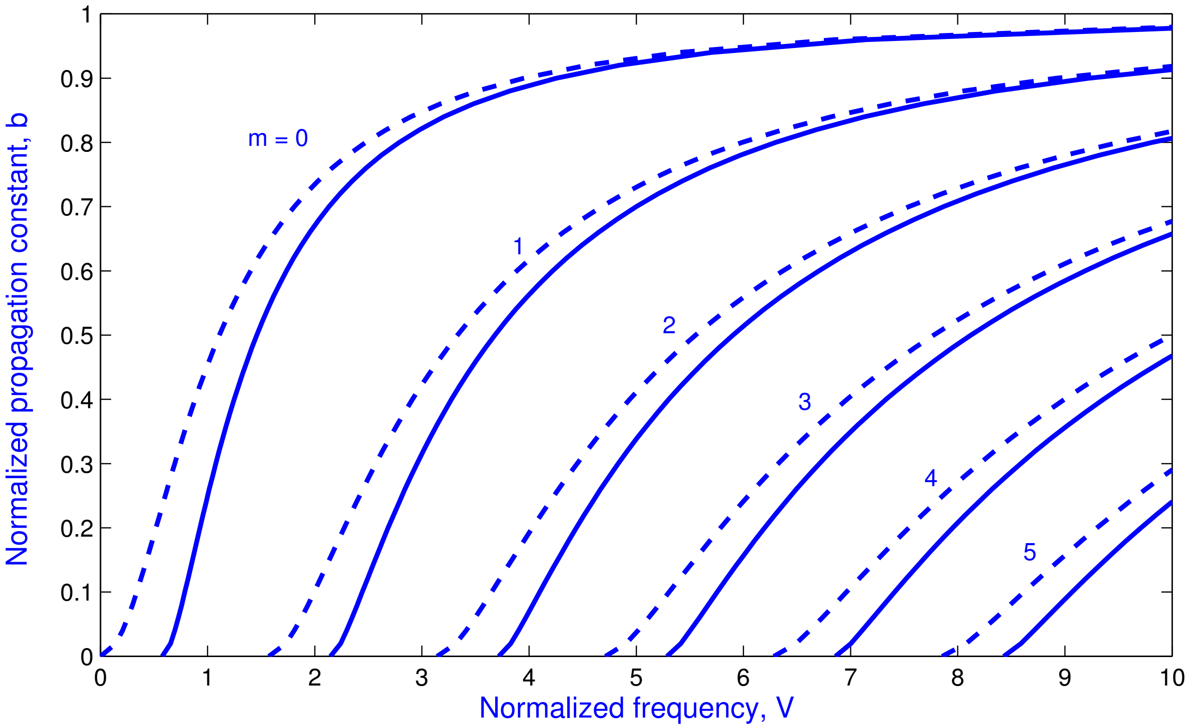

Solid lines ($\delta = 5$); dashed lines ($\delta = 0$).

Mode-Cutoff Condition

- Cutoff condition corresponds to the value of V for which mode ceases to decay exponentially in one of the cladding layers.
- It is obtained by setting $b = 0$ in eigenvalue equation:

$$V_m(\mathrm{TE}) = \frac{m\pi}{2} + \frac{1}{2}\tan^{-1}\sqrt{\delta}.$$

- Eigenvalue equation for the TM modes:

$$2V\sqrt{1-b} = m\pi + \tan^{-1}\left(\frac{n_1^2}{n_s^2}\sqrt{\frac{b}{1-b}}\right) + \tan^{-1}\left(\frac{n_1^2}{n_c^2}\sqrt{\frac{b+\delta}{1-b}}\right).$$

- The cutoff condition found by setting $b = 0$:

$$V_m(\mathrm{TM}) = \frac{m\pi}{2} + \frac{1}{2}\tan^{-1}\left(\frac{n_1^2}{n_c^2}\sqrt{\delta}\right).$$

Mode-Cutoff Condition

- For a symmetric waveguide ($\delta = 0$), these two conditions reduce to a single condition, $V_m = m\pi/2$.
- TE and TM modes for a given value of m have the same cutoff.
- A single-mode waveguide is realized if V parameter of the waveguide satisfies

$$V \equiv k_0 d \sqrt{n_1^2 - n_s^2} < \frac{\pi}{2}$$

- Fundamental mode always exists for a symmetric waveguide.
- An asymmetric waveguide with $2V < \tan^{-1}\sqrt{\delta}$ does not support any bounded mode.

Spatial Distribution of Modes

$$E_y(x) = \begin{cases} B_c \exp[-q_1(x-d)]; & x > d, \\ A\cos(px-\phi) \quad ; & |x| \le d \\ B_s \exp[q_2(x+d)] \quad ; & x < -d, \end{cases}$$

- Boundary conditions: $B_c = A\cos(pd-\phi)$, $\quad B_s = A\cos(pd+\phi)$
- A is related to total power $P = \frac{1}{2}\int_{-\infty}^{\infty} \hat{z}\cdot(\mathbf{E}\times\mathbf{H})\,dx$:

$$P = \frac{\beta}{2\omega\mu_0}\int_{-\infty}^{\infty} |E_y(x)|^2\,dx = \frac{\beta A^2}{4\omega\mu_0}\left(2d + \frac{1}{q_1} + \frac{1}{q_2}\right).$$

- Fraction of power propagating inside the waveguide layer:

$$\Gamma = \frac{\int_{-d}^{d} |E_y(x)|^2 dx}{\int_{-\infty}^{\infty} |E_y(x)|^2 dx} = \frac{2d + \sin^2(pd-\phi)/q_1 + \sin^2(pd+\phi)/q_2}{2d + 1/q_1 + 1/q_2}.$$

- For fundamental mode $\Gamma \ll 1$ when $V \ll \pi/2$.

Back
Close

Rectangular Waveguides

- Rectangular waveguide confines light in both x and y dimensions.
- The high-index region in the middle core layer has a finite width $2w$ and is surrounded on all sides by lower-index materials.
- Refractive index can be different on all sides of a rectangular waveguide.

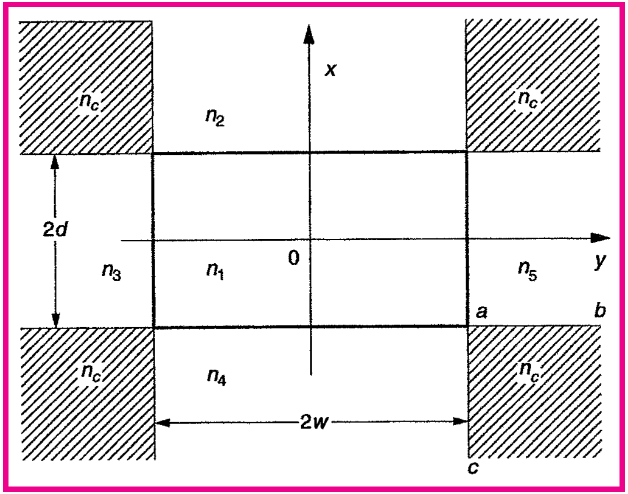

Modes of Rectangular Waveguides

- To simplify the analysis, all shaded cladding regions are assumed to have the same refractive index n_c.
- A numerical approach still necessary for an exact solution.
- Approximate analytic solution possible with two simplifications; Marcatili, *Bell Syst. Tech. J.* **48**, 2071 (1969).
  - ⋆ Ignore boundary conditions associated with hatched regions.
  - ⋆ Assume core-cladding index differences are small on all sides.
- Problem is then reduced to solving two planar-waveguide problems in the x and y directions.

Modes of Rectangular Waveguides

- One can find TE- and TM-like modes for which either E_z or H_z is nearly negligible compared to other components.
- Modes denoted as E^x_{mn} and E^y_{mn} obtained by solving two coupled eigenvalue equations.

$$
\begin{aligned}
2p_x d &= m\pi + \tan^{-1}\left(\frac{n_1^2 q_2}{n_2^2 p_x}\right) + \tan^{-1}\left(\frac{n_1^2 q_4}{n_4^2 p_x}\right), \\
2p_y w &= n\pi + \tan^{-1}\left(\frac{q_3}{p_y}\right) + \tan^{-1}\left(\frac{q_5}{p_y}\right), \\
p_x^2 &= n_1^2 k_0^2 - \beta^2 - p_y^2, \quad p_y^2 = n_1^2 k_0^2 - \beta^2 - p_x^2, \\
q_2^2 &= \beta^2 + p_y^2 - n_2^2 k_0^2, \quad q_4^2 = \beta^2 + p_y^2 - n_4^2 k_0^2, \\
q_3^2 &= \beta^2 + p_x^2 - n_3^2 k_0^2, \quad q_5^2 = \beta^2 + p_x^2 - n_5^2 k_0^2,
\end{aligned}
$$

Effective-Index Method

- Effective-index method appropriate when thickness of a rectangular waveguide is much smaller than its width ($d \ll w$).
- Planar waveguide problem in the x direction is solved first to obtain the effective mode index $n_e(y)$.
- n_e is a function of y because of a finite waveguide width.
- In the y direction, we use a waveguide of width $2w$ such that $n_y = n_e$ if $|y| < w$ but equals n_3 or n_5 outside of this region.
- Single-mode condition is found to be

$$V_x = k_0 d\sqrt{n_1^2 - n_4^2} < \pi/2, \qquad V_y = k_0 w\sqrt{n_e^2 - n_5^2} < \pi/2$$

Design of Rectangular Waveguides

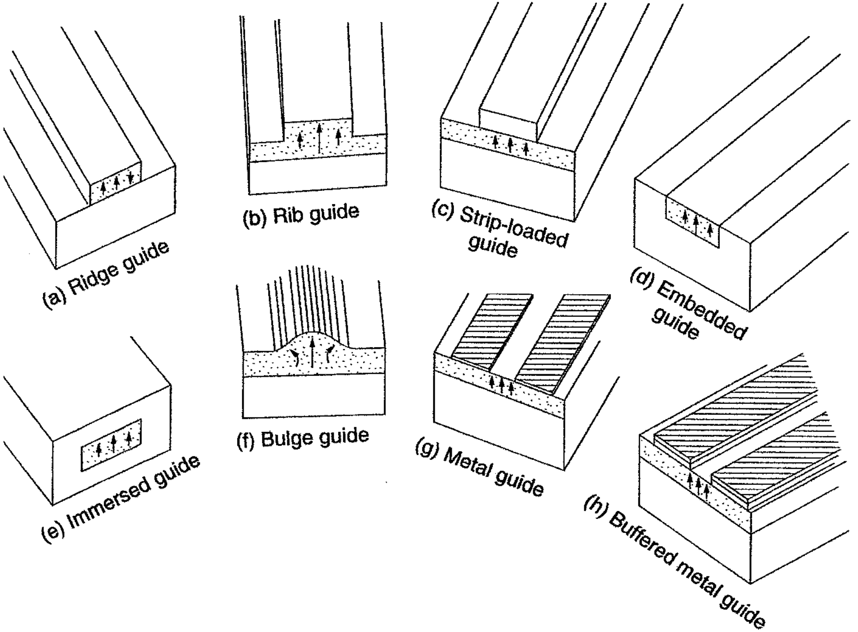

- In (g) core layer is covered with two metal stripes.
- Losses can be reduced by using a thin buffer layer (h).

Materials for Waveguides

- Semiconductor Waveguides: GaAs, InP, etc.
- Electro-Optic Waveguides: mostly $LiNbO_3$.
- Glass Waveguides: silica (SiO_2), SiON.
  - ⋆ Silica-on-silicon technology
  - ⋆ Laser-written waveguides
- Silicon-on-Insulator Technology
- Polymers Waveguides: Several organic polymers

Semiconductor Waveguides

Useful for semiconductor lasers, modulators, and photodetectors.

- Semiconductors allow fabrication of electrically active devices.
- Semiconductors belonging to III–V Group often used.
- Two semiconductors with different refractive indices needed.
- They must have different bandgaps but same lattice constant.
- Nature does not provide such semiconductors.

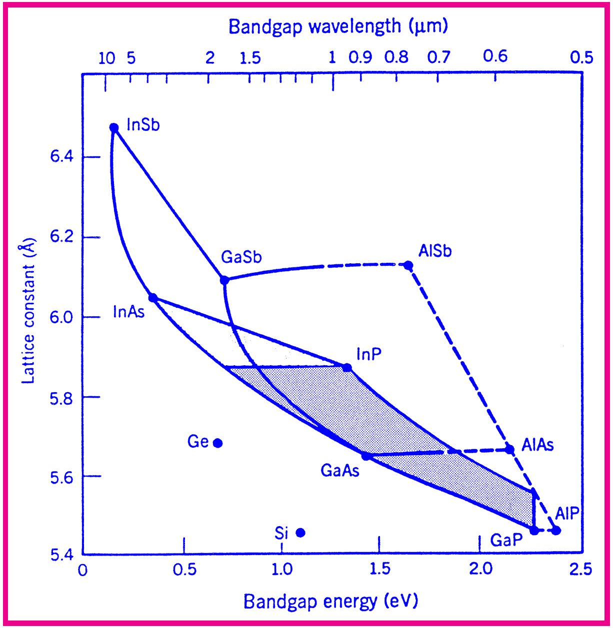

Ternary and Quaternary Compounds

- A fraction of the lattice sites in a binary semiconductor (GaAs, InP, etc.) is replaced by other elements.
- Ternary compound $Al_xGa_{1-x}As$ is made by replacing a fraction x of Ga atoms by Al atoms.
- Bandgap varies with x as

$$E_g(x) = 1.424 + 1.247x \qquad (0 < x < 0.45).$$

- Quaternary compound $In_{1-x}Ga_xAs_yP_{1-y}$ useful in the wavelength range 1.1 to 1.6 μm.
- For matching lattice constant to InP substrate, $x/y = 0.45$.
- Bandgap varies with y as $E_g(y) = 1.35 - 0.72y + 0.12y^2$.

Fabrication Techniques

Epitaxial growth of multiple layers on a base substrate (GaAs or InP).

Three primary techniques:

- Liquid-phase epitaxy (LPE)
- Vapor-phase epitaxy (VPE)
- Molecular-beam epitaxy (MBE)

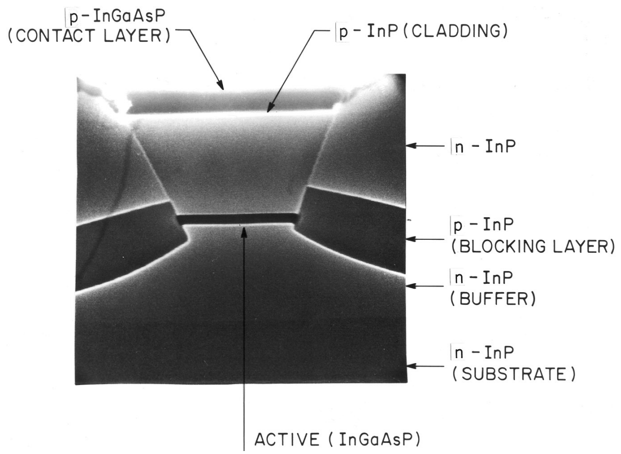

VPE is also called chemical-vapor deposition (CVD).

Metal-organic chemical-vapor deposition (MOCVD) is often used in practice.

Quantum-Well Technology

- Thickness of the core layer plays a central role.
- If it is small enough, electrons and holes act as if they are confined to a quantum well.
- Confinement leads to quantization of energy bands into subbands.
- Joint density of states acquires a staircase-like structure.
- Useful for making modern quantum-well, quantum wire, and quantum-dot lasers.
- in MQW lasers, multiple core layers (thickness 5–10 nm) are separated by transparent barrier layers.
- Use of intentional but controlled strain improves performance in *strained* quantum wells.

Doped Semiconductor Waveguides

- To build a laser, one needs to inject current into the core layer.
- This is accomplished through a p–n junction formed by making cladding layers p- and n-types.
- n-type material requires a dopant with an extra electron.
- p-type material requires a dopant with one less electron.
- Doping creates free electrons or holes within a semiconductor.
- Fermi level lies in the middle of bandgap for undoped (intrinsic) semiconductors.
- In a heavily doped semiconductor, Fermi level lies inside the conduction or valence band.

p–n junctions

- Fermi level continuous across the p–n junction in thermal equilibrium.
- A built-in electric field separates electrons and holes.
- Forward biasing reduces the built-in electric field.
- An electric current begins to flow: $I = I_s[\exp(qV/k_BT) - 1]$.
- Recombination of electrons and holes generates light.

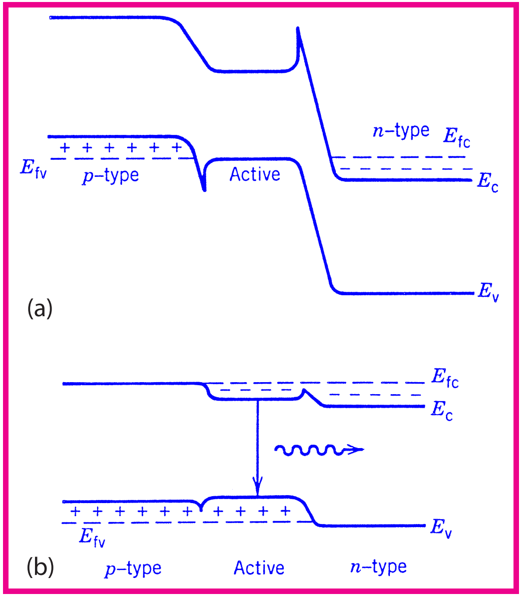

Electro-Optic Waveguides

- Use Pockels effect to change refractive index of the core layer with an external voltage.
- Common electro-optic materials: $LiNbO_3$, $LiTaO_3$, $BaTiO_3$.
- $LiNbO_3$ used commonly for making optical modulators.
- For any anisotropic material $D_i = \varepsilon_0 \sum_{j=1}^{3} \varepsilon_{ij} E_j$.
- Matrix ε_{ij} can be diagonalized by rotating the coordinate system along the principal axes.
- Impermeability tensor $\eta_{ij} = 1/\varepsilon_{ij}$ describes changes induced by an external field as $\eta_{ij}(\mathbf{E}^a) = \eta_{ij}(0) + \sum_k r_{ijk} \mathbf{E}_k^a$.
- Tensor r_{ijk} is responsible for the electro-optic effect.

Lithium Niobate Waveguides

- $LiNbO_3$ waveguides do not require an epitaxial growth.
- A popular technique employs diffusion of metals into a $LiNbO_3$ substrate, resulting in a low-loss waveguide.
- The most commonly used element: Titanium (Ti).
- Diffusion of Ti atoms within $LiNbO_3$ crystal increases refractive index and forms the core region.
- Out-diffusion of Li atoms from substrate should be avoided.
- Surface flatness critical to ensure a uniform waveguide.

$LiNbO_3$ Waveguides

- A proton-exchange technique is also used for $LiNbO_3$ waveguides.
- A low-temperature process ($\sim 200^\circ$C) in which Li ions are replaced with protons when the substrate is placed in an acid bath.
- Proton exchange increases the extraordinary part of refractive index but leaves the ordinary part unchanged.
- Such a waveguide supports only TM modes and is useful for some applications because of its polarization selectivity.
- High-temperature annealing used to stabilizes the index difference.
- Accelerated aging tests predict a lifetime of over 25 years at a temperature as high as 95°C.

$LiNbO_3$ Waveguides

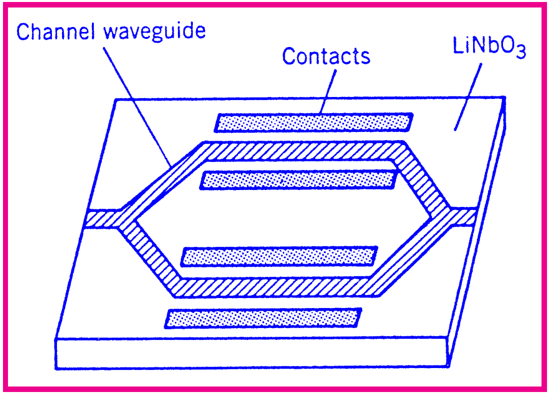

- Electrodes fabricated directly on the surface of wafer (or on an optically transparent buffer layer.
- An adhesion layer (typically Ti) first deposited to ensure that metal sticks to $LiNbO_3$.
- Photolithography used to define the electrode pattern.

Silica Glass Waveguides

- Silica layers deposited on top of a Si substrate.
- Employs the technology developed for integrated circuits.
- Fabricated using flame hydrolysis with reactive ion etching.
- Two silica layers are first deposited using flame hydrolysis.
- Top layer converted to core by doping it with germania.
- Both layers solidified by heating at 1300°C (consolidation process).
- Photolithography used to etch patterns on the core layer.
- Entire structure covered with a cladding formed using flame hydrolysis. A thermo-optic phase shifter often formed on top.

Silica-on-Silicon Technique

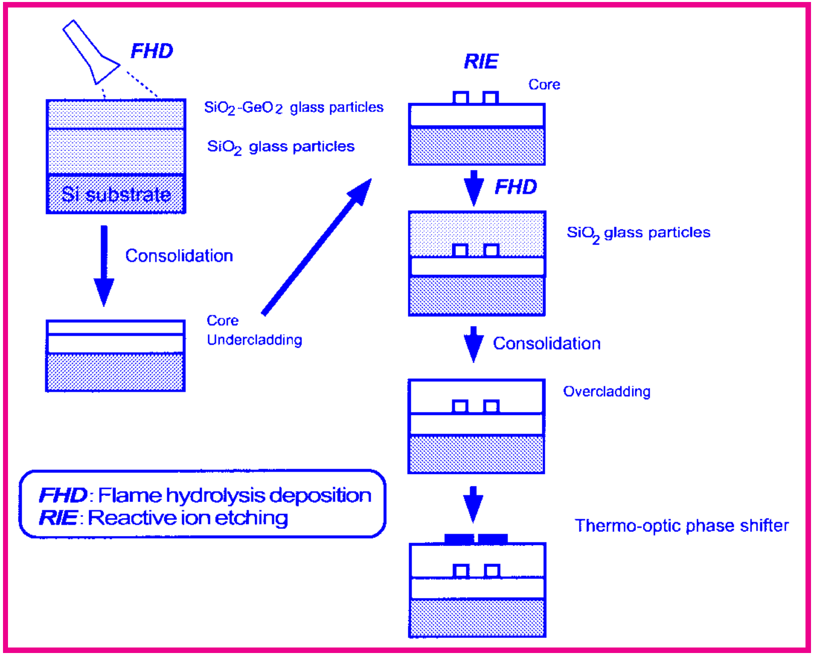

Steps used to form silica waveguides on top of a Si Substrate

Silica Waveguide properties

- Silica-on-silicon technology produces uniform waveguides.
- Losses depend on the core-cladding index difference $\Delta = (n_1 - n_2)/n_1$.
- Losses are low for small values of Δ (about 0.017 dB/cm for $\Delta = 0.45\%$).
- Higher values of Δ often used for reducing device length.
- Propagation losses ~0.1 dB/cm for $\Delta = 2\%$.
- Planar lightwave circuits: Multiple waveguides and optical components integrated over the same silicon substrate.
- Useful for making compact WDM devices ($\sim 5 \times 5$ cm^2).
- Large insertion losses when a PLC is connected to optical fibers.

Packaged PLCs

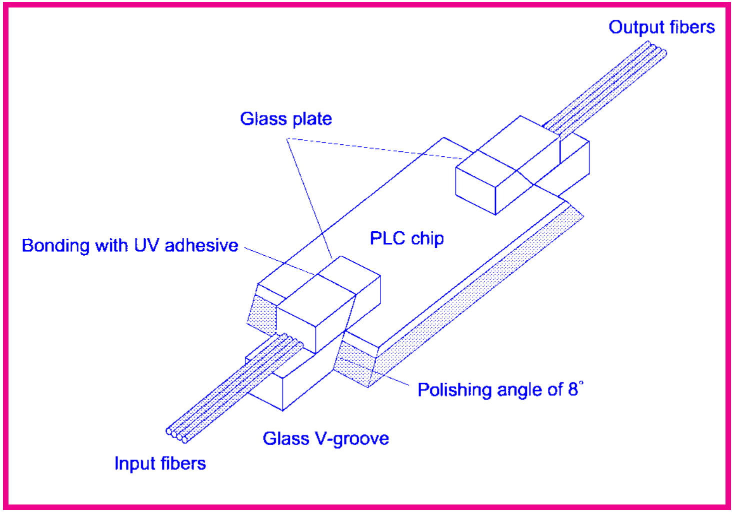

- Package design for minimizing insertion losses.
- Fibers inserted into V-shaped grooves formed on a glass substrate.
- Glass substrate connected to the PLC chip using an adhesive.
- A glass plate placed on top of V grooves is bonded to the PLC chip

with the same adhesive.

Silicon Oxynitride Waveguides

- Employ Si substrate but use SiON for the core layer.
- SiON alloy is made by combining SiO_2 with Si_3N_4, two dielectrics with refractive indices of 1.45 and 2.01.
- Refractive index of SiON layer can vary from 1.45–2.01.
- SiON film deposited using plasma-enhanced chemical vapor deposition (SiH_4 combined with N_2O and NH_3).
- Low-pressure chemical vapor deposition also used (SiH_2Cl_2 combined with O_2 and NH_3).
- Photolithography pattern formed on a 200-nm-thick chromium layer.
- Propagation losses typically <0.2 dB/cm.

Laser-Written Waveguides

- CW or pulsed light from a laser used for "writing" waveguides in silica and other glasses.
- Photosensitivity of germanium-doped silica exploited to enhance refractive index in the region exposed to a UV laser.
- Absorption of 244-nm light from a KrF laser changes refractive index by $\sim 10^{-4}$ only in the region exposed to UV light.
- Index changes $>10^{-3}$ can be realized with a 193-nm ArF laser.
- A planar waveguide formed first through CVD, but core layer is doped with germania.
- An UV beam focused to $\sim 1\ \mu$m scanned slowly to enhance n selectively. UV-written sample then annealed at 80°C.

Laser-Written Waveguides

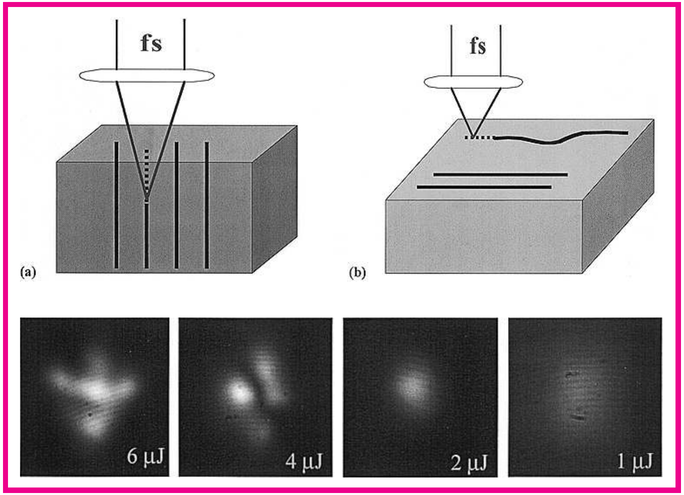

- Femtosecond pulses from a Ti:sapphire laser can be used to write waveguides in bulk glasses.
- Intense pulses modify the structure of silica through multiphoton absorption.
- Refractive-index changes $\sim 10^{-2}$ are possible.

Silicon-on-Insulator Technology

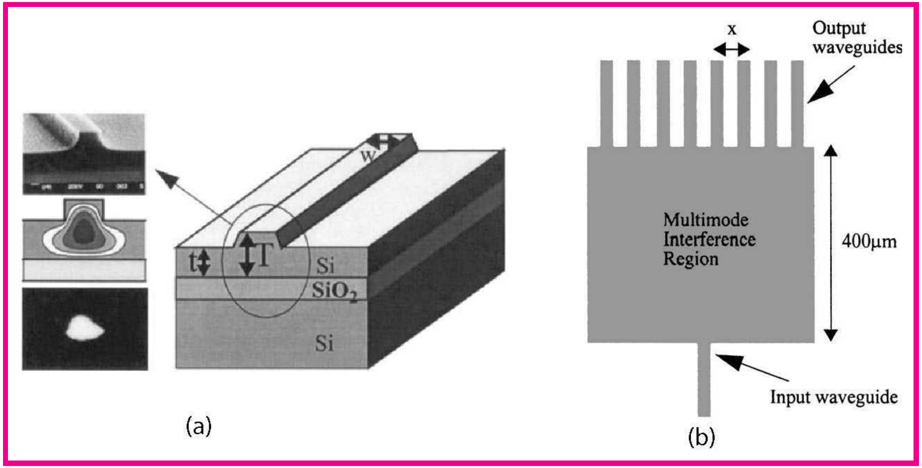

- Core waveguide layer is made of Si ($n_1 = 3.45$).
- A silica layer under the core layer is used for lower cladding.
- Air on top acts as the top cladding layer.
- Tightly confined waveguide mode because of large index difference.
- Silica layer formed by implanting oxygen, followed with annealing.

Polymer Waveguides

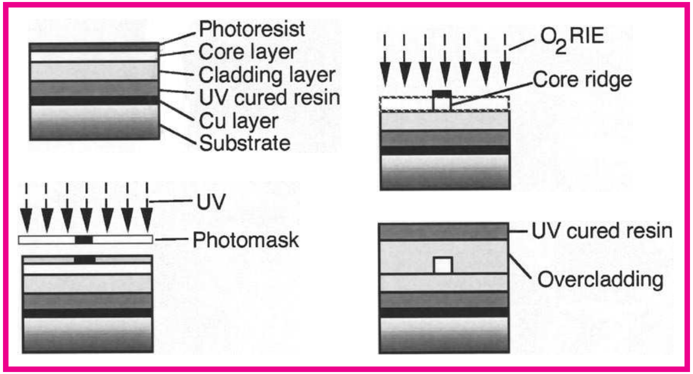

- Polymers such as halogenated acrylate, fluorinated polyimide, and deuterated polymethylmethacrylate (PMMA) have been used.
- Polymer films can be fabricated on top of Si, glass, quartz, or plastic through spin coating.
- Photoresist layer on top used for reactive ion etching of the core layer through a photomask.

Optical Fibers

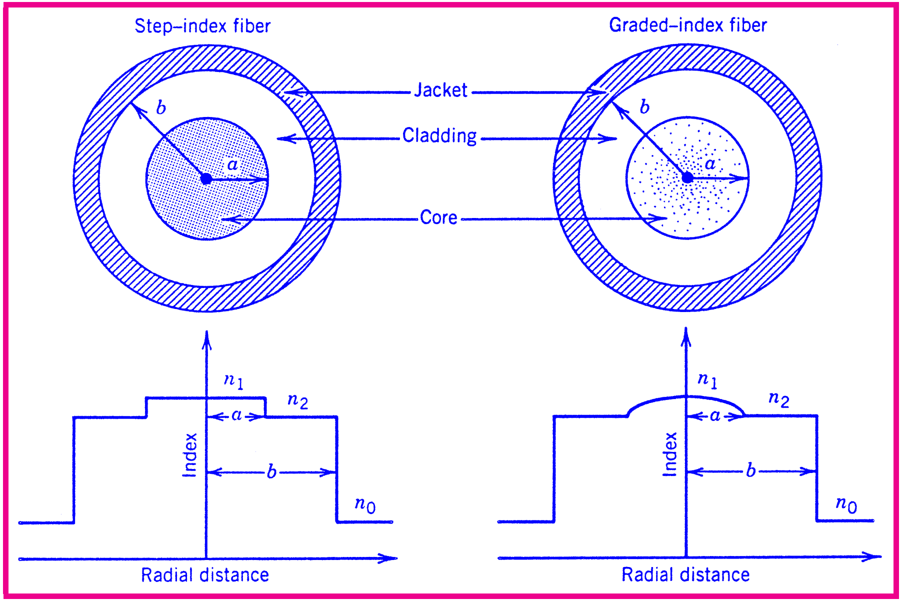

- Contain a central core surrounded by a lower-index cladding
- Two-dimensional waveguides with cylindrical symmetry
- Graded-index fibers: Refractive index varies inside the core

Total internal reflection

- Refraction at the air–glass interface: $n_0 \sin\theta_i = n_1 \sin\theta_r$
- Total internal reflection at the core-cladding interface if $\phi > \phi_c = \sin^{-1}(n_2/n_1)$.

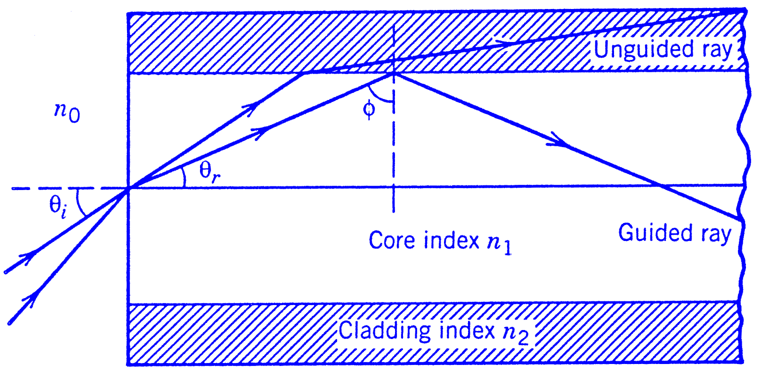

Numerical Aperture: Maximum angle of incidence

$$n_0 \sin\theta_i^{\max} = n_1 \sin(\pi/2 - \phi_c) = n_1 \cos\phi_c = \sqrt{n_1^2 - n_2^2}$$

Modal Dispersion

- Multimode fibers suffer from modal dispersion.
- Shortest path length $L_{\min} = L$ (along the fiber axis).
- Longest path length for the ray close to the critical angle

$$L_{\max} = L/\sin\phi_c = L(n_1/n_2).$$

- **Pulse broadening:** $\Delta T = (L_{\max} - L_{\min})(n_1/c)$.
- Modal dispersion: $\Delta T/L = n_1^2\Delta/(n_2 c)$.
- Limitation on the bit rate

$$\Delta T < T_B = 1/B; \quad B\Delta T < 1; \quad BL < \frac{n_2 c}{n_1^2 \Delta}.$$

- Single-mode fibers essential for high performance.

Graded-Index Fibers

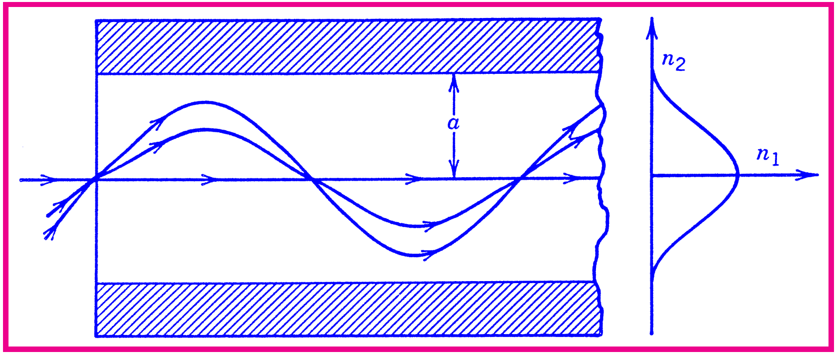

- Refractive index $n(\rho) = \begin{cases} n_1[1-\Delta(\rho/a)^\alpha]; & \rho < a, \\ n_1(1-\Delta) = n_2 \ ; & \rho \geq a. \end{cases}$
- Ray path obtained by solving $\frac{d^2\rho}{dz^2} = \frac{1}{n}\frac{dn}{d\rho}$.
- For $\alpha = 2$, $\rho = \rho_0 \cos(pz) + (\rho_0'/p)\sin(pz)$.
- All rays arrive simultaneously at periodic intervals.
- Limitation on the Bit Rate: $BL < \frac{8c}{n_1\Delta^2}$.

Back
Close

Fiber Design

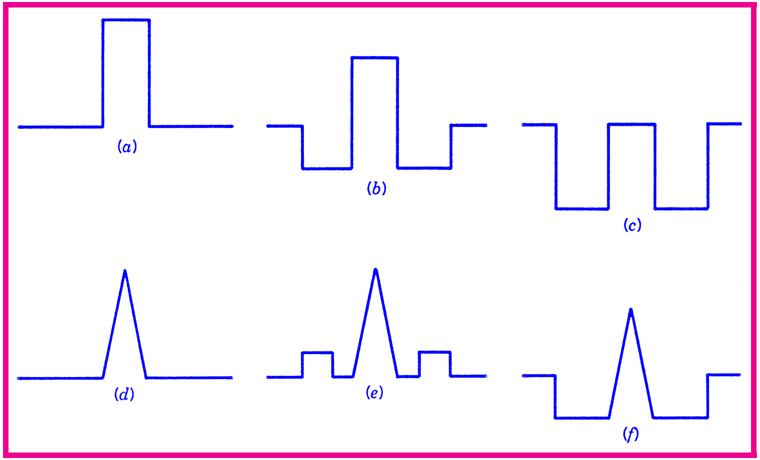

- Core doped with GeO_2; cladding with fluorine.
- Index profile rectangular for standard fibers.
- Triangular index profile for dispersion-shifted fibers.
- Raised or depressed cladding for dispersion control.

Silica Fibers

Two-Stage Fabrication

- **Preform:** Length 1 m, diameter 2 cm; correct index profile.
- Preform is drawn into fiber using a draw tower.

Preform Fabrication Techniques

- Modified chemical vapor deposition (MCVD).
- Outside vapor deposition (OVD).
- Vapor Axial deposition (VAD).

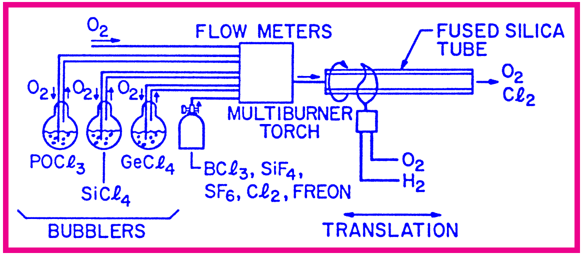

Fiber Draw Tower

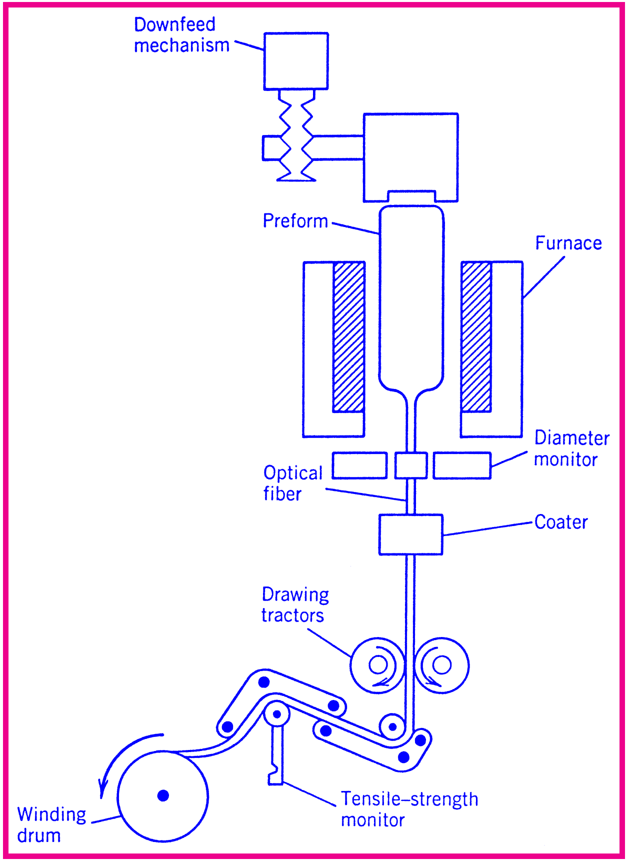

Plastic Fibers

- Multimode fibers (core diameter as large as 1 mm).
- Large NA results in high coupling efficiency.
- Use of plastics reduces cost but loss exceeds 50 dB/km.
- Useful for data transmission over short distances (<1 km).
- 10-Gb/s signal transmitted over 0.5 km (1996 demo).
- Ideal solution for transferring data between computers.
- Commonly used polymers:
  - ⋆ polymethyl methacrylate (PMMA), polystyrene
  - ⋆ polycarbonate, poly(perfluoro-butenylvinyl) ether

Plastic Fibers

- Preform made with the interfacial gel polymerization method.
- A cladding cylinder is filled with a mixture of monomer (same used for cladding polymer), index-increasing dopant, a chemical for initiating polymerization, and a chain-transfer agent.
- Cylinder heated to a 95°C and rotated on its axis for a period of up to 24 hours.
- Core polymerization begins near cylinder wall.
- Dopant concentration increases toward core center.
- This technique automatically creates a gradient in the core index.

Microstructure Fibers

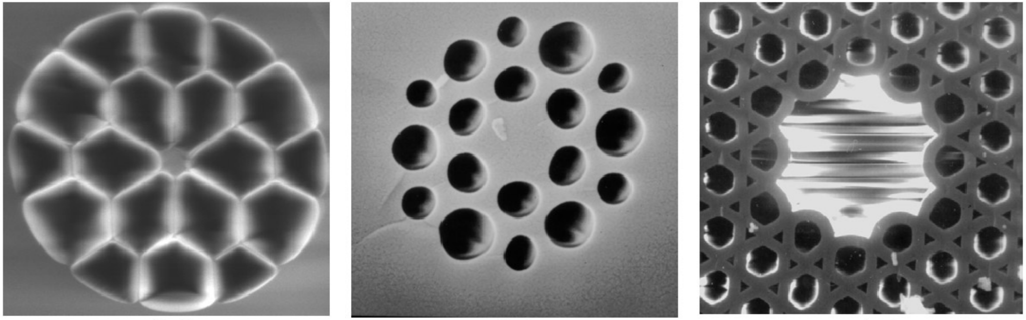

(a) (b) (c)

- New types of fibers with air holes in cladding region.
- Air holes reduce the index of the cladding region.
- Narrow core (2 μm or so) results in tighter mode confinement.
- Air-core fibers guide light through the photonic-crystal effect.
- Preform made by stacking silica tubes in a hexagonal pattern.

The Institute of OPTICS

UNIVERSITY of ROCHESTER

Fiber Modes

- Maxwell's equations in the Fourier domain lead to

$$\nabla^2\tilde{\mathbf{E}} + n^2(\omega)k_0^2\tilde{\mathbf{E}} = 0.$$

- $n = n_1$ inside the core but changes to n_2 in the cladding.
- Useful to work in cylindrical coordinates ρ, ϕ, z.
- Common to choose E_z and H_z as independent components.
- Equation for E_z in cylindrical coordinates:

$$\frac{\partial^2 E_z}{\partial \rho^2} + \frac{1}{\rho}\frac{\partial E_z}{\partial \rho} + \frac{1}{\rho^2}\frac{\partial^2 E_z}{\partial \phi^2} + \frac{\partial^2 E_z}{\partial z^2} + n^2 k_0^2 E_z = 0.$$

- H_z satisfies the same equation.

Fiber Modes (cont.)

- Use the method of separation of variables:

$$E_z(\rho, \phi, z) = F(\rho)\Phi(\phi)Z(z).$$

- We then obtain three ODEs:

$$d^2Z/dz^2 + \beta^2 Z = 0,$$

$$d^2\Phi/d\phi^2 + m^2\Phi = 0,$$

$$\frac{d^2F}{d\rho^2} + \frac{1}{\rho}\frac{dF}{d\rho} + \left(n^2k_0^2 - \beta^2 - \frac{m^2}{\rho^2}\right)F = 0.$$

- β and m are two constants (m must be an integer).
- First two equations can be solved easily to obtain

$$Z(z) = \exp(i\beta z), \qquad \Phi(\phi) = \exp(im\phi).$$

- $F(\rho)$ satisfies the Bessel equation.

Fiber Modes (cont.)

- General solution for E_z and H_z:

$$E_z = \begin{cases} AJ_m(p\rho)\exp(im\phi)\exp(i\beta z)\,; & \rho \le a, \\ CK_m(q\rho)\exp(im\phi)\exp(i\beta z); & \rho > a. \end{cases}$$

$$H_z = \begin{cases} BJ_m(p\rho)\exp(im\phi)\exp(i\beta z)\,; & \rho \le a, \\ DK_m(q\rho)\exp(im\phi)\exp(i\beta z); & \rho > a. \end{cases}$$

$$p^2 = n_1^2 k_0^2 - \beta^2, \quad q^2 = \beta^2 - n_2^2 k_0^2.$$

- Other components can be written in terms of E_z and H_z:

$$E_\rho = \frac{i}{p^2}\left(\beta\frac{\partial E_z}{\partial\rho} + \mu_0\frac{\omega}{\rho}\frac{\partial H_z}{\partial\phi}\right), \qquad E_\phi = \frac{i}{p^2}\left(\frac{\beta}{\rho}\frac{\partial E_z}{\partial\phi} - \mu_0\omega\frac{\partial H_z}{\partial\rho}\right),$$

$$H_\rho = \frac{i}{p^2}\left(\beta\frac{\partial H_z}{\partial\rho} - \varepsilon_0 n^2\frac{\omega}{\rho}\frac{\partial E_z}{\partial\phi}\right), \qquad H_\phi = \frac{i}{p^2}\left(\frac{\beta}{\rho}\frac{\partial H_z}{\partial\phi} + \varepsilon_0 n^2\omega\frac{\partial E_z}{\partial\rho}\right).$$

Eigenvalue Equation

- Boundary conditions: E_z, H_z, E_ϕ, and H_ϕ should be continuous across the *core–cladding interface*.

- Continuity of E_z and H_z at $\rho = a$ leads to
  $AJ_m(pa) = CK_m(qa), \quad BJ_m(pa) = DK_m(qa).$

- Continuity of E_ϕ and H_ϕ provides two more equations.

- Four equations lead to the eigenvalue equation

$$\left[\frac{J_m'(pa)}{pJ_m(pa)} + \frac{K_m'(qa)}{qK_m(qa)}\right]\left[\frac{J_m'(pa)}{pJ_m(pa)} + \frac{n_2^2}{n_1^2}\frac{K_m'(qa)}{qK_m(qa)}\right]$$

$$= \frac{m^2}{a^2}\left(\frac{1}{p^2} + \frac{1}{q^2}\right)\left(\frac{1}{p^2} + \frac{n_2^2}{n_1^2}\frac{1}{q^2}\right)$$

$$p^2 = n_1^2 k_0^2 - \beta^2, \quad q^2 = \beta^2 - n_2^2 k_0^2.$$

Eigenvalue Equation

- Eigenvalue equation involves Bessel functions and their derivatives. It needs to be solved numerically.
- Noting that $p^2 + q^2 = (n_1^2 - n_2^2)k_0^2$, we introduce the dimensionless V parameter as

$$V = k_0 a \sqrt{n_1^2 - n_2^2}.$$

- Multiple solutions for β for a given value of V.
- Each solution represents an optical mode.
- Number of modes increases rapidly with V parameter.
- Effective mode index $\bar{n} = \beta / k_0$ lies between n_1 and n_2 for all bound modes.

Effective Mode Index

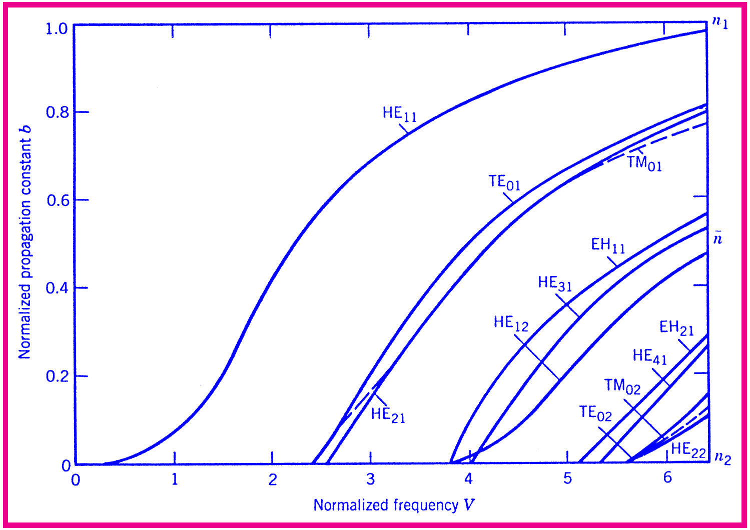

- Useful to introduce a normalized quantity

$$b = (\bar{n} - n_2)/(n_1 - n_2), \quad (0 < b < 1).$$

- Modes quantified through $\beta(\omega)$ or $b(V)$.

Classification of Fiber Modes

- In general, both E_z and H_z are nonzero (hybrid modes).
- Multiple solutions occur for each value of m.
- Modes denoted by HE_{mn} or EH_{mn} ($n = 1, 2, \ldots$) depending on whether H_z or E_z dominates.
- TE and TM modes exist for $m = 0$ (called TE_{0n} and TM_{0n}).
- Setting $m = 0$ in the eigenvalue equation, we obtain two equations

$$\left[\frac{J_m'(pa)}{pJ_m(pa)} + \frac{K_m'(qa)}{qK_m(qa)}\right] = 0, \qquad \left[\frac{J_m'(pa)}{pJ_m(pa)} + \frac{n_2^2}{n_1^2}\frac{K_m'(qa)}{qK_m(qa)}\right] = 0$$

- These equations govern TE_{0n} and TM_{0n} modes of fiber.

Linearly Polarized Modes

- Eigenvalue equation simplified considerably for weakly guiding fibers ($n_1 - n_2 \ll 1$):

$$\left[\frac{J_m'(pa)}{pJ_m(pa)} + \frac{K_m'(qa)}{qK_m(qa)}\right]^2 = \frac{m^2}{a^2}\left(\frac{1}{p^2} + \frac{1}{q^2}\right)^2.$$

- Using properties of Bessel functions, the eigenvalue equation can be written in the following compact form:

$$p\frac{J_{l-1}(pa)}{J_l(pa)} = -q\frac{K_{l-1}(qa)}{K_l(qa)},$$

  where $l = 1$ for TE and TM modes, $l = m - 1$ for HE modes, and $l = m + 1$ for EH modes.

- $\text{TE}_{0,n}$ and $\text{TM}_{0,n}$ modes are degenerate. Also, $\text{HE}_{m+1,n}$ and $\text{EH}_{m-1,n}$ are degenerate in this approximation.

Back
Close

Linearly Polarized Modes

- Degenerate modes travel at the same velocity through fiber.
- Any linear combination of degenerate modes will travel without change in shape.
- Certain linearly polarized combinations produce LP_{mn} modes.
  - ⋆ LP_{0n} is composed of of HE_{1n}.
  - ⋆ LP_{1n} is composed of $\mathrm{TE}_{0n} + \mathrm{TM}_{0n} + \mathrm{HE}_{2n}$.
  - ⋆ LP_{mn} is composed of $\mathrm{HE}_{m+1,n} + \mathrm{EH}_{m-1,n}$.
- Historically, LP modes were obtained first using a simplified analysis of fiber modes.

Fundamental Fiber Mode

- A mode ceases to exist when $q = 0$ (no decay in the cladding).
- TE_{01} and TM_{01} reach cutoff when $J_0(V) = 0$.
- This follows from their eigenvalue equation

$$p\frac{J_0(pa)}{J_1(pa)} = -q\frac{K_0(qa)}{K_1(qa)}$$

after setting $q = 0$ and $pa = V$.

- Single-mode fibers require $V < 2.405$ (first zero of J_0).
- They transport light through the fundamental HE_{11} mode.
- This mode is almost linearly polarized ($|E_z|^2 \ll |E_x|^2$)

$$E_x(\rho,\phi,z) = \begin{cases} A[J_0(p\rho)/J_0(pa)]e^{i\beta z}\,; & \rho \le a, \\ A[K_0(q\rho)/K_0(qa)]e^{i\beta z}; & \rho > a. \end{cases}$$

Fundamental Fiber Mode

- Use of Bessel functions is not always practical.
- It is possible to approximate spatial distribution of HE_{11} mode with a Gaussian for V in the range 1 to 2.5.
- $E_x(\rho, \phi, z) \approx A \exp(-\rho^2/w^2) e^{i\beta z}$.
- Spot size w depends on V parameter.

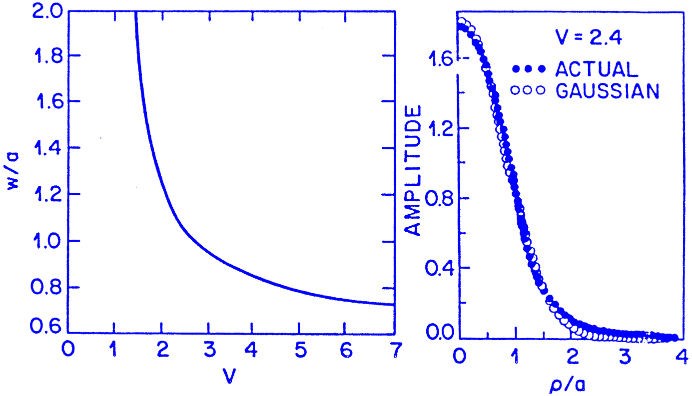

(a) (b)

Single-Mode Properties

- Spot size: $w/a \approx 0.65 + 1.619V^{-3/2} + 2.879V^{-6}$.
- Mode index:

$$\bar{n} = n_2 + b(n_1 - n_2) \approx n_2(1 + b\Delta),$$

$$b(V) \approx (1.1428 - 0.9960/V)^2.$$

- Confinement factor:

$$\Gamma = \frac{P_{\text{core}}}{P_{\text{total}}} = \frac{\int_0^a |E_x|^2 \rho \, d\rho}{\int_0^\infty |E_x|^2 \rho \, d\rho} = 1 - \exp\left(-\frac{2a^2}{w^2}\right).$$

- $\Gamma \approx 0.8$ for $V = 2$ but drops to 0.2 for $V = 1$.
- Mode properties completely specified if V parameter is known.

Fiber Birefringence

- Real fibers exhibit some birefringence $(\bar{n}_x \neq \bar{n}_y)$.
- Modal birefringence quite small $(B_m = |\bar{n}_x - \bar{n}_y| \sim 10^{-6})$.
- Beat length: $L_B = \lambda / B_m$.
- State of polarization evolves periodically.
- Birefringence varies randomly along fiber length (PMD) because of stress and core-size variations.

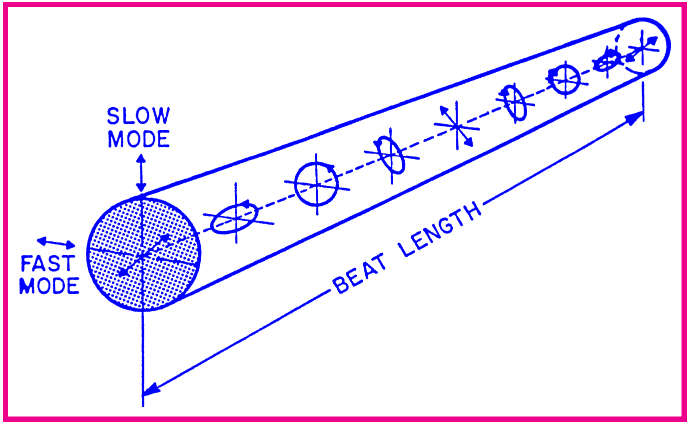

Fiber Losses

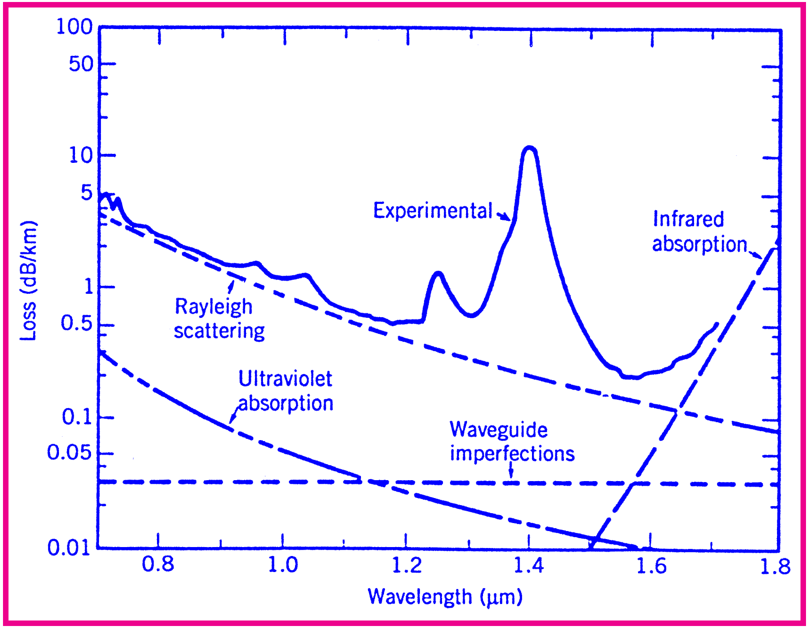

Definition: $P_{\text{out}} = P_{\text{in}} \exp(-\alpha L)$, $\quad \alpha$ (dB/km) $= 4.343\alpha$.

- Material absorption (silica, impurities, dopants)
- Rayleigh scattering (varies as λ^{-4})

Losses of Plastic Fibers

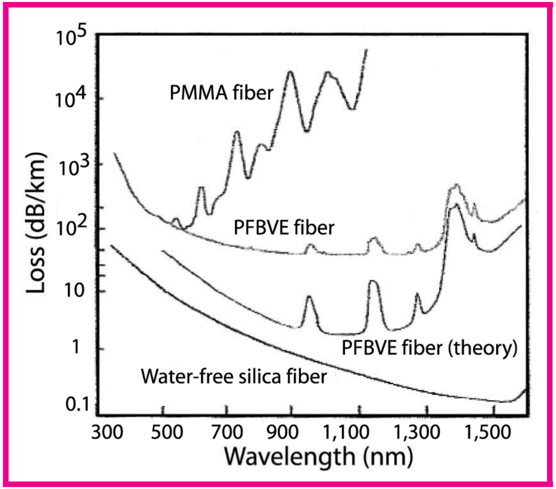

- Large absorption losses of plastics result from vibrational modes of molecular bonds (C—C, C—O, C—H, and O—H).
- Transition-metal impurities (Fe, Co, Ni, Mn, and Cr) absorb strongly in the range 0.6–1.6 μm.
- Residual water vapors produce strong peak near 1390 nm.

Fiber Dispersion

- Origin: Frequency dependence of the mode index $n(\omega)$:

$$\beta(\omega) = \bar{n}(\omega)\omega/c = \beta_0 + \beta_1(\omega - \omega_0) + \beta_2(\omega - \omega_0)^2 + \cdots,$$

where ω_0 is the carrier frequency of optical pulse.

- *Transit time* for a fiber of length L: $T = L/v_g = \beta_1 L.$

- Different frequency components travel at different speeds and arrive at different times at output end (pulse broadening).

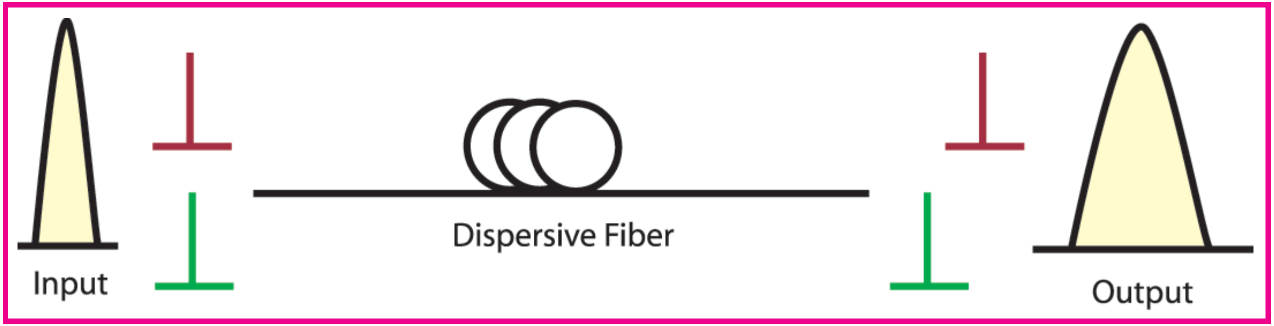

Fiber Dispersion (continued)

- Pulse broadening governed by group-velocity dispersion:

$$\Delta T = \frac{dT}{d\omega}\Delta\omega = \frac{d}{d\omega}\frac{L}{v_g}\Delta\omega = L\frac{d\beta_1}{d\omega}\Delta\omega = L\beta_2\Delta\omega,$$

where $\Delta\omega$ is pulse bandwidth and L is fiber length.

- GVD parameter: $\beta_2 = \left(\frac{d^2\beta}{d\omega^2}\right)_{\omega=\omega_0}$.

- Alternate definition: $D = \frac{d}{d\lambda}\left(\frac{1}{v_g}\right) = -\frac{2\pi c}{\lambda^2}\beta_2$.

- Limitation on the bit rate: $\Delta T < T_B = 1/B$, or

$$B(\Delta T) = BL\beta_2\Delta\omega \equiv BLD\Delta\lambda < 1.$$

Material Dispersion

- Refractive index of of any material is frequency dependent.
- Material dispersion governed by the Sellmeier equation

$$n^2(\omega) = 1 + \sum_{j=1}^{M} \frac{B_j \omega_j^2}{\omega_j^2 - \omega^2}.$$

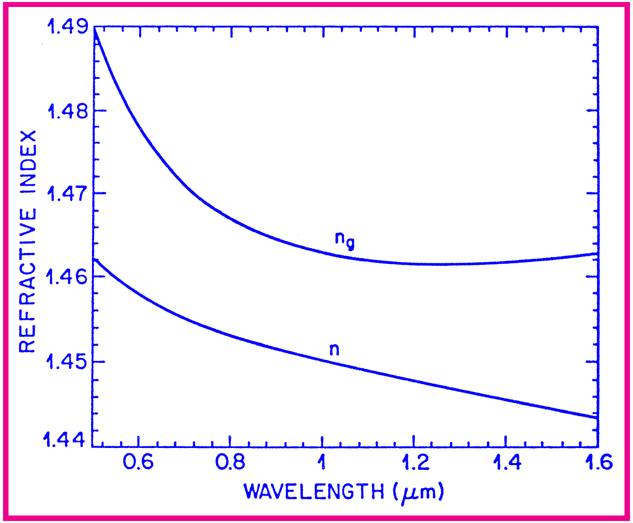

Waveguide Dispersion

- Mode index $\bar{n}(\omega) = n_1(\omega) - \delta n_W(\omega)$.
- Material dispersion D_M results from $n_1(\omega)$ (index of silica).
- Waveguide dispersion D_W results from $\delta n_W(\omega)$ and depends on core size and dopant distribution.
- Total dispersion $D = D_M + D_W$ can be controlled.

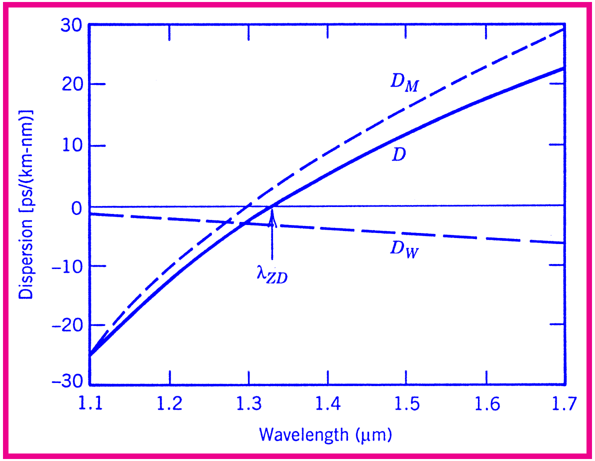

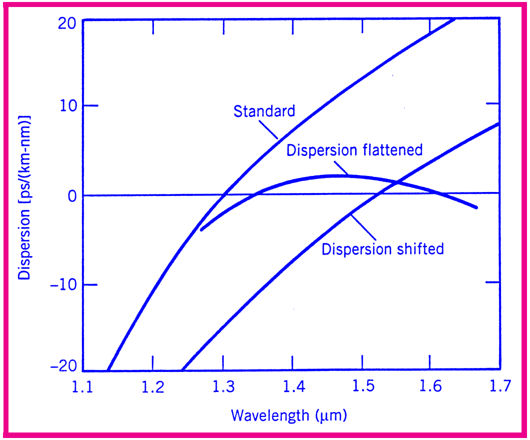

The Institute of OPTICS

UNIVERSITY of ROCHESTER

Dispersion in Microstructure Fibers

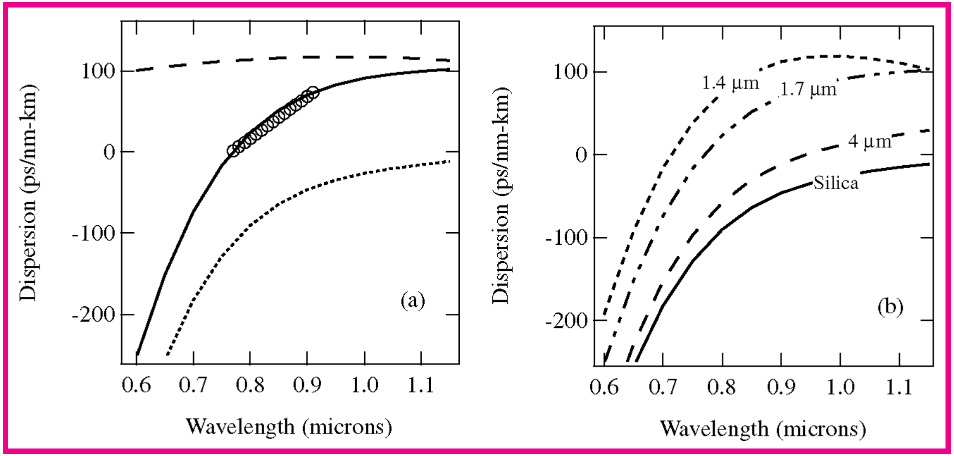

- Air holes in cladding and a small core diameter help to shift ZDWL in the region near 800 nm.
- Waveguide dispersion D_W is very large in such fibers.
- Useful for supercontinuum generation using mode-locking pulses from a Ti:sapphire laser.

Higher-Order Dispersion

- Dispersive effects do not disappear at $\lambda = \lambda_{\text{ZD}}$.
- D cannot be made zero at all frequencies within the pulse spectrum.
- Higher-order dispersive effects are governed by the dispersion slope $S = dD/d\lambda$.
- S can be related to third-order dispersion β_3 as

$$S = (2\pi c/\lambda^2)^2 \beta_3 + (4\pi c/\lambda^3)\beta_2.$$

- At $\lambda = \lambda_{\text{ZD}}$, $\beta_2 = 0$, and S is proportional to β_3.

Commercial Fibers

Fiber Type and Trade Name	$A_{\rm eff}$ (μm^2)	$\lambda_{\rm ZD}$ (nm)	D (C band) ps/(km-nm)	Slope S ps/(km-nm^2)
Corning SMF-28	80	1302–1322	16 to 19	0.090
Lucent AllWave	80	1300–1322	17 to 20	0.088
Alcatel ColorLock	80	1300–1320	16 to 19	0.090
Corning Vascade	101	1300–1310	18 to 20	0.060
TrueWave-RS	50	1470–1490	2.6 to 6	0.050
Corning LEAF	72	1490–1500	2 to 6	0.060
TrueWave-XL	72	1570–1580	-1.4 to -4.6	0.112
Alcatel TeraLight	65	1440–1450	5.5 to 10	0.058

The Institute of OPTICS

UNIVERSITY of ROCHESTER

Polarization-Mode Dispersion

- Real fibers exhibit some birefringence ($\bar{n}_x \neq \bar{n}_y$).
- Orthogonally polarized components of a pulse travel at different speeds. The relative delay is given by

$$\Delta T = \left| \frac{L}{v_{gx}} - \frac{L}{v_{gy}} \right| = L|\beta_{1x} - \beta_{1y}| = L(\Delta\beta_1).$$

- Birefringence varies randomly along fiber length (PMD) because of stress and core-size variations.
- RMS Pulse broadening:

$$\sigma_T \approx (\Delta\beta_1)\sqrt{2l_c L} \equiv D_p\sqrt{L}.$$

- PMD parameter $D_p \sim$ 0.01–10 ps/$\sqrt{\text{km}}$
- PMD can degrade the system performance considerably (especially for old fibers).

Back
Close

Pulse Propagation Equation

- Optical Field at frequency ω at $z = 0$:

$$\tilde{\mathbf{E}}(\mathbf{r}, \omega) = \hat{\mathbf{x}} F(x, y) \tilde{B}(0, \omega) \exp(i\beta z).$$

- Optical field at a distance z:

$$\tilde{B}(z, \omega) = \tilde{B}(0, \omega) \exp(i\beta z).$$

- Expand $\beta(\omega)$ is a Taylor series around ω_0:

$$\beta(\omega) = \bar{n}(\omega)\frac{\omega}{c} \approx \beta_0 + \beta_1(\Delta\omega) + \frac{\beta_2}{2}(\Delta\omega)^2 + \frac{\beta_3}{6}(\Delta\omega)^3.$$

- Introduce Pulse envelope:

$$B(z, t) = A(z, t) \exp[i(\beta_0 z - \omega_0 t)].$$

Back
Close

Pulse Propagation Equation

- Pulse envelope is obtained using

$$A(z,t) = \frac{1}{2\pi}\int_{-\infty}^{\infty} d(\Delta\omega)\tilde{A}(0,\Delta\omega)\exp\left[i\beta_1 z\Delta\omega + \frac{i}{2}\beta_2 z(\Delta\omega)^2 + \frac{i}{6}\beta_3 z(\Delta\omega)^3 - i(\Delta\omega)t\right].$$

- Calculate $\partial A/\partial z$ and convert to time domain by replacing $\Delta\omega$ with $i(\partial A/\partial t)$.

- Final equation:

$$\frac{\partial A}{\partial z} + \beta_1\frac{\partial A}{\partial t} + \frac{i\beta_2}{2}\frac{\partial^2 A}{\partial t^2} - \frac{\beta_3}{6}\frac{\partial^3 A}{\partial t^3} = 0.$$

- With the transformation $t' = t - \beta_1 z$ and $z' = z$, it reduces to

$$\frac{\partial A}{\partial z'} + \frac{i\beta_2}{2}\frac{\partial^2 A}{\partial t'^2} - \frac{\beta_3}{6}\frac{\partial^3 A}{\partial t'^3} = 0.$$

Pulse Propagation Equation

- If we neglect third-order dispersion, pulse evolution is governed by

$$\frac{\partial A}{\partial z} + \frac{i\beta_2}{2}\frac{\partial^2 A}{\partial t^2} = 0.$$

- Compare with the paraxial equation governing diffraction:

$$2ik\frac{\partial A}{\partial z} + \frac{\partial^2 A}{\partial x^2} = 0.$$

- Slit-diffraction problem identical to pulse propagation problem.
- The only difference is that β_2 can be positive or negative.
- Many results from diffraction theory can be used for pulses.
- A Gaussian pulse should spread but remain Gaussian in shape.

Major Nonlinear Effects

- Self-Phase Modulation (SPM)
- Cross-Phase Modulation (XPM)
- Four-Wave Mixing (FWM)
- Stimulated Brillouin Scattering (SBS)
- Stimulated Raman Scattering (SRS)

Origin of Nonlinear Effects in Optical Fibers

- Third-order nonlinear susceptibility $\chi^{(3)}$.
- Real part leads to SPM, XPM, and FWM.
- Imaginary part leads to SBS and SRS.

Self-Phase Modulation (SPM)

- Refractive index depends on intensity as

$$n'_j = n_j + \bar{n}_2 I(t).$$

- $\bar{n}_2 = 2.6 \times 10^{-20}$ m^2/W for silica fibers.
- Propagation constant: $\beta' = \beta + k_0 \bar{n}_2 P/A_{\text{eff}} \equiv \beta + \gamma P$.
- Nonlinear parameter: $\gamma = 2\pi \bar{n}_2/(A_{\text{eff}}\lambda)$.
- Nonlinear Phase shift:

$$\phi_{\text{NL}} = \int_0^L (\beta' - \beta)\, dz = \int_0^L \gamma P(z)\, dz = \gamma P_{\text{in}} L_{\text{eff}}.$$

- Optical field modifies its own phase (SPM).
- Phase shift varies with time for pulses (chirping).

SPM-Induced Chirp

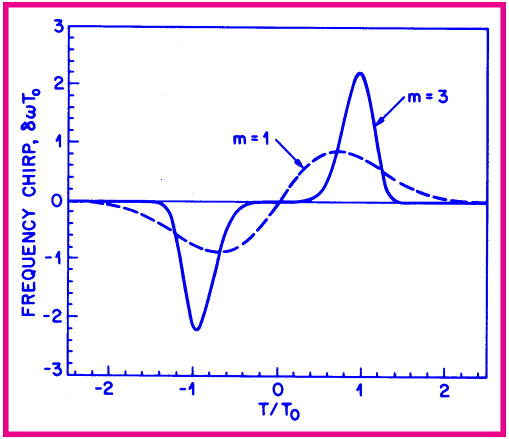

- SPM-induced chirp depends on the pulse shape.
- Gaussian pulses ($m = 1$): Nearly linear chirp across the pulse.
- Super-Gaussian pulses ($m = 1$): Chirping only near pulse edges.
- SPM broadens spectrum of unchirped pulses; spectral narrowing possible in the case of chirped pulses.

Nonlinear Schrödinger Equation

- Nonlinear effects can be included by adding a nonlinear term to the equation used earlier for dispersive effects.
- This equation is known as the Nonlinear Schrödinger Equation:

$$\frac{\partial A}{\partial z} + \frac{i\beta_2}{2}\frac{\partial^2 A}{\partial t^2} = i\gamma|A|^2 A.$$

- Nonlinear parameter: $\gamma = 2\pi\bar{n}_2/(A_{\rm eff}\lambda)$.
- Fibers with large $A_{\rm eff}$ help through reduced γ.
- Known as large effective-area fiber or LEAF.
- Nonlinear effects leads to formation of optical solitons.

Cross-Phase Modulation (XPM)

- Refractive index seen by one wave depends on the intensity of other copropagating channels.

$$E(\mathbf{r},t) = A_a(z,t)F_a(x,y)\exp(i\beta_{0a}z - i\omega_a t)$$

$$+A_b(z,t)F_b(x,y)\exp(i\beta_{0b}z - i\omega_b t)],$$

- Propagation constants are found to be modified as

$$\beta_a' = \beta_a + \gamma_a(|A_a|^2 + 2|A_b|^2), \qquad \beta_b' = \beta_b + \gamma_b(|A_b|^2 + 2|A_a|^2).$$

- Nonlinear phase shifts produced become

$$\phi_a^{\rm NL} = \gamma_a L_{\rm eff}(P_a + 2P_b), \qquad \phi_b^{\rm NL} = \gamma_b L_{\rm eff}(P_b + 2P_a).$$

- The second term is due to XPM.

The Institute of OPTICS — UNIVERSITY of ROCHESTER

Impact of XPM

- In the case of a WDM system, total nonlinear phase shift is

$$\phi_j^{\mathrm{NL}} = \gamma L_{\mathrm{eff}} \left(P_j + 2 \sum_{m \neq j} P_m \right).$$

- Phase shift varies from bit to bit depending on the bit pattern in neighboring channels.
- It leads to interchannel crosstalk and affects system performance considerably.
- XPM is also beneficial for applications such as optical switching, wavelength conversion, etc.
- Mathematically, XPM effects are governed by two coupled NLS equations.

Four-Wave Mixing

- FWM converts two photons from one or two pump beams into two new frequency-shifted photons.
- Energy conservation: $\omega_1 + \omega_2 = \omega_3 + \omega_4$.
- Degenerate FWM: $2\omega_1 = \omega_3 + \omega_4$.
- Momentum conservation or phase matching is required.
- FWM efficiency governed by phase mismatch:

$$\Delta = \beta(\omega_3) + \beta(\omega_4) - \beta(\omega_1) - \beta(\omega_2).$$

- In the degenerate case $(\omega_1 = \omega_2)$, $\omega_3 = \omega_1 + \Omega$, and $\omega_4 = \omega_1 - \Omega$.
- Expanding β in a Taylor series, $\Delta = \beta_2 \Omega^2$.
- FWM becomes important for WDM systems designed with low-dispersion fibers.

FWM: Good or Bad?

- FWM leads to interchannel crosstalk in WDM systems.
- It can be avoided through dispersion management.

On the other hand . . .
FWM can be used beneficially for

- Parametric amplification
- Optical phase conjugation
- Demultiplexing of OTDM channels
- Wavelength conversion of WDM channels
- Supercontinuum generation

Brillouin Scattering

- Scattering of light from acoustic waves (electrostriction).
- Energy and momentum conservation laws require $\Omega_B = \omega_p - \omega_s$ and $\mathbf{k}_A = \mathbf{k}_p - \mathbf{k}_s$.
- Brillouin shift: $\Omega_B = |k_A| v_A = 2v_A |k_p| \sin(\theta/2)$.
- Only possibility: $\theta = \pi$ for single-mode fibers (backward propagating Stokes wave).
- Using $k_p = 2\pi\bar{n}/\lambda_p$, $\nu_B = \Omega_B/2\pi = 2\bar{n}v_A/\lambda_p$.
- With $v_A = 5.96$ km/s and $\bar{n} = 1.45$, $\nu_B \approx 11$ GHz near 1.55 μm.
- Stokes wave grows from noise.
- Not a very efficient process at low pump powers.

Stimulated Brillouin Scattering

- Becomes a stimulated process at high input power levels.
- Governed by two coupled equations:

$$\frac{dI_p}{dz} = -g_B I_p I_s - \alpha_p I_p, \qquad -\frac{dI_s}{dz} = +g_B I_p I_s - \alpha_s I_s.$$

- Brillouin gain has a narrow Lorentzian spectrum ($\Delta\nu \sim 20$ MHz).

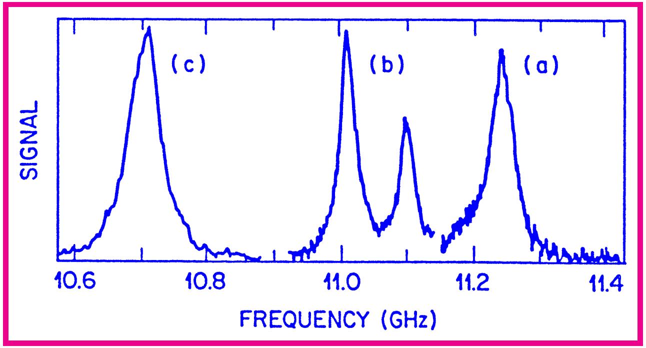

SBS Threshold

- Threshold condition: $g_B P_{\text{th}} L_{\text{eff}} / A_{\text{eff}} \approx 21$.
- Effective fiber length: $L_{\text{eff}} = [1 - \exp(-\alpha L)]/\alpha$.
- Effective core area: $A_{\text{eff}} \approx$ 50–80 μm^2.
- Peak Brillouin gain: $g_B \approx 5 \times 10^{-11}$ m/W.
- Low threshold power for long fibers ($\sim$5 mW).
- Most of the power reflected backward after the SBS threshold.

Threshold can be increased using

- Phase modulation at frequencies >0.1 GHz.
- Sinusoidal strain along the fiber.
- Nonuniform core radius or dopant density.

Back
Close

Stimulated Raman Scattering

- Scattering of light from vibrating molecules.
- Scattered light shifted in frequency.
- Raman gain spectrum extends over 40 THz.
- Raman shift at Gain peak: $\Omega_R = \omega_p - \omega_s \sim 13$ THz).

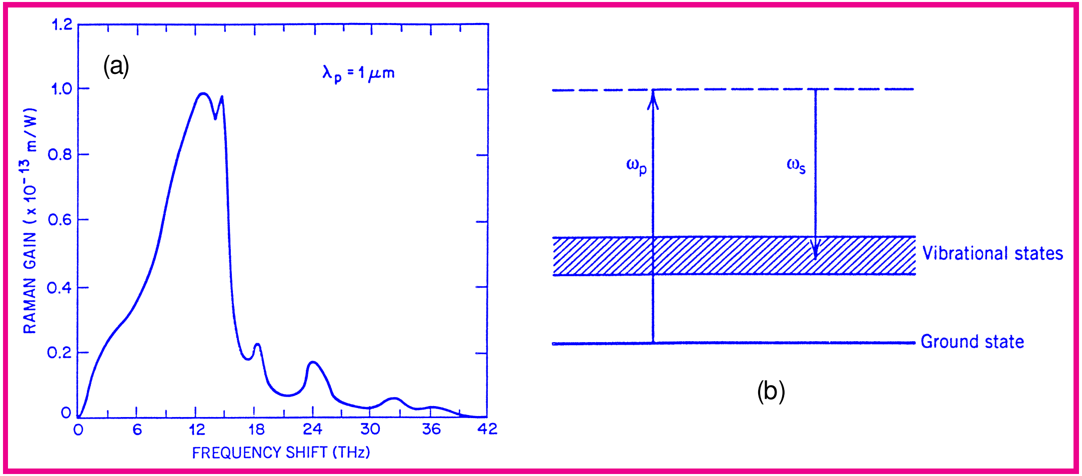

Back

Close

The Institute of OPTICS

UNIVERSITY of ROCHESTER

SRS Threshold

- SRS governed by two coupled equations:

$$\frac{dI_p}{dz} = -g_R I_p I_s - \alpha_p I_p$$

$$\frac{dI_s}{dz} = g_R I_p I_s - \alpha_s I_s.$$

- Threshold condition: $g_R P_{\text{th}} L_{\text{eff}}/A_{\text{eff}} \approx 16$.
- Peak Raman gain: $g_R \approx 6 \times 10^{-14}$ m/W near 1.5 μm.
- Threshold power relatively large ($\sim$ 0.6 W).
- SRS is not of concern for single-channel systems.
- Leads to interchannel crosstalk in WDM systems.

Fiber Components

- Fibers can be used to make many optical components.
- Passive components
  - ⋆ Directional Couplers
  - ⋆ Fiber Gratings
  - ⋆ Fiber Interferometers
  - ⋆ Isolators and Circulators
- Active components
  - ⋆ Doped-Fiber Amplifiers
  - ⋆ Raman and Parametric Amplifiers
  - ⋆ CW and mode-locked Fiber Lasers

Directional Couplers

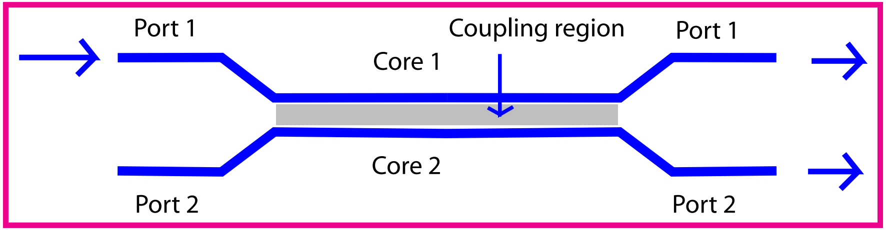

- Four-port devices (two input and two output ports).
- Output can be split in two different directions; hence the name *directional couplers*.
- Can be fabricated using fibers or planar waveguides.
- Two waveguides are identical in symmetric couplers.
- Evanescent coupling of modes in two closely spaced waveguides.
- Overlapping of modes in the central region leads to power transfer.

Theory of Directional Couplers

- Coupled-mode theory commonly used for couplers.
- Begin with the Helmholtz equation $\nabla^2\tilde{\mathbf{E}} + \tilde{n}^2 k_0^2 \tilde{\mathbf{E}} = 0$.
- $\tilde{n}(x,y) = n_0$ everywhere except in the region occupied by two cores.
- Approximate solution:

$$\tilde{\mathbf{E}}(\mathbf{r},\omega) \approx \hat{e}[\tilde{A}_1(z,\omega)F_1(x,y) + \tilde{A}_2(z,\omega)F_2(x,y)]e^{i\beta z}.$$

- $F_m(x,y)$ corresponds to the mode supported by the each waveguide:

$$\frac{\partial^2 F_m}{\partial x^2} + \frac{\partial^2 F_m}{\partial y^2} + [n_m^2(x,y)k_0^2 - \bar{\beta}_m^2]F_m = 0.$$

- A_1 and A_2 vary with z because of the mode overlap.

Coupled-Mode Equations

- Coupled-mode theory deals with amplitudes A_1 and A_2.
- We substitute assumed solution in Helmholtz equation, multiply by F_1^* or F_2^*, and integrate over x–y plane to obtain

$$\frac{d\tilde{A}_1}{dz} = i(\bar{\beta}_1 - \beta)\tilde{A}_1 + i\kappa_{12}\tilde{A}_2,$$
$$\frac{d\tilde{A}_2}{dz} = i(\bar{\beta}_2 - \beta)\tilde{A}_2 + i\kappa_{21}\tilde{A}_1,$$

- Coupling coefficient is defined as

$$\kappa_{mp} = \frac{k_0^2}{2\beta}\int\int_{-\infty}^{\infty}(\tilde{n}^2 - n_p^2)F_m^* F_p \, dx\, dy,$$

- Modes are normalized such that $\int\int_{-\infty}^{\infty} |F_m(x,y)|^2 \, dx\, dy = 1$.

Time-Domain Coupled-Mode Equations

- Expand $\bar{\beta}_m(\omega)$ in a Taylor series around the carrier frequency ω_0 as

$$\bar{\beta}_m(\omega) = \beta_{0m} + (\omega - \omega_0)\beta_{1m} + \tfrac{1}{2}(\omega - \omega_0)^2\beta_{2m} + \cdots,$$

- Replace $\omega - \omega_0$ by $i(\partial/\partial t)$ while taking inverse Fourier transform

$$\begin{aligned}
\frac{\partial A_1}{\partial z} + \frac{1}{v_{g1}}\frac{\partial A_1}{\partial t} + \frac{i\beta_{21}}{2}\frac{\partial^2 A_1}{\partial t^2} &= i\kappa_{12}A_2 + i\delta_a A_1, \\
\frac{\partial A_2}{\partial z} + \frac{1}{v_{g2}}\frac{\partial A_2}{\partial t} + \frac{i\beta_{22}}{2}\frac{\partial^2 A_2}{\partial t^2} &= i\kappa_{21}A_1 - i\delta_a A_2,
\end{aligned}$$

where $v_{gm} \equiv 1/\beta_{1m}$ and

$$\delta_a = \tfrac{1}{2}(\beta_{01} - \beta_{02}), \qquad \beta = \tfrac{1}{2}(\beta_{01} + \beta_{02}).$$

- For a symmetric coupler, $\delta_a = 0$ and $\kappa_{12} = \kappa_{21} \equiv \kappa$.

Back
Close

Power-Transfer Characteristics

- Consider first the simplest case of a CW beam incident on one of the input ports of a coupler.

- Setting time-dependent terms to zero we obtain

$$\frac{dA_1}{dz} = i\kappa_{12}A_2 + i\delta_a A_1, \qquad \frac{dA_2}{dz} = i\kappa_{21}A_1 - i\delta_a A_2.$$

- Eliminating dA_2/dz, we obtain a simple equation for A_1:

$$\frac{d^2A_1}{dz^2} + \kappa_e^2 A_1 = 0, \qquad \kappa_e = \sqrt{\kappa^2 + \delta_a^2} \quad (\kappa = \sqrt{\kappa_{12}\kappa_{21}}).$$

- General solution when $A_1(0) = A_0$ and $A_2(0) = 0$:

$$\begin{aligned} A_1(z) &= A_0[\cos(\kappa_e z) + i(\delta_a/\kappa_e)\sin(\kappa_e z)], \\ A_2(z) &= A_0(i\kappa_{21}/\kappa_e)\sin(\kappa_e z). \end{aligned}$$

Power-Transfer Characteristics

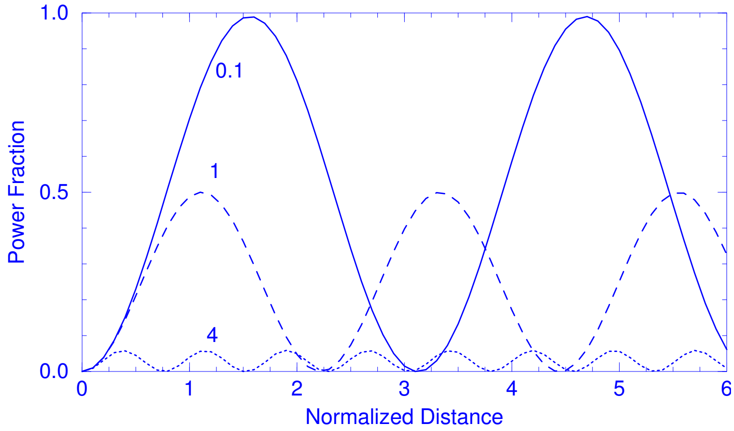

- Even though $A_2 = 0$ at $z = 0$, some power is transferred to the second core as light propagates inside a coupler.
- Power transfer follows a periodic pattern.
- Maximum power transfer occurs for $\kappa_e z = m\pi/2$.
- Coupling length is defined as $L_c = \pi/(2\kappa_e)$.

Symmetric Coupler

- Maximum power transfer occurs for a symmetric coupler $(\delta_a = 0)$
- General solution for a symmetric coupler of length L:

$$\begin{aligned} A_1(L) &= A_1(0)\cos(\kappa L) + iA_2(0)\sin(\kappa L) \\ A_2(L) &= iA_1(0)\sin(\kappa L) + A_2(0)\cos(\kappa L) \end{aligned}$$

- This solution can be written in a matrix form as

$$\begin{pmatrix} A_1(L) \\ A_2(L) \end{pmatrix} = \begin{pmatrix} \cos(\kappa L) & i\sin(\kappa L) \\ i\sin(\kappa L) & \cos(\kappa L) \end{pmatrix} \begin{pmatrix} A_1(0) \\ A_2(0) \end{pmatrix}.$$

- When $A_2(0) = 0$ (only one beam injected), output fields become

$$A_1(L) = A_1(0)\cos(\kappa L), \qquad A_2(L) = iA_2(0)\sin(\kappa L)$$

- A coupler acts as a beam splitter; notice 90° phase shift for the cross port.

Transfer Matrix of a Coupler

- Concept of a transfer matrix useful for couplers because a single matrix governs all its properties.
- Introduce $\rho = P_1(L)/P_0 = \cos^2(\kappa L)$ as a fraction of input power P_0 remaining in the same port of coupler.
- Transfer matrix can then be written as

$$T_c = \begin{pmatrix} \sqrt{\rho} & i\sqrt{1-\rho} \\ i\sqrt{1-\rho} & \sqrt{\rho} \end{pmatrix}.$$

- This matrix is symmetric to ensure that the coupler behaves the same way if direction of light propagation is reversed.
- The 90° phase shift important for many applications.

Applications of Directional Couplers

- Simplest application of a fiber coupler is as an optical tap.
- If ρ is close to 1, a small fraction of input power is transferred to the other core.
- Another application consists of dividing input power equally between the two output ports ($\rho = \frac{1}{2}$).
- Coupler length L is chosen such that $\kappa L = \pi/4$ or $L = L_c/2$. Such couplers are referred to as 3-dB couplers.
- Couplers with $L = L_c$ transfer all input power to the cross port.
- By choosing coupler length appropriately, power can be divided between two output ports in an arbitrary manner.

Coupling Coefficient

- Length of a coupler required depends on κ.
- Value of κ depends on the spacing d between two cores.
- For a symmetric coupler, κ can be approximated as

$$\kappa = \frac{\pi V}{2k_0 n_1 a^2} \exp[-(c_0 + c_1 \bar{d} + c_2 \bar{d}^2)] \quad (\bar{d} = d/a).$$

- Constants c_0, c_1, and c_2 depend only on V.
- Accurate to within 1% for values of V and $\bar{d}$ in the range $1.5 \leq V \leq 2.5$ and $2 \leq \bar{d} \leq 4.5$.
- As an example, $\kappa \sim 1$ cm^{-1} for $\bar{d} = 3$ but it reduces to 0.01 cm^{-1} when $\bar{d}$ exceeds 5.

Supermodes of a Coupler

- Are there launch conditions for which no power transfer occurs?
- Under what conditions $\tilde{A}_1$ and $\tilde{A}_2$ become z-independent?

$$\frac{d\tilde{A}_1}{dz} = i(\bar{\beta}_1 - \beta)\tilde{A}_1 + i\kappa_{12}\tilde{A}_2,$$
$$\frac{d\tilde{A}_2}{dz} = i(\bar{\beta}_2 - \beta)\tilde{A}_2 + i\kappa_{21}\tilde{A}_1,$$

- This can occur when the ratio $f = \tilde{A}_2(0)/\tilde{A}_1(0)$ satisfies

$$f = \frac{\beta - \bar{\beta}_1}{\kappa_{12}} = \frac{\kappa_{21}}{\beta - \bar{\beta}_2}.$$

- This equation determines β for supermodes

$$\beta_{\pm} = \tfrac{1}{2}(\bar{\beta}_1 + \bar{\beta}_2) \pm \sqrt{\delta_a^2 + \kappa^2}.$$

Supermodes of a Coupler

- Spatial distribution corresponding to two eigenvalues is given by $F_\pm(x,y) = (1+f_\pm^2)^{-1/2}[F_1(x,y) + f_\pm F_2(x,y)]$.
- These two specific linear combinations of F_1 and F_2 constitute the supermodes of a fiber coupler.
- In the case of a symmetric coupler, $f_\pm = \pm 1$, and supermodes become even and odd combinations of F_1 and F_2.
- When input conditions are such that a supermode is excited, no power transfer occurs between two cores of a coupler.
- When light is incident on one core, both supermodes are excited.
- Two supermodes travel at different speeds and develop a relative phase shift that is responsible for periodic power transfer between two cores.

Effects of Fiber Dispersion

- Coupled-mode equations for a symmetric coupler:

$$
\begin{aligned}
\frac{\partial A_1}{\partial z} + \frac{i\beta_2}{2}\frac{\partial^2 A_1}{\partial T^2} &= i\kappa A_2 \\
\frac{\partial A_2}{\partial z} + \frac{i\beta_2}{2}\frac{\partial^2 A_2}{\partial T^2} &= i\kappa A_1
\end{aligned}
\tag{1}
$$

- GVD effects negligible if coupler length $L \ll L_D = T_0^2/|\beta_2|$.
- GVD has no effect on couplers for which $L_D \gg L_c$.
- L_D exceeds 1 km for $T_0 > 1$ ps but typically $L_c < 10$ m.
- GVD effects important only for ultrashort pulses ($T_0 < 0.1$ ps).
- Picosecond pulses behave in the same way as CW beams.
- Pulse energy transferred to neighboring core periodically.

Dispersion of Coupling Coefficient

- Frequency dependence of κ cannot be ignored in all cases:

$$\kappa(\omega) \approx \kappa_0 + (\omega - \omega_0)\kappa_1 + \tfrac{1}{2}(\omega - \omega_0)^2\kappa_2,$$

- Modified coupled-mode equations become

$$\begin{aligned} \frac{\partial A_1}{\partial z} + \kappa_1 \frac{\partial A_2}{\partial T} + \frac{i\beta_2}{2}\frac{\partial^2 A_1}{\partial T^2} + \frac{i\kappa_2}{2}\frac{\partial^2 A_2}{\partial T^2} &= i\kappa_0 A_2, \\ \frac{\partial A_2}{\partial z} + \kappa_1 \frac{\partial A_1}{\partial T} + \frac{i\beta_2}{2}\frac{\partial^2 A_2}{\partial T^2} + \frac{i\kappa_2}{2}\frac{\partial^2 A_1}{\partial T^2} &= i\kappa_0 A_1. \end{aligned}$$

- Approximate solution when $\beta_2 = 0$ and $\kappa_2 = 0$:

$$\begin{aligned} A_1(z,T) &= \tfrac{1}{2}\left[A_0(T - \kappa_1 z)e^{i\kappa_0 z} + A_0(T + \kappa_1 z)e^{-i\kappa_0 z}\right], \\ A_2(z,T) &= \tfrac{1}{2}\left[A_0(T - \kappa_1 z)e^{i\kappa_0 z} - A_0(T + \kappa_1 z)e^{-i\kappa_0 z}\right], \end{aligned}$$

- Pulse splits into two subpulses after a few coupling lengths.

Fiber Gratings

- Silica fibers exhibit a photosensitive effect.
- Refractive index can be changed permanently when fiber is exposed to UV radiation.
- Photosensitivity was discovered in 1978 by chance.
- Used routinely to make fiber Bragg gratings in which mode index varies in a periodic fashion along fiber length.
- Fiber gratings can be designed to operate over a wide range of wavelengths.
- Most useful in the wavelength region 1.55 μm because of its relevance to fiber-optic communication systems.
- Fiber gratings act as a narrowband optical filter.

Bragg Diffraction

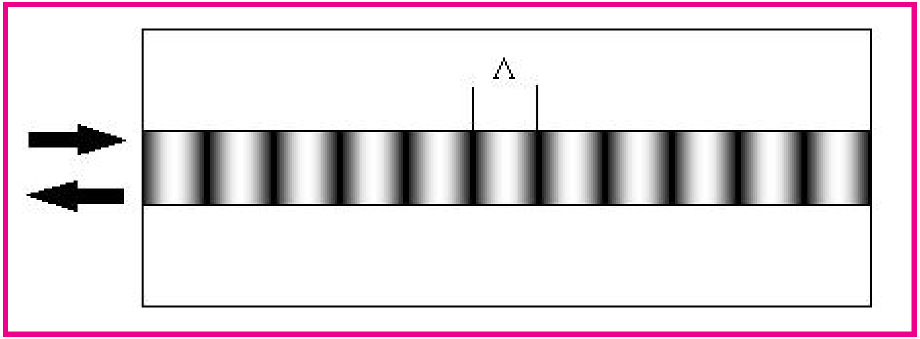

- Bragg diffraction must satisfy the phase-matching condition
  $\mathbf{k}_i - \mathbf{k}_d = m\mathbf{k}_g, \qquad k_g = 2\pi/\Lambda.$
- In single-mode fibers, all three vectors lie along fiber axis.
- Since $\mathbf{k}_d = -\mathbf{k}_i$, diffracted light propagates backward.
- A fiber grating acts as a reflector for a specific wavelength for which $k_g = 2k_i$, or $\lambda = 2\bar{n}\Lambda$.
- This condition is known as the *Bragg condition*.

First Fiber Grating

- In a 1978 experiment, Hill et al. launched blue light from an argon-ion laser into a 1-m-long fiber.
- Reflected power increased with time and became nearly 100%.
- Mechanism behind grating formation was understood much later.
- The 4% reflection occurring at the fiber ends creates a standing-wave pattern.
- Two-photon absorption changes glass structure changes and alters refractive index in a periodic fashion.
- Grating becomes stronger with time because it enhances the visibility of fringe pattern.
- By 1989, a holographic technique was used to form the fringe pattern directly using a 244-nm UV laser.

Photosensitivity of Fibers

- Main Mechanism: Formation of defects in the core of a Ge-doped silica fiber.
- Ge atoms in fiber core leads to formation of oxygen-deficient bonds (Si–Ge, Si–Si, and Ge–Ge bonds).
- Absorption of 244-nm radiation breaks defect bonds.
- Modifications in glass structure change absorption spectrum.
- Refractive index also changes through Kramers–Kronig relation

$$\Delta n(\omega') = \frac{c}{\pi} \int_0^\infty \frac{\Delta\alpha(\omega)\, d\omega}{\omega^2 - \omega'^2}.$$

- Typically, Δn is $\sim 10^{-4}$ near 1.5 μm, but it can exceed 0.001 in fibers with high Ge concentration.

Back
Close

Photosensitivity of Fibers

- Standard telecommunication fibers not suitable for forming Bragg gratings (<3% of Ge atoms results in small index changes.
- Photosensitivity can be enhanced using dopants such as phosphorus, boron, and aluminum.
- $\Delta n > 0.01$ possible by soaking fiber in hydrogen gas at high pressures (200 atm).
- Density of Ge–Si oxygen-deficient bonds increases in hydrogen-soaked fibers.
- Once hydrogenated, fiber needs to be stored at low temperature to maintain its photosensitivity.
- Gratings remain intact over long periods of time.

Fabrication Techniques

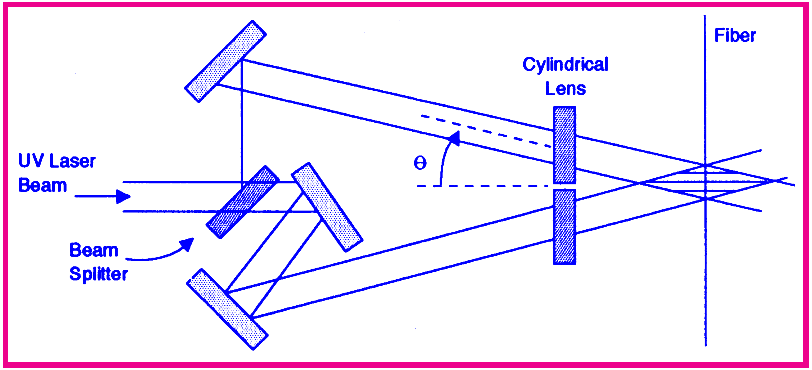

- A dual-beam holographic technique is used commonly.
- Cylindrical lens is used to expand UV beam along fiber length.
- Fringe pattern formed on fiber surface creates an index grating.
- Grating period Λ related to $\lambda_{\rm uv}$ as $\Lambda = \lambda_{\rm uv}/(2\sin\theta)$.
- Λ can be varied over a wide range by changing θ.
- Wavelength reflected by grating is set by $\lambda = 2\bar{n}\Lambda$.

The Institute of OPTICS

UNIVERSITY of ROCHESTER

Fabrication Techniques

- Several variations of the basic technique have been developed.
- Holographic technique requires a UV laser with excellent temporal and spatial coherence.
- Excimer lasers used commonly have relatively poor beam quality.
- It is difficult to maintain fringe pattern over fiber core over a duration of several minutes.
- Fiber gratings can be written using excimer laser pulses.
- Pulse energies required are close to 40 mJ for 20-ns pulses.
- Exposure time reduced considerably, relaxing coherence requirements.

Phase-Mask Technique

- Commercial production makes use of a phase-mask technique.
- Phase mask acts as a master grating that is transferred to the fiber using a suitable method.
- A patterned layer of chromium is deposited on a quartz substrate using electron-beam lithography and reactive ion etching.
- Demands on the temporal and spatial coherence of UV beam are much less stringent when a phase mask is used.
- Even a non-laser source such as a UV lamp can be used.
- Quality of fiber grating depends completely on the master phase mask.

Phase-Mask Interferometer

- Phase mask can also be used to form an interferometer.
- UV laser beam falls normally on the phase mask and is diffracted into several beams through Raman–Nath scattering.
- The zeroth-order is blocked or cancelled with a suitable technique.
- Two first-order diffracted beams interfere on fiber surface and form a fringe pattern.
- Grating period equals one-half of phase mask period.
- This method is tolerant of any beam-pointing instability.
- Relatively long gratings can be made with this technique.
- Use of a single silica block that reflects two beams internally forms a compact interferometer.

Point-by-Point Fabrication

- Grating is fabricated onto a fiber period by period.
- This technique bypasses the need of a master phase mask.
- Short sections ($w < |\Lambda$) of fiber exposed to a single high-energy UV pulse.
- Spot size of UV beam focused tightly to a width w.
- Fiber moved by a distance $\Lambda - w$ before next pulse arrives.
- A periodic index pattern can be created in this manner.
- Only short fiber gratings (<1 cm) can be produced because of time-consuming nature of this method.
- Most suitable for long-period gratings.

Grating Theory

- Refractive index of fiber mode varies periodically as

$$\tilde{n}(\omega, z) = \bar{n}(\omega) + \delta n_g(z) = \sum_{m=-\infty}^{\infty} \delta n_m \exp[2\pi i m(z/\Lambda)].$$

- Total field $\tilde{E}$ in the Helmholtz equation has the form

$$\tilde{E}(\mathbf{r}, \omega) = F(x,y)[\tilde{A}_f(z,\omega)\exp(i\beta_B z) + \tilde{A}_b(z,\omega)\exp(-i\beta_B z)],$$

where $\beta_B = \pi/\Lambda$ is the Bragg wave number.

- If we assume $\tilde{A}_f$ and $\tilde{A}_b$ vary slowly with z and keep only nearly phase-matched terms, we obtain coupled-mode equations

$$\frac{\partial \tilde{A}_f}{\partial z} = i\delta(\omega)\tilde{A}_f + i\kappa\tilde{A}_b,$$
$$-\frac{\partial \tilde{A}_b}{\partial z} = i\delta(\omega)\tilde{A}_b + i\kappa\tilde{A}_f,$$

The Institute of OPTICS

UNIVERSITY of ROCHESTER

Coupled-Mode Equations

- Coupled-mode equations look similar to those obtained for couplers with one difference: Second equations has a negative derivative
- This is expected because of backward propagation of A_b.
- Parameter $\delta(\omega) = \beta(\omega) - \beta_B$ measures detuning from the Bragg wavelength.
- Coupling coefficient κ is defined as

$$\kappa = \frac{k_0 \iint_{-\infty}^{\infty} \delta n_1 |F(x,y)|^2 \,dx\,dy}{\iint_{-\infty}^{\infty} |F(x,y)|^2 \,dx\,dy}.$$

- For a sinusoidal grating, $\delta n_g = n_a \cos(2\pi z/\Lambda)$, $\delta n_1 = n_a/2$ and $\kappa = \pi n_a/\lambda$.

Time-Domain Coupled-Mode Equations

- Coupled-mode equations can be converted to time domain by expanding $\beta(\omega)$ as

$$\beta(\omega) = \beta_0 + (\omega - \omega_0)\beta_1 + \tfrac{1}{2}(\omega - \omega_0)^2\beta_2 + \tfrac{1}{6}(\omega - \omega_0)^3\beta_3 + \cdots,$$

- Replacing $\omega - \omega_0$ with $i(\partial/\partial t)$, we obtain

$$\begin{aligned} \frac{\partial A_f}{\partial z} + \frac{1}{v_g}\frac{\partial A_f}{\partial t} + \frac{i\beta_2}{2}\frac{\partial^2 A_f}{\partial t^2} &= i\delta_0 A_f + i\kappa A_b, \\ -\frac{\partial A_b}{\partial z} + \frac{1}{v_g}\frac{\partial A_b}{\partial t} + \frac{i\beta_2}{2}\frac{\partial^2 A_b}{\partial t^2} &= i\delta_0 A_b + i\kappa A_f, \end{aligned}$$

- $\delta_0 = (\omega_0 - \omega_B)/v_g$ and $v_g = 1/\beta_1$ is the group velocity.
- When compared to couplers, The only difference is the $-$ sign appearing in the second equation.

Photonic Bandgap

- In the case of a CW beam, the general solution is

$$\tilde{A}_f(z) = A_1 \exp(iqz) + A_2 \exp(-iqz),$$
$$\tilde{A}_b(z) = B_1 \exp(iqz) + B_2 \exp(-iqz),$$

- Constants A_1, A_2, B_1, and B_2 satisfy

$$(q-\delta)A_1 = \kappa B_1, \qquad (q+\delta)B_1 = -\kappa A_1,$$
$$(q-\delta)B_2 = \kappa A_2, \qquad (q+\delta)A_2 = -\kappa B_2.$$

- These relations are satisfied if q obeys

$$q = \pm\sqrt{\delta^2 - \kappa^2}.$$

- This dispersion relation is of paramount importance for gratings.

Dispersion Relation of Gratings

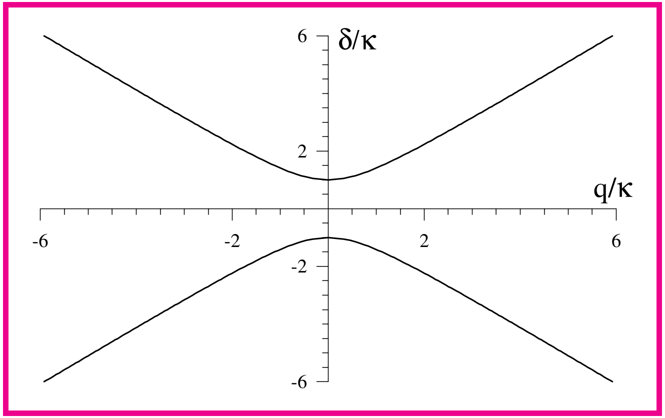

- If frequency of incident light is such that $-\kappa < \delta < \kappa$, q becomes purely imaginary.
- Most of the incident field is reflected under such conditions.
- The range $|\delta| \leq \kappa$ is called the *photonic bandgap* or *stop band*.
- Outside this band, propagation constant of light is modified by the grating to become $\beta_e = \beta_B \pm q$.

Grating Dispersion

- Since q depends on ω, grating exhibits dispersive effects.
- Grating-induced dispersion adds to the material and waveguide dispersions associated with a waveguide.
- To find its magnitude, we expand β_e in a Taylor series:

$$\beta_e(\omega) = \beta_0^g + (\omega - \omega_0)\beta_1^g + \tfrac{1}{2}(\omega - \omega_0)^2\beta_2^g + \tfrac{1}{6}(\omega - \omega_0)^3\beta_3^g + \cdots,$$

where $\beta_m^g = \frac{d^m q}{d\omega^m} \approx \left(\frac{1}{v_g}\right)^m \frac{d^m q}{d\delta^m}$.

- Group velocity $V_G = 1/\beta_1^g = \pm v_g\sqrt{1 - \kappa^2/\delta^2}$.
- For $|\delta| \gg \kappa$, optical pulse is unaffected by grating.
- As $|\delta|$ approaches κ, group velocity decreases and becomes zero at the edges of a stop band.

Grating Dispersion

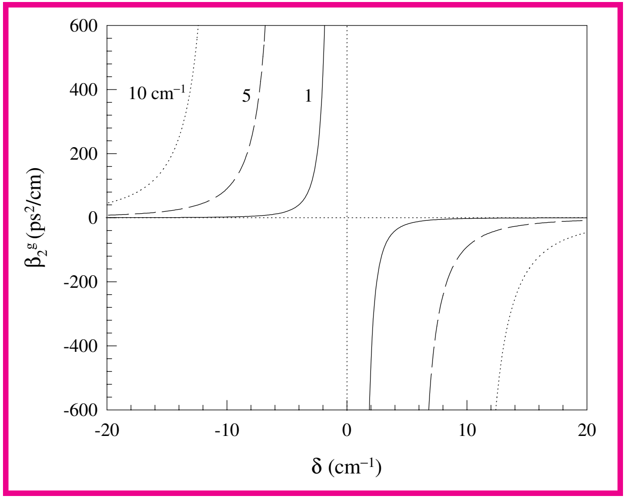

- Second- and third-order dispersive properties are governed by

$$\beta_2^g = -\frac{\mathrm{sgn}(\delta)\kappa^2/v_g^2}{(\delta^2-\kappa^2)^{3/2}}, \qquad \beta_3^g = \frac{3|\delta|\kappa^2/v_g^3}{(\delta^2-\kappa^2)^{5/2}}.$$

- GVD anomalous for $\delta > 0$ and normal for $\delta < 0$.

Grating as an Optical Filter

- What happens to optical pulses incident on a fiber grating?
- If pulse spectrum falls entirely within the stop band, pulse is reflected by the grating.
- If a part of pulse spectrum is outside the stop band, that part is transmitted by the grating.
- Clearly, shape of reflected and transmitted pulses will be quite different depending on detuning from Bragg wavelength.
- We can calculate reflection and transmission coefficients for each spectral component and then integrate over frequency.
- In the linear regime, a fiber grating acts as an optical filter.

Grating Reflectivity

- Reflection coefficient can be calculated from the solution

$$\begin{aligned}\tilde{A}_f(z) &= A_1 \exp(iqz) + r(q) B_2 \exp(-iqz)\\ \tilde{A}_b(z) &= B_2 \exp(-iqz) + r(q) A_1 \exp(iqz)\\ r(q) &= \frac{q-\delta}{\kappa} = -\frac{\kappa}{q+\delta}.\end{aligned}$$

- Reflection coefficient $r_g = \frac{\tilde{A}_b(0)}{\tilde{A}_f(0)} = \frac{B_2 + r(q)A_1}{A_1 + r(q)B_2}$.
- Using boundary condition $\tilde{A}_b(L) = 0$, $B_2 = -r(q)A_1 \exp(2iqL)$.
- Using this value of B_2, we obtain

$$r_g(\delta) = \frac{i\kappa \sin(qL)}{q\cos(qL) - i\delta \sin(qL)}.$$

Grating Reflectivity

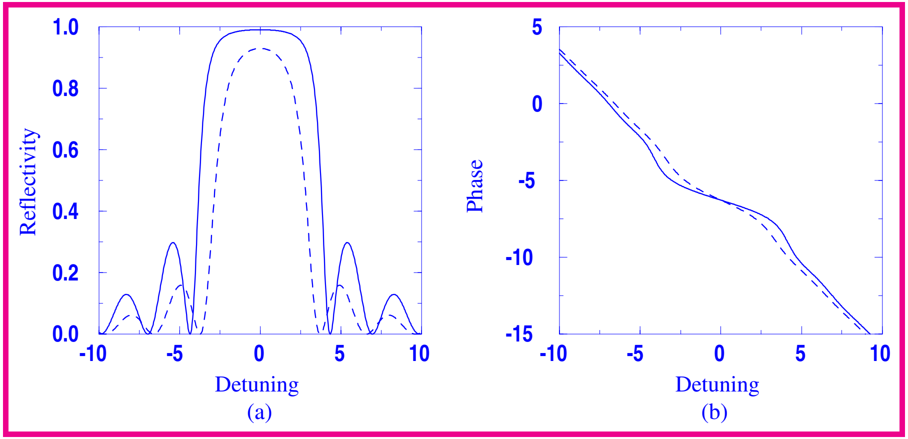

- $\kappa L = 2$ (dashed line); $\kappa L = 3$ (solid line).
- Reflectivity approaches 100% for $\kappa L = 3$ or larger.
- $\kappa = 2\pi\delta n_1/\lambda$ can be used to estimate grating length.
- For $\delta n_1 \approx 10^{-4}$, $\lambda = 1.55\ \mu$m, $L > 5$ 5 mm to yield $\kappa L > 2$.

Grating Apodization

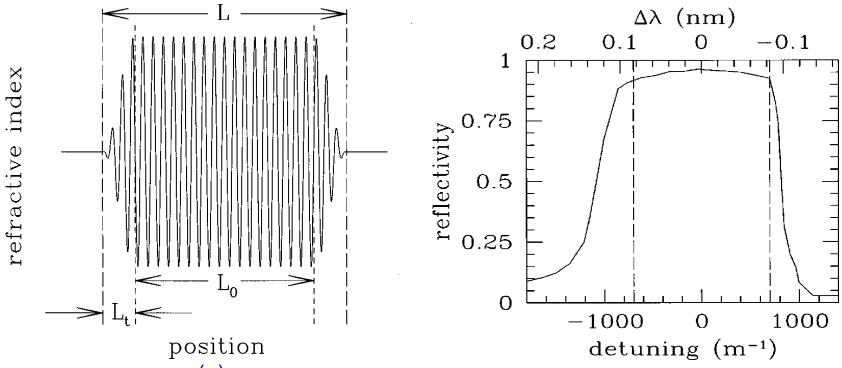

(a) (b)

- Reflectivity sidebands originate from a Fabry–Perot cavity formed by weak reflections occurring at the grating ends.
- An apodization technique is used to remove these sidebands.
- Intensity of the UV beam across the grating is varied such that it drops to zero gradually near the two grating ends.
- κ increases from zero to its maximum value in the center.

Grating Properties

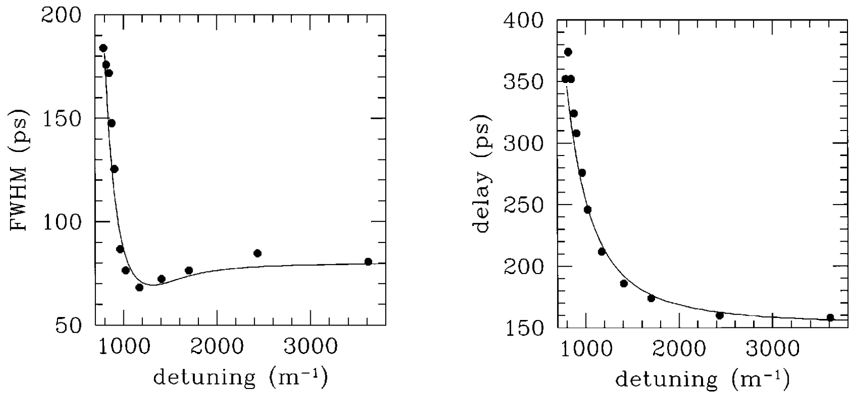

(a) (b)

- 80-ps pulses transmitted through an apodized grating.
- Pulses were delayed considerably close to a stop-band edge.
- Pulse width changed because of grating-induced GVD effects.
- Slight compression near $\delta = 1200\ \mathrm{m}^{-1}$ is due to SPM.

Nonuniform Gratings

- Grating parameters κ and δ become z-dependent in a nonuniform grating.
- Examples of nonuniform gratings include chirped gratings, phase-shifted gratings, and superstructure gratings.
- In a chirped grating, optical period $\bar{n}\Lambda$ changes along grating length.
- Since $\lambda_B = 2\bar{n}\Lambda$ sets the Bragg wavelength, stop band shifts along the grating length.
- Mathematically, δ becomes z-dependent.
- Chirped gratings have a much wider stop band because it is formed by a superposition of multiple stop bands.

Chirped Fiber Gratings

- Linearly chirped gratings are commonly used in practice.
- Bragg wavelength λ_B changes linearly along grating length.
- They can be fabricated either by varying physical period Λ or by changing $\bar{n}$ along z.
- To change Λ, fringe spacing is made nonuniform by interfering beams with different curvatures.
- A cylindrical lens is often used in one arm of interferometer.
- Chirped fiber gratings can also be fabricated by tilting or stretching the fiber, using strain or temperature gradients, or stitching multiple uniform sections.

Chirped Fiber Gratings

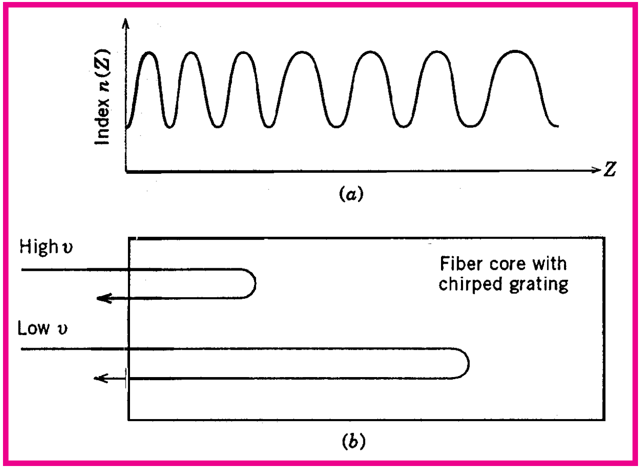

- Useful for dispersion compensation in lightwave systems.
- Different spectral components reflected by different parts of grating.
- Reflected pulse experiences a large amount of GVD.
- Nature of GVD (normal vs. anomalous) is controllable.

Superstructure Gratings

- Gratings have a single-peak transfer function.
- Some applications require optical filters with multiple peaks.
- Superstructure gratings have multiple equally spaced peaks.
- Grating designed such that κ varies periodically along its length. Such doubly periodic devices are also called *sampled gratings*.
- Such a structure contain multiple grating sections with constant spacing among them.
- It can be made by blocking small regions during fabrication such that $\kappa = 0$ in the blocked regions.
- It can also be made by etching away parts of a grating.

Fiber Interferometers

- Two passive components—couplers and gratings—can be combined to form a variety of fiber-based optical devices.
- Four common ones among them are
  - ⋆ Ring and Fabry–Perot resonators
  - ⋆ Sagnac-Loop interferometers
  - ⋆ Mach–Zehnder interferometers
  - ⋆ Michelson interferometers
- Useful for optical switching and other WDM applications.

Fiber-Ring Resonators

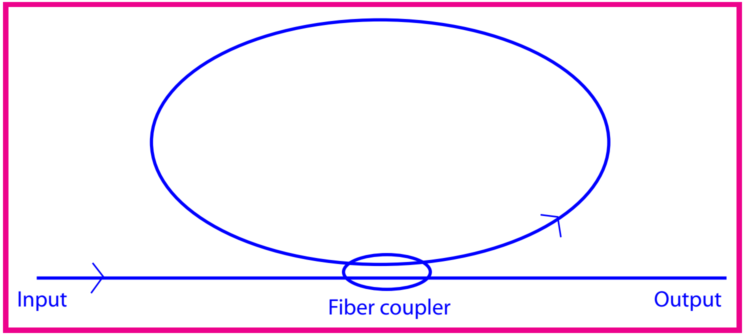

- Made by connecting input and output ports of one core of a directional coupler to form a ring.
- Transmission characteristics obtained using matrix relation

$$\begin{pmatrix} A_f \\ A_i \end{pmatrix} = \begin{pmatrix} \sqrt{\rho} & i\sqrt{1-\rho} \\ i\sqrt{1-\rho} & \sqrt{\rho} \end{pmatrix} \begin{pmatrix} A_c \\ A_t \end{pmatrix}.$$

- After one round trip, $A_f/A_c = \exp[-\alpha L/2 + i\beta(\omega)L] \equiv \sqrt{a}e^{i\phi}$ where $a = \exp(-\alpha L) \leq 1$ and $\phi(\omega) = \beta(\omega)L$.

Transmission Spectrum

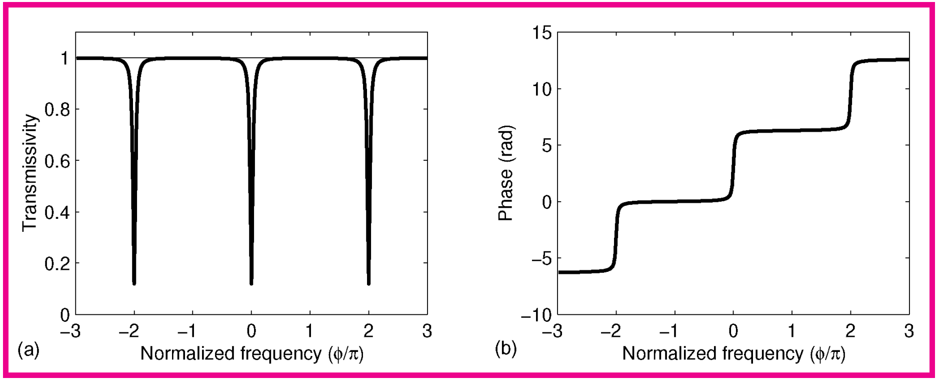

- The transmission coefficient is found to be

$$t_r(\omega) \equiv \sqrt{T_r} e^{i\phi_t} = \frac{A_t}{A_i} = \frac{\sqrt{a} - \sqrt{\rho} e^{-i\phi}}{1 - \sqrt{a\rho} e^{i\phi}} e^{i(\pi+\phi)}.$$

- Spectrum shown for $a = 0.95$ and $\rho = 0.9$.
- If $a = 1$ (no loss), $T_r = 1$ (all-pass resonator) but phase varies as

$$\phi_t(\omega) = \pi + \phi + 2\tan^{-1} \frac{\sqrt{\rho} \sin\phi}{1 - \sqrt{\rho} \cos\phi}.$$

All-Pass Resonators

- Frequency dependence of transmitted phase for all-pass resonators can be used for many applications.
- Different frequency components of a pulse are delayed by different amounts near a cavity resonance.
- A ring resonator exhibits GVD (similar to a fiber grating).
- Since group delay $\tau_d = d\phi_t/d\omega$, GVD parameter is given by $\beta_2 = \frac{1}{L}\frac{d^2\phi_t}{d\omega^2}$.
- A fiber-ring resonator can be used for dispersion compensation.
- If a single ring does not provide enough dispersion, several rings can be cascaded in series.
- Such a device can compensate dispersion of multiple channels.

Fabry–Perot Resonators

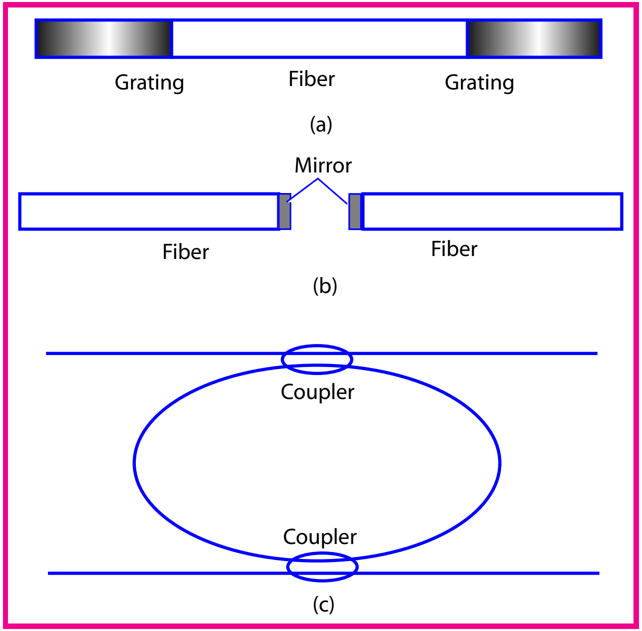

- Use of couplers and gratings provides an all-fiber design.
- Transmissivity can be calculated by adding contributions of successive round trips to transmitted field.

The Institute of OPTICS

UNIVERSITY of ROCHESTER

Transmission Spectrum

- Transmitted field:

$$A_t = A_i e^{i\pi}(1-R_1)^{1/2}(1-R_2)^{1/2}\left[1+\sqrt{R_1R_2}e^{i\phi_R}+R_1R_2e^{2i\phi_R}+\cdots\right],$$

- Phase shift during a single round trip: $\phi_R = 2\beta(\omega)L$.
- When $R_m = R_1 = R_2$, $\qquad A_t = \frac{(1-R_m)A_i e^{i\pi}}{1-R_m\exp(2i\phi_R)}$.
- Transmissivity is given by the Airy formula

$$T_R = \left|\frac{A_t}{A_i}\right|^2 = \frac{(1-R_m)^2}{(1-R_m)^2+4R_m\sin^2(\phi_R/2)}.$$

- Round-trip phase shift $\phi_R = (\omega-\omega_0)\tau_r$, where τ_r is the round-trip time.

Free Spectral Range and Finesse

- Sharpness of resonance peaks quantified through the finesse

$$F_R = \frac{\text{Peak bandwidth}}{\text{Free spectral range}} = \frac{\pi\sqrt{R_m}}{1-R_m},$$

- Free spectral range $\Delta\nu_L$ is obtained from phase-matching condition

$$2[\beta(\omega+2\pi\Delta\nu_L)-\beta(\omega)]L = 2\pi.$$

- $\Delta\nu_L = 1/\tau_r$, where $\tau_r = 2L/v_g$ is the round-trip time.
- FP resonators are useful as an optical filter with periodic passbands.
- Center frequencies of passbands can be tuned by changing physical mirror spacing or by modifying the refractive index.

Sagnac Interferometers

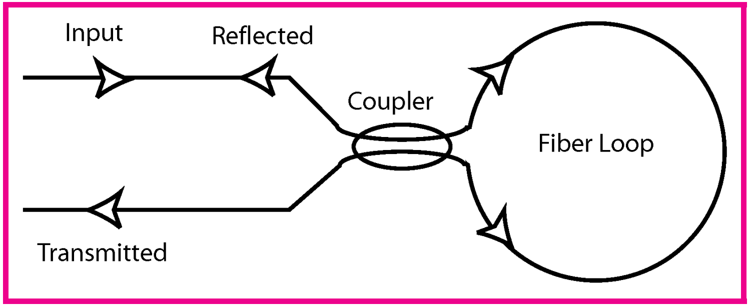

- Made by connecting two output ports of a fiber coupler to form a fiber loop.
- No feedback mechanism; all light entering exits after a round trip.
- Two counterpropagating parts share the same optical path and interfere at the coupler coherently.
- Their phase difference determines whether input beam is reflected or transmitted.

Fiber-Loop Mirrors

- When a 3-dB fiber coupler is used, any input is totally reflected.
- Such a device is called the fiber-loop mirror.
- Fiber-loop mirror can be used for all-optical switching by exploiting nonlinear effects such as SPM and XPM.
- Such a *nonlinear* optical loop mirror transmits a high-power signal while reflecting it at low power levels.
- Useful for many applications such as mode locking, wavelength conversion, and channel demultiplexing.

Nonlinear Fiber-Loop Mirrors

- Input field splits into two parts: $A_f = \sqrt{\rho}A_0, \quad A_b = i\sqrt{1-\rho}\,A_0$.
- After one round trip, $A'_f = A_f \exp[i\phi_0 + i\gamma(|A_f|^2 + 2|A_b|^2)L]$, $A'_b = A_b \exp(i\phi_0 + i\gamma(|A_b|^2 + 2|A_f|^2)L]$.
- Reflected and transmitted fields after fiber coupler:

$$\begin{pmatrix} A_t \\ A_r \end{pmatrix} = \begin{pmatrix} \sqrt{\rho} & i\sqrt{1-\rho} \\ i\sqrt{1-\rho} & \sqrt{\rho} \end{pmatrix} \begin{pmatrix} A'_f \\ A'_b \end{pmatrix}.$$

- Transmissivity $T_S \equiv |A_t|^2/|A_0|^2$ of the Sagnac loop:

$$T_S = 1 - 2\rho(1-\rho)\{1 + \cos[(1-2\rho)\gamma P_0 L]\},$$

- If $\rho \neq 1/2$, fiber-loop mirror can act as an optical switch.

Nonlinear Transmission Characteristics

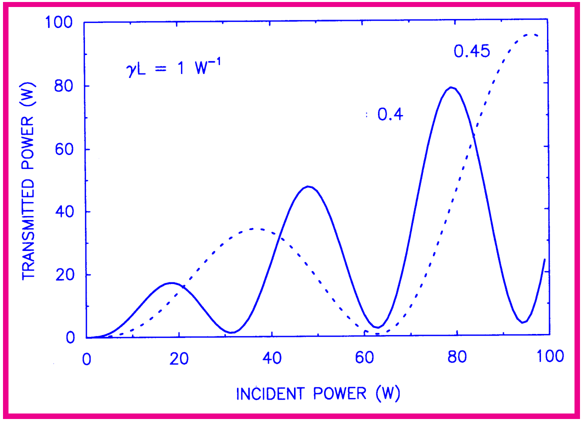

- At low powers, little light is transmitted if ρ is close to 0.5.
- At high powers, SPM-induced phase shift leads to 100% transmission whenever $|1-2\rho|\gamma P_0 L = (2m-1)\pi$.
- Switching power for $m = 1$ is 31 W for a 100-m-long fiber loop when $\rho = 0.45$ and $\gamma = 10\ \mathrm{W}^{-1}/\mathrm{km}$.
- It can be reduced by increasing loop length or γ.

Nonlinear Switching

- Most experiments use short optical pulses with high peak powers.
- In a 1989 experiment, 180-ps pulses were injected into a 25-m Sagnac loop.
- Transmission increased from a few percent to 60% as peak power was increased beyond 30 W.
- Only the central part of the pulse was switched.
- Shape deformation can be avoided by using solitons.
- Switching threshold can be reduced by incorporating a fiber amplifier within the loop.

Nonlinear Amplifying-Loop Mirror

- If amplifier is located close to the fiber coupler, it introduces an asymmetry beneficial to optical switching.
- Even a 50:50 coupler ($\rho = 0.5$) can be used for switching.
- In one direction pulse is amplified as it enters the loop.
- Counterpropagating pulse is amplified just before it exits the loop.
- Since powers in two directions differ by a large amount, differential phase shift can be quite large.
- Transmissivity of loop mirror is given by

$$T_S = 1 - 2\rho(1-\rho)\{1 + \cos[(1 - \rho - G\rho)\gamma P_0 L]\}.$$

- Switching power $P_0 = 2\pi/[(G-1)\gamma L]$.

Back
Close

Nonlinear Amplifying-Loop Mirror

- Since $G \sim 30$ dB, switching power is reduced considerably.
- Such a device can switch at peak power levels below 1 mW.
- In a 1990 experiment, 4.5 m of Nd-doped fiber was spliced within a 306-m fiber loop formed with a 3-dB coupler.
- Switching was observed using 10-ns pulses.
- Switching power was about 0.9 W even when amplifier provided only 6-dB gain.
- A semiconductor optical amplifier inside a 17-m fiber loop produced switching at 250 μW with 10-ns pulses.

Dispersion-Unbalanced Sagnac Loops

- Sagnac interferometer can also be unbalanced by using a fiber whose GVD varies along the loop length.
- A dispersion-decreasing fiber or several fibers with different dispersive properties can be used.
- In the simplest case Sagnac loop is made with two types of fibers.
- Sagnac interferometer is unbalanced as counterpropagating waves experience different GVD during a round trip.
- Such Sagnac loops remain balanced for CW beams.
- As a result, optical pulses can be switched to output port while any CW background noise is reflected.
- Such a device can improve the SNR of a noisy signal.

XPM-Induced Switching

- XPM can also be used for all-optical switching.
- A control signal is injected into the Sagnac loop such that it propagates in only one direction.
- It induces a nonlinear phase shift through XPM in that direction.
- In essence, control signal unbalances the Sagnac loop.
- As a result, a low-power CW signal is reflected in the absence of a control pulse but is transmitted in its presence.
- As early as 1989, a 632-nm CW signal was switched using intense 532-nm picosecond pump pulses with 25-W peak power.
- Walk-off effects induced by group-velocity mismatch affect the device. It is better to us orthogonally polarized control at the same wavelength.

Mach–Zehnder Interferometers

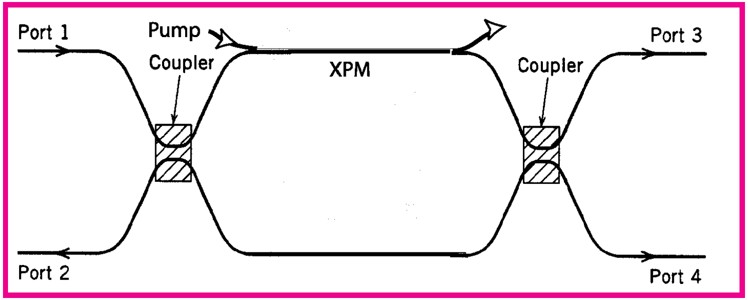

- A Mach–Zehnder (MZ) interferometer is made by connecting two fiber couplers in series.
- Such a device has the advantage that nothing is reflected back toward the input port.
- MZ interferometer can be unbalanced by using different path lengths in its two arms.
- This feature also makes it susceptible to environmental fluctuations.

Transmission Characteristics

- Taking into account both the linear and nonlinear phase shifts, optical fields at the second coupler are given by

$$A_1 = \sqrt{\rho_1} A_0 \exp(i\beta_1 L_1 + i\rho_1 \gamma |A_0|^2 L_1),$$
$$A_2 = i\sqrt{1-\rho_1} A_0 \exp[i\beta_2 L_2 + i(1-\rho_1)\gamma |A_0|^2 L_2],$$

- Transmitted fields from two ports:

$$\begin{pmatrix} A_3 \\ A_4 \end{pmatrix} = \begin{pmatrix} \sqrt{\rho_2} & i\sqrt{1-\rho_2} \\ i\sqrt{1-\rho_2} & \sqrt{\rho_2} \end{pmatrix} \begin{pmatrix} A_1 \\ A_2 \end{pmatrix}.$$

- Transmissivity of the bar port is given by

$$T_b = \rho_1\rho_2 + (1-\rho_1)(1-\rho_2) - 2[\rho_1\rho_2(1-\rho_1)(1-\rho_2)]^{1/2} \cos(\phi_L + \phi_{\rm NL}),$$

- $\phi_L = \beta_1 L_1 - \beta_2 L_2$ and $\phi_{\rm NL} = \gamma P_0[\rho_1 L_1 - (1-\rho_1)L_2]$.

Transmission Characteristics

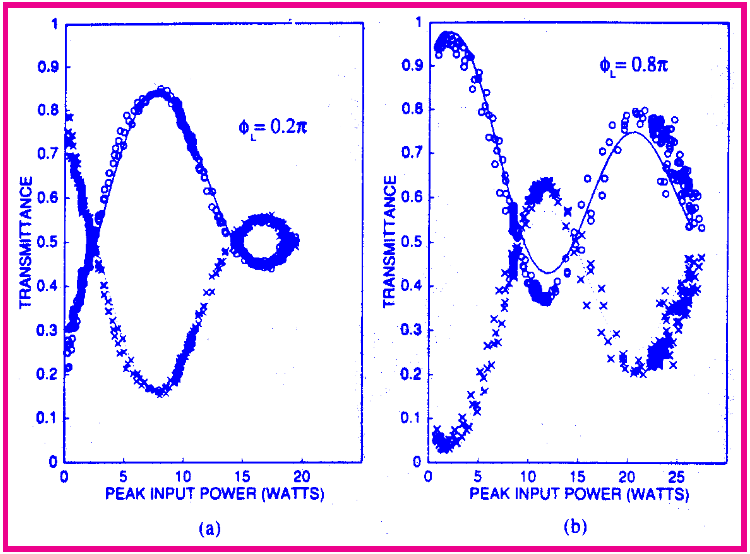

- Nonlinear switching for two values of ϕ_L.
- A dual-core fiber was used to make the interferometer $(L_1 = L_2)$.
- This configuration avoids temporal fluctuations occurring invariably when two separate fiber pieces are used.

XPM-Induced Switching

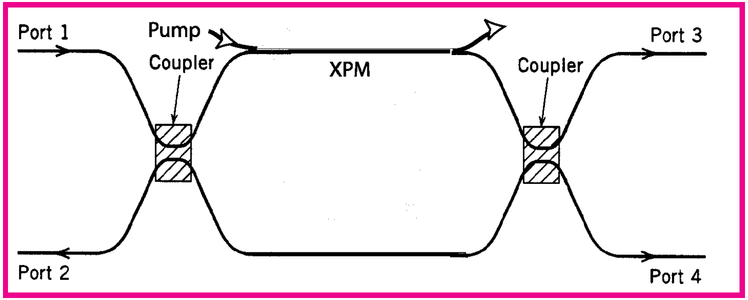

- Switching is also possible through XPM-induced phase shift.
- Control beam propagates in one arm of the MZ interferometer.
- MZ interferometer is balanced in the absence of control, and signal appears at port 4.
- When control induces a π phase shift through XPM, signal is directed toward port 3.
- Switching power can be lowered by reducing effective core area A_{eff} of fiber.

Michelson Interferometers

- Can be made by splicing Bragg gratings at the output ports of a fiber coupler.
- It functions like a MZ interferometer.
- Light propagating in its two arms interferes at the same coupler where it was split.
- Acts as a nonlinear mirror, similar to a Sagnac interferometer.
- Reflectivity $R_M = \rho^2 + (1-\rho)^2 - 2\rho(1-\rho)\cos(\phi_L + \phi_{\rm NL})$.
- Nonlinear characteristics similar to those of a Sagnac loop.
- Often used for passive mode locking of lasers (additive-pulse mode locking).

Isolators and Circulators

- Isolators and circulators fall into the category of nonreciprocal devices.
- Such a device breaks the time-reversal symmetry inherent in optics.
- It requires that device behave differently when the direction of light propagation is reversed.
- A static magnetic field must be applied to break time-reversal symmetry.
- Device operation is based on the Faraday effect.
- Faraday effect: Changes in the state of polarization of an optical beam in a magneto-optic medium in the presence of a magnetic field.

Faraday Effect

- Refractive indices of some materials become different for RCP and LCP components in the presence of a magnetic field.
- On a more fundamental level, Faraday effect has its origin in the motion of electrons in the presence of a magnetic field.
- It manifests as a change in the state of polarization as the beam propagates through the medium.
- Polarization changes depend on the direction of magnetic field but not on the direction in which light is traveling.
- Mathematically, two circularly polarized components propagate with $\beta^{\pm} = n^{\pm}(\omega/c)$.
- Circular birefringence depends on magnetic field as $\delta n = n^{+} - n^{-} = K_F H_{\mathrm{dc}}$.

Faraday Rotator

- Relative phase shift between RCP and LCP components is

$$\delta\phi = (\omega/c)K_F H_{\mathrm{dc}} l_M = V_c H_{\mathrm{dc}} l_M,$$

  where $V_c = (\omega/c)K_F$ is the Verdet constant.

- Plane of polarization of light is rotated by an angle $\theta_F = \frac{1}{2}\delta\phi$.

- Most commonly used material: terbium gallium garnet with Verdet constant of $\sim$0.1 rad/(Oe-cm).

- Useful for making a device known as the Faraday rotator.

- Magnetic field and medium length are chosen to induce 45° change in direction of linearly polarized light.

Optical Isolators

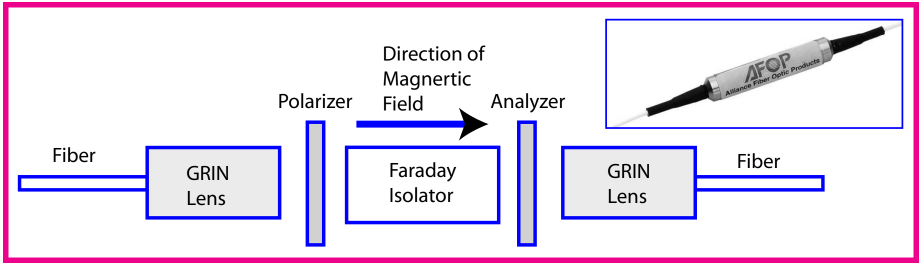

- Optical analog of a rectifying diode.
- Uses a Faraday rotator sandwiched between two polarizers.
- Second polarizer tilted at 45° from first polarizer.
- Polarization-independent isolators process orthogonally polarized components separately and combine them at the output end.
- Commercial isolators provide better than 30-dB isolation in a compact package (4 cm×5 mm wide).

Optical Circulators

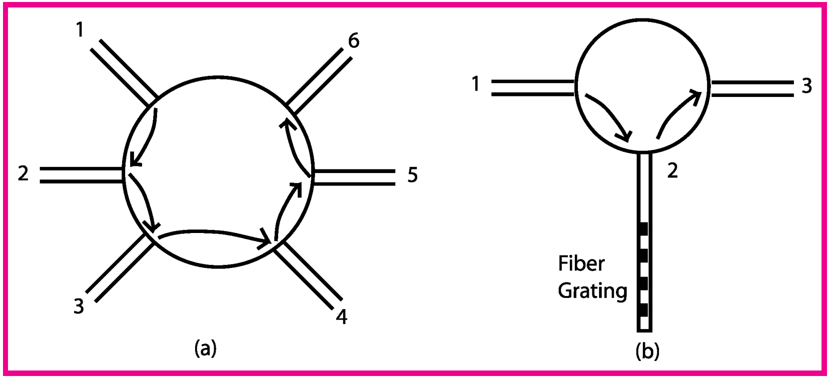

- A circulator directs backward propagating light does to another port rather than discarding it, resulting in a three-port device.
- More ports can be added if necessary.
- Such devices are called circulators because they direct light to different ports in a circular fashion.
- Design of optical circulators becomes increasingly complex as the number of ports increases.

Active Fiber Components

- No electrical pumping possible as silica is an insulator.
- Active components can be made but require optical pumping.
- Fiber core is often doped with a rare-earth element to realize optical gain through optical pumping.
- Active Fiber components
  - ⋆ Doped-Fiber Amplifiers
  - ⋆ Raman Amplifiers (SRS)
  - ⋆ Parametric Amplifiers (FWM)
  - ⋆ CW and mode-locked Fiber Lasers

Doped-Fiber Amplifiers

- Core doped with a rare-earth element during manufacturing.
- Many different elements such as erbium, neodymium, and ytterbium, can be used to make fiber amplifiers (and lasers).
- Amplifier properties such as operating wavelength and gain bandwidth are set by the dopant.
- Silica fiber plays the passive role of a host.
- Erbium-doped fiber amplifiers (EDFAs) operate near 1.55 μm and are used commonly for lightwave systems.
- Yb-doped fiber are useful for high-power applications.
- Yb-doped fiber lasers can emit > 1 kW of power.

Optical Pumping

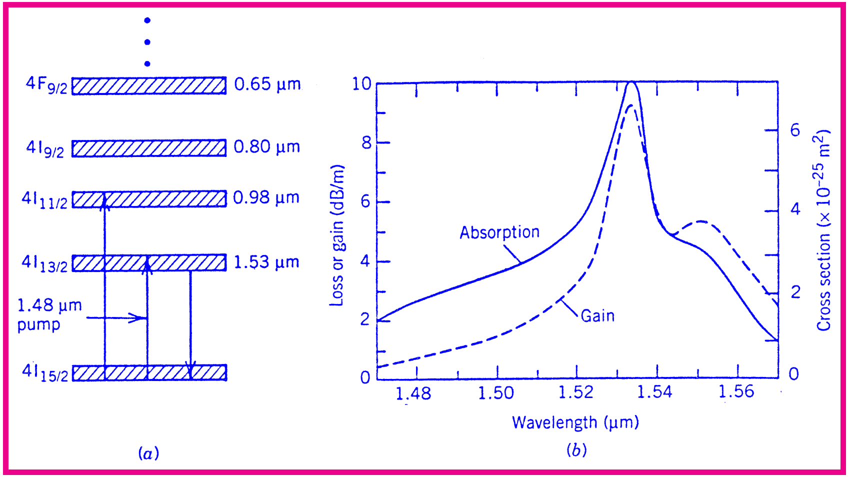

- Optical gain realized when a doped fiber is pumped optically.
- In the case of EDFAs, semiconductor lasers operating near 0.98- and 1.48-μm wavelengths are used.
- 30-dB gain can be realized with only 10–15 mW of pump power.
- Efficiencies as high as 11 dB/mW are possible.

Amplifier Gain

- Gain coefficient can be written as

$$g(\omega) = \frac{g_0(P_p)}{1 + (\omega - \omega_0)^2 T_2^2 + P/P_s}.$$

- T_2 is the dipole relaxation time (typically <1 ps).
- Fluorescence time T_1 can vary from 1 μs–10 ms depending on the rare-earth element used (10 ms for EDFAs).
- Amplification of a CW signal is governed by $dP/dz = g(\omega)P$.
- When $P/P_s \ll 1$, solution is $P(z) = P(0)\exp(gz)$.
- Amplifier gain G is defined as

$$G(\omega) = P_{\text{out}}/P_{\text{in}} = P(L)/P(0) = \exp[g(\omega)L].$$

Gain Spectrum

- For $P \ll P_s$, small-signal gain is of the form

$$g(\omega) = \frac{g_0}{1 + (\omega - \omega_0)^2 T_2^2}.$$

- Lorentzian Gain spectrum with a FWHM $\Delta\nu_g = \frac{1}{\pi T_2}$.
- Amplifier gain $G(\omega)$ has a peak value $G_0 = \exp(g_0 L)$.
- Its FWHM is given by $\Delta\nu_A = \Delta\nu_g \left[\frac{\ln 2}{\ln(G_0/2)}\right]^{1/2}$.
- Amplifier bandwidth is smaller than gain bandwidth.
- Gain spectrum of EDFAs has a double-peak structure with a bandwidth >35 nm.
- EDFAs can provide amplification over a wide spectral region (1520–1610 nm).

Amplifier Noise

- All amplifiers degrade SNR of the amplified signal because of spontaneous emission.
- SNR degradation quantified through the noise figure F_n defined as $F_n = (\text{SNR})_{\text{in}}/(\text{SNR})_{\text{out}}$.
- In general, F_n depends on several detector parameters related to thermal noise.
- For an ideal detector (no thermal noise)

$$F_n = 2n_{\text{sp}}(1 - 1/G) + 1/G \approx 2n_{\text{sp}}.$$

- Spontaneous emission factor $n_{\text{sp}} = N_2/(N_2 - N_1)$.
- For a fully inverted amplifier $(N_2 \gg N_1)$, $n_{\text{sp}} = 1$.
- 51-dB gain realized with $F_n = 3.1$ dB at 48 mW pump power.

Amplifier Design

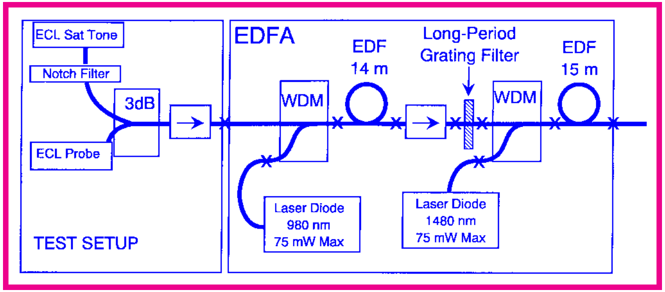

- EDFAs are designed to provide uniform gain over the entire C band (1530–1570 nm).
- An optical filter is used for gain flattening.
- It often contains several long-period fiber gratings.
- Two-stage design helps to reduce the noise level as it permits to place optical filter in the middle.
- Noise figure is set by the first stage.

Amplifier Design

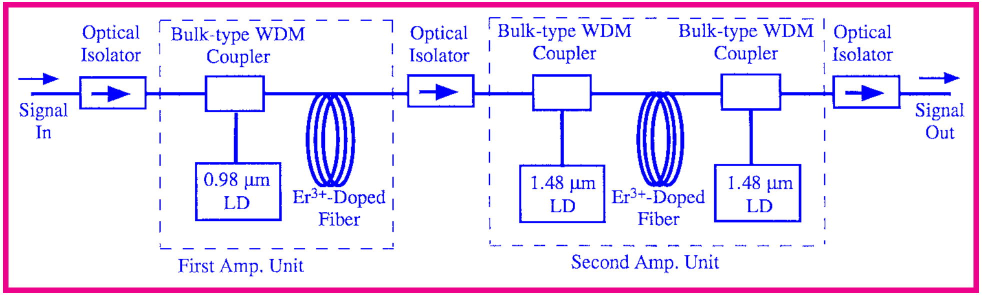

- A two-stage design is used for L-band amplifiers operating in the range 1570–1610 nm.
- First stage pumped at 980 nm and acts as a traditional EDFA.
- Second stage has a long doped fiber (200 m or so) and is pumped bidirectionally using 1480-nm lasers.
- An optical isolator blocks the backward-propagating ASE.
- Such cascaded amplifiers provide flat gain with relatively low noise level levels.

Raman Amplifiers

- A Raman amplifier uses stimulated Raman scattering (SRS) for signal amplification.
- SRS is normally harmful for WDM systems.
- The same process useful for making Raman amplifiers.
- Raman amplifiers can provide large gain over a wide bandwidth in any spectral region using a suitable pump.
- Require long fiber lengths ($>$1 km) compared with EDFAs.
- Fiber used for data transmission can itself be employed as a Raman-gain medium.
- This scheme is referred to as distributed Raman amplification.

Raman Amplifiers

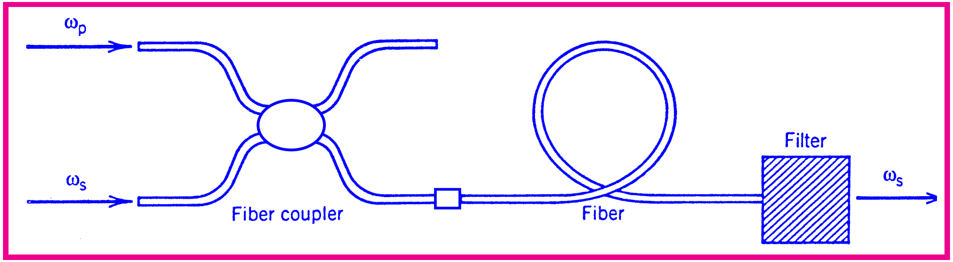

- Similar to EDFAs, Raman amplifiers must be pumped optically.
- Pump and signal injected into the fiber through a fiber coupler.
- Pump power is transferred to the signal through SRS.
- Pump and signal counterpropagate in the backward-pumping configuration often used in practice.
- Signal amplified exponentially as e^{gL} with

$$g(\omega) = g_R(\omega)(P_p/A_{\text{eff}}).$$

Raman Gain and Bandwidth

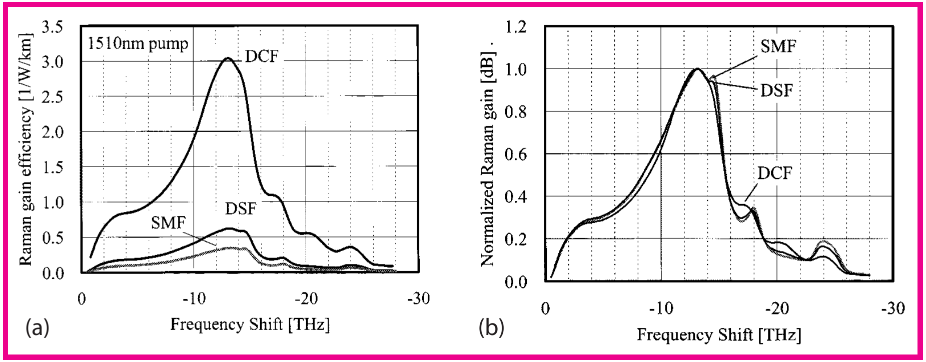

- Raman gain spectrum $g_R(\Omega)$ has a broad peak located near 13 THz.
- The ratio g_R/A_{eff} is a measure of Raman-gain efficiency and depends on fiber design.
- A dispersion-compensating fiber (DCF) can be 8 times more efficient than a standard silica fiber.
- Gain bandwidth $\Delta\nu_g$ is about 6 THz.
- Multiple pumps can be used make gain spectrum wider and flatter.

Single-Pump Raman Amplification

- Governed by a set of two coupled nonlinear equations:

$$\frac{dP_s}{dz} = \frac{g_R}{A_{\rm eff}} P_p P_s - \alpha_s P_s, \qquad \eta \frac{dP_p}{dz} = -\frac{\omega_p}{\omega_s} \frac{g_R}{A_{\rm eff}} P_p P_s - \alpha_p P_p,$$

- $\eta = \pm 1$ depending on the pumping configuration.
- In practice, $P_p \gg P_s$, and pump depletion can be ignored.
- $P_p(z) = P_0 \exp(-\alpha_p z)$ in the forward-pumping case.
- Signal equation is then easily integrated to obtain

$$P_s(L) = P_s(0) \exp(g_R P_0 L_{\rm eff}/A_{\rm eff} - \alpha_s L) \equiv G(L) P_s(0),$$

where $L_{\rm eff} = [1 - \exp(-\alpha_p L)]/\alpha_p$.

Bidirectional Pumping

- In the case of backward-pumping, boundary condition becomes $P_p(L) = P_0$.
- Solution of pump equation becomes $P_p(z) = P_0 \exp[-\alpha_p(L-z)]$.
- Same amplification factor as for forward pumping.
- In the case of bidirectional pumping, the solution is

$$P_s(z) \equiv G(z)P_s(0) = P_s(0)\exp\left(\frac{g_R}{A_{\text{eff}}}\int_0^z P_p(z)\,dz - \alpha_s L\right),$$

  where $P_p(z) = P_0\{f_p \exp(-\alpha_p z) + (1-f_p)\exp[-\alpha_p(L-z)]\}$.
- P_0 is total power and f_p is its fraction in forward direction.
- Amplifier properties depend on f_p.

Bidirectional Pumping

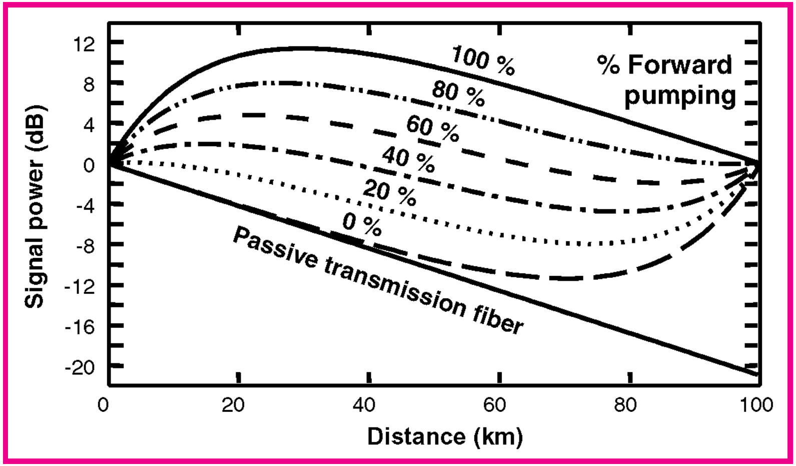

- Change in signal power along a 100-km-long Raman amplifier as f_p is varied in the range 0 to 1.
- In all cases, $g_R/A_{\text{eff}} = 0.7$ W^{-1}/km, $\alpha_s = 0.2$ dB/km, $\alpha_p = 0.25$ dB/km, and $G(L) = 1$.
- Which pumping configuration is better from a system standpoint?

Back
Close

Forward or Backward Pumping?

- Forward pumping superior from the noise viewpoint.
- Backward pumping better in practice as it reduces nonlinear effects (signal power small throughout fiber link).
- Accumulated nonlinear phase shift induced by SPM is given by

$$\phi_{\rm NL} = \gamma \int_0^L P_s(z)\,dz = \gamma P_s(0) \int_0^L G(z)\,dz.$$

- Increase in $\phi_{\rm NL}$ because of Raman amplification is quantified by the ratio

$$R_{\rm NL} = \frac{\phi_{\rm NL}(\text{pump on})}{\phi_{\rm NL}(\text{pump off})} = L_{\rm eff}^{-1} \int_0^L G(z)\,dz.$$

- This ratio is smallest for backward pumping.

Multiple-Pump Raman Amplification

- Raman amplifiers need high pump powers.
- Gain spectrum is 20–25 nm wide but relatively nonuniform.
- Both problems can be solved using multiple pump lasers at suitably optimized wavelengths.
- Even though Raman gain spectrum of each pump is not very flat, it can be broadened and flattened using multiple pumps.
- Each pump creates its own nonuniform gain profile over a specific spectral range.
- Superposition of several such spectra can create relatively flat gain over a wide spectral region.

Example of Raman Gain Spectrum

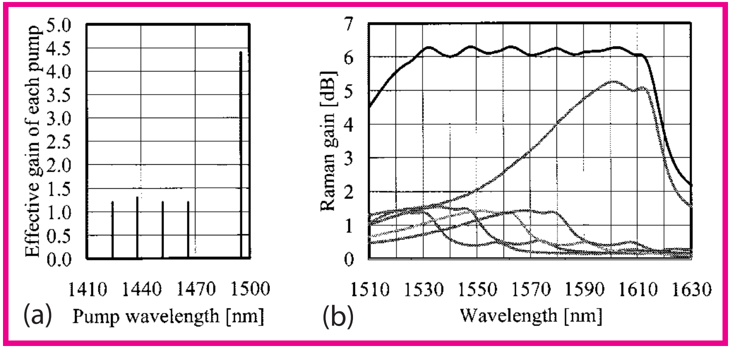

- Five pump lasers operating at 1,420, 1,435, 1,450, 1,465, and 1,495 nm are used.
- Individual pump powers chosen to provide uniform gain over a 80-nm bandwidth (top trace).
- Raman gain is polarization-sensitive. Polarization problem is solved using two orthogonally polarized pump lasers at each wavelength.
- It can also be solved by depolarizing output of each pump laser.

The Institute of OPTICS

UNIVERSITY of ROCHESTER

Example of Raman Gain Spectrum

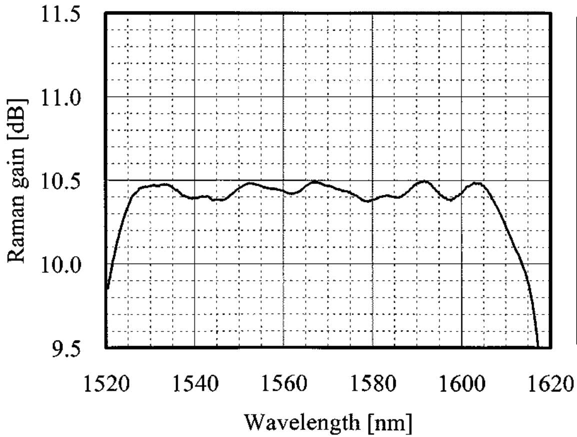

Frequency [THz]	Power [mW]
212.2	91
211.1	98
210.2	95
209.2	52
208.2	52
207.3	39
206.2	38
205.3	29
204.2	35
203.3	33
200.1	51
199.3	32

- Measured Raman gain for a Raman amplifier pumped with 12 lasers.
- Pump powers used (shown on the right) were below 100 mW for each pump laser.
- Pump powers and wavelengths are design parameters obtained by solving a complex set of equations.

Noise in Raman Amplifiers

- Spontaneous Raman scattering adds noise to the amplified signal.
- Noise is temperature dependent as it depends on phonon population in the vibrational state.
- Evolution of signal is governed by

$$\frac{dA_s}{dz} = \frac{g_R}{2A_{\text{eff}}} P_p(z) A_s - \frac{\alpha_s}{2} A_s + f_n(z,t),$$

- $f_n(z,t)$ is modeled as a Gaussian stochastic process with

$$\langle f_n(z,t) f_n(z',t') \rangle = n_{\text{sp}} h\nu_0 g_R P_p(z) \delta(z-z') \delta(t-t'),$$

- $n_{\text{sp}}(\Omega) = [1 - \exp(-\hbar\Omega/k_B T)]^{-1}, \quad \Omega = \omega_p - \omega_s.$

Noise in Raman Amplifiers

- Integrating over amplifier length, $A_s(L) = \sqrt{G(L)}A_s(0) + A_{\rm sp}$:

$$A_{\rm sp} = \sqrt{G(L)} \int_0^L \frac{f_n(z,t)}{\sqrt{G(z)}} dz, \quad G(z) = \exp\left(\int_0^z [g_R P_p(z') - \alpha_s]\, dz'\right).$$

- Spontaneous power added to the signal is given by

$$P_{\rm sp} = n_{\rm sp} h\nu_0 g_R B_{\rm opt} G(L) \int_0^L \frac{P_p(z)}{G(z)} dz,$$

- $B_{\rm opt}$ is the bandwidth of the Raman amplifier (or optical filter).
- Total noise power higher by factor of 2 when both polarization components are considered.

The Institute of OPTICS — UNIVERSITY of ROCHESTER

Noise in Raman Amplifiers

- Noise figure of a Raman amplifier is given by

$$F_n = \frac{P_{\rm sp}}{Gh\nu_0\Delta f} = n_{\rm sp} g_R \frac{B_{\rm opt}}{\Delta f}\int_0^L \frac{P_p(z)}{G(z)}\,dz.$$

- Common to introduce the concept of an *effective noise figure* as $F_{\rm eff} = F_n \exp(-\alpha_s L)$.
- $F_{\rm eff}$ can be less than 1 (negative on the decibel scale).
- Physically speaking, distributed gain counteracts fiber losses and results in better SNR compared with lumped amplifiers.
- Forward pumping results in less noise because Raman gain is concentrated toward the input end.

The Institute of OPTICS

UNIVERSITY of ROCHESTER

Parametric Amplifiers

- Make use of four-wave mixing (FWM) in optical fibers.
- Two pumps (at ω_1 and ω_2) launched with the signal at ω_3.
- The idler field generated internally at a frequency $\omega_4 = \omega_1 + \omega_2 - \omega_3$.
- Signal and idler both amplified through FWM.
- Such a device can amplify signal by 30–40 dB if a phase-matching condition is satisfied.
- It can also act as a wavelength converter.
- Idler phase is reverse of the signal (phase conjugation).

Simple Theory

- FWM is described by a set of 4 coupled nonlinear equations.
- These equations must be solved numerically in general.
- If we assume intense pumps (negligible depletion), and treat pump powers as constant, signal and idler fields satisfy

$$\frac{dA_3}{dz} = 2i\gamma[(P_1+P_2)A_3 + \sqrt{P_1P_2}e^{-i\theta}A_4^*],$$
$$\frac{dA_4^*}{dz} = -2i\gamma[(P_1+P_2)A_4^* + \sqrt{P_1P_2}e^{i\theta}A_3],$$

- $P_1 = |A_1|^2$ and $P_2 = |A_2|^2$ are pump powers.
- $\theta = [\Delta\beta - 3\gamma(P_1+P_2)]z$ represents total phase mismatch.
- Linear part $\Delta\beta = \beta_3 + \beta_4 - \beta_1 - \beta_2$, where $\beta_j = \tilde{n}_j\omega_j/c$.

Signal and Idler Equations

- Two coupled equations can be solved analytically as they are linear first-order ODEs.
- Notice that A_3 couples to A_4^* (phase conjugation).
- Introducing $B_j = A_j \exp[-2i\gamma(P_1 + P_2)z]$, we obtain the following set of two equations:

$$\frac{dB_3}{dz} = 2i\gamma\sqrt{P_1 P_2} e^{-i\kappa z} B_4^*,$$
$$\frac{dB_4^*}{dz} = -2i\gamma\sqrt{P_1 P_2} e^{i\kappa z} B_3,$$

- Phase mismatch: $\kappa = \Delta\beta + \gamma(P_1 + P_2)$.
- $\kappa = 0$ is possible if pump wavelength lies close to ZDWL but in the anomalous-dispersion regime of the fiber.

Parametric Gain

- General solution for signal and idler fields:

$$B_3(z) = (a_3 e^{gz} + b_3 e^{-gz}) \exp(-i\kappa z/2),$$
$$B_4^*(z) = (a_4 e^{gz} + b_4 e^{-gz}) \exp(i\kappa z/2),$$

- a_3, b_3, a_4, and b_4 are determined from boundary conditions.
- Parametric gain g depends on pump powers as

$$g = \sqrt{(\gamma P_0 r)^2 - (\kappa/2)^2}, \quad r = 2\sqrt{P_1 P_2}/P_0, \quad P_0 = P_1 + P_2.$$

- In the degenerate case, single pump provides both photons for creating a pair of signal and idler photons.
- In this case $P_1 = P_2 = P_0$ and $r = 1$.
- Maximum gain $g_{\max} = \gamma P_0$ occurs when $\kappa = 0$.

Single-Pump Parametric Amplifiers

- A single pump is used to pump a parametric amplifier.
- Assuming $P_4(0) = 0$ (no input at idler frequency), signal and idler powers at $z = L$ are

$$\begin{aligned} P_3(L) &= P_3(0)[1 + (1 + \kappa^2/4g^2)\sinh^2(gL)], \\ P_4(L) &= P_3(0)(1 + \kappa^2/4g^2)\sinh^2(gL), \end{aligned}$$

- Parametric gain $g = \sqrt{(\gamma P_0)^2 - (\kappa/2)^2}$.
- Amplification factor $G_p = \frac{P_3(L)}{P_3(0)} = 1 + (\gamma P_0/g)^2 \sinh^2(\gamma P_0 L)$.
- When phase matching is perfect $(\kappa = 0)$ and $gL \gg 1$

$$G_p = 1 + \sinh^2(\gamma P_0 L) \approx \frac{1}{4}\exp(2\gamma P_0 L).$$

Single-Pump Parametric Amplifiers

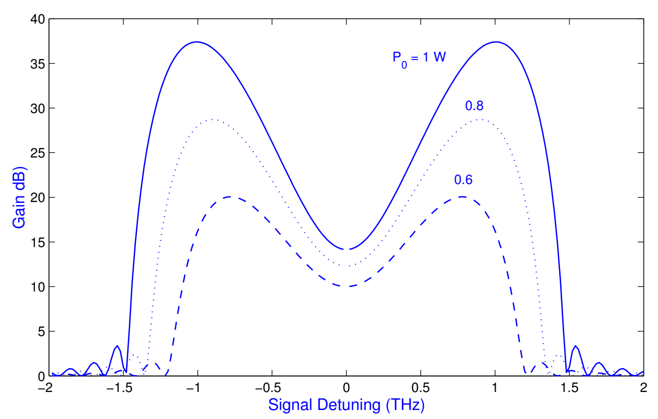

- G_p as a function of pump-signal detuning $\omega_s - \omega_p$.
- Pump wavelength close to the zero-dispersion wavelength.
- 500-m-long fiber with $\gamma = 10$ W^{-1}/km and $\beta_2 = -0.5$ ps^2/km.
- Peak gain is close to 38 dB at a 1-W pump level and occurs when signal is detuned by 1 THz from pump wavelength.

Single-Pump Parametric Amplifiers

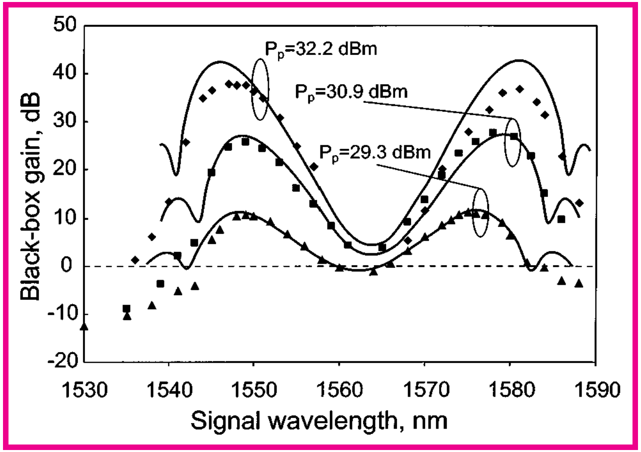

- Experimental results agree with simple FWM theory.
- 500-m-long fiber with $\gamma = 11$ W^{-1}/km.
- Output of a DFB laser was boosted to 2 W using two EDFAs.
- It was necessary to broaden pump spectrum from 10 MHz to $>$1 GHz to suppress SBS.

Dual-Pump Parametric Amplifiers

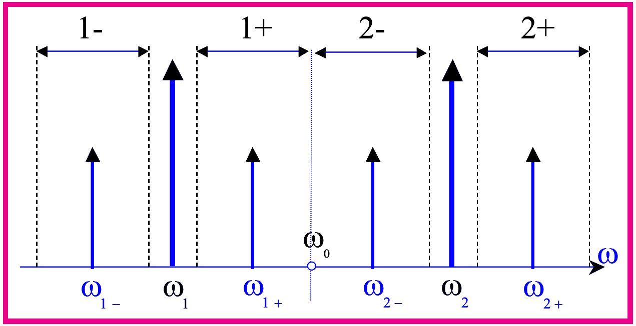

- Pumps positioned on opposite sides of ZDWL.
- Multiple FWM processes general several idler bands.
- Degenerate FWM : $\omega_1 + \omega_1 \longrightarrow \omega_{1+} + \omega_{1-}$.
- Nondegenerate FWM: $\omega_1 + \omega_2 \longrightarrow \omega_{1+} + \omega_{2-}$.
- Additional gain through combinations

$$\omega_1 + \omega_{1+} \longrightarrow \omega_2 + \omega_{2-}, \qquad \omega_2 + \omega_{1+} \longrightarrow \omega_1 + \omega_{2+}.$$

Dual-Pump Parametric Amplifiers

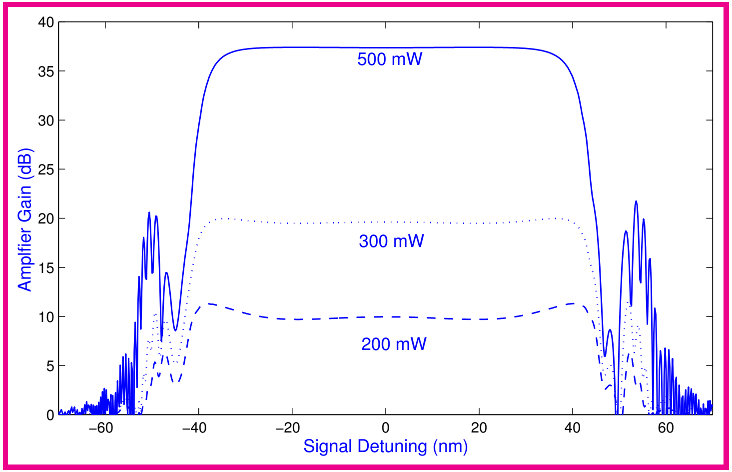

- Examples of gain spectra at three pump-power levels.
- A 500-m-long fiber used with $\gamma = 10\ \mathrm{W}^{-1}$/km, ZDWL = 1570 nm, $\beta_3 = 0.038$ ps^3/km, and $\beta_4 = 1 \times 10^{-4}$ ps^3/km.
- Two pumps at 1525 and 1618 nm (almost symmetric around ZDWL) with 500 mW of power.

Dual-Pump Parametric Amplifiers

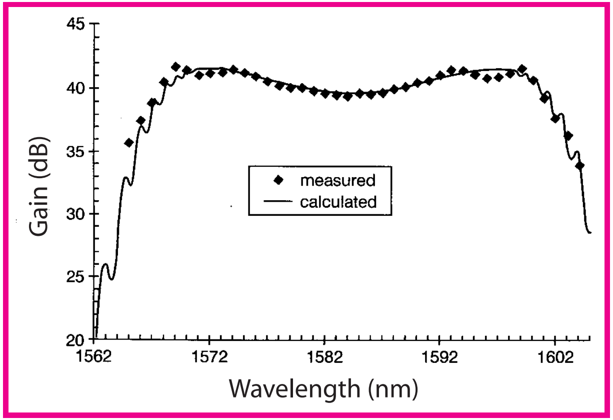

- Measured gain (symbols) for pump powers of 600 and 200 mW at 1,559 and 1,610 nm, respectively.
- Unequal input pump powers were used because of SRS.
- SBS was avoided by modulating pump phases at 10 GHz.
- Theoretical fit required inclusion of Raman-induced transfer of powers between the pumps, signal, and idlers.

Polarization effects

- Parametric gain is negligible when pump and signal are orthogonally polarized (and maximum when they are copolarized).
- Parametric gain can vary widely depending on SOP of input signal.
- This problem can be solved by using two orthogonally polarized pumps with equal powers.
- Linearly polarized pumps in most experiments.
- Amplifier gain is reduced drastically compared with the copolarized case.
- Much higher values of gain are possible if two pumps are chosen to be circularly polarized.

Back
Close

Polarization effects

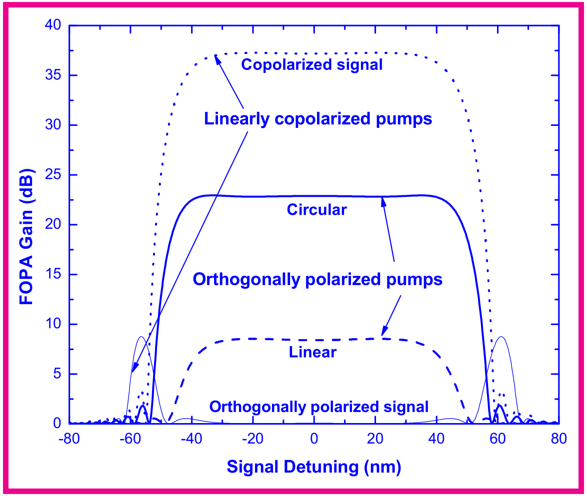

- Two pumps at 1,535 and 1,628 nm launched with 0.5 W powers.
- Gain reduced to 8.5 dB for linearly polarized pumps but increases to 23 dB when pumps are circularly polarized.
- Reason: Angular momentum should be conserved.

Fiber Lasers

- Any amplifier can be converted into a laser by placing it inside a cavity designed to provide optical feedback.
- Fiber lasers can use a Fabry–Perot cavity if mirrors are butt-coupled to its two ends.
- Alignment of such a cavity is not easy.
- Better approach: deposit dielectric mirrors onto the polished ends of a doped fiber.
- Since pump light passes through the same mirrors, dielectric coatings can be easily damaged.
- A WDM fiber coupler can solve this problem.
- Another solution is to use fiber gratings as mirrors.

Ring-Cavity Design

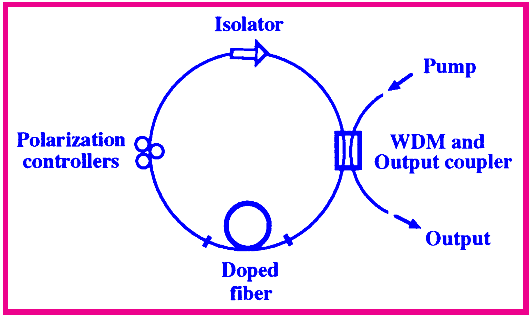

- A ring cavity is often used for fiber lasers.
- It can be made without using any mirrors.
- Two ports of a WDM coupler connected to form a ring cavity.
- An isolator is inserted for unidirectional operation.
- A polarization controller is needed for conventional fibers that do not preserve polarization.

Figure-8 Cavity

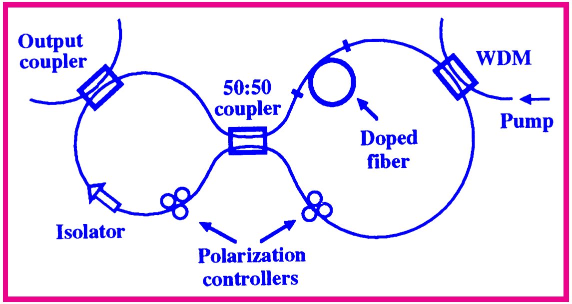

- Ring cavity on right acts as a nonlinear amplifying-loop mirror.
- Nonlinear effects play important role in such lasers.
- At low powers, loop transmissivity is small, resulting in large cavity losses for CW operation.
- Sagnac loop becomes transmissive for pulses whose peak power exceeds a critical value.
- A figure-8 cavity permits passive mode locking without any active elements.

CW Fiber Lasers

- EDFLs exhibit low threshold (<10 mW pump power) and a narrow line width (<10 kHz).
- Tunable over a wide wavelength range (>50 nm).
- A rotating grating can be used (Wyatt, Electon. Lett.,1989).
- Many other tuning techniques have been used.

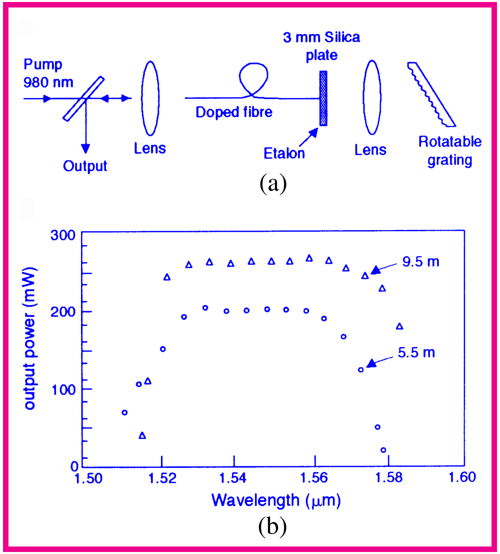

Multiwavelength Fiber Lasers

- EDFLs can be designed to emit light at several wavelengths simultaneously.
- Such lasers are useful for WDM applications.
- A dual-frequency fiber laser was demonstrated in 1993 using a coupled-cavity configuration.
- A comb filter (e.g., a Fabry–Perot filter) is often used for this purpose.
- In a recent experiment, a fiber-ring laser provided output at 52 channels, designed to be 50 GHz apart.

Mode-Locked Fiber Lasers

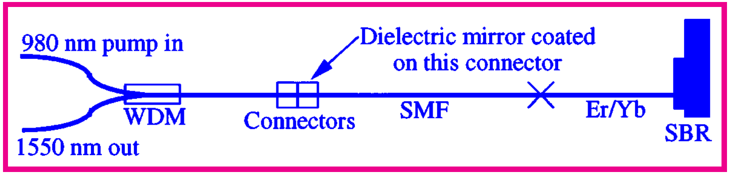

- Saturable absorbers commonly used for passive mode locking.
- A saturable Bragg reflector often used for this purpose.
- Dispersion and SPM inside fibers play an important role and should be included.
- 15 cm of doped fiber is spliced to a 30-cm section of standard fiber for dispersion control.
- Pulse widths below 0.5 ps formed over a wide range of average GVD ($\beta_2 = -2$ to -14 ps^2/km).
- Harmonic mode locking was found to occur for short cavity lengths.

Nonlinear Fiber-Loop Mirrors

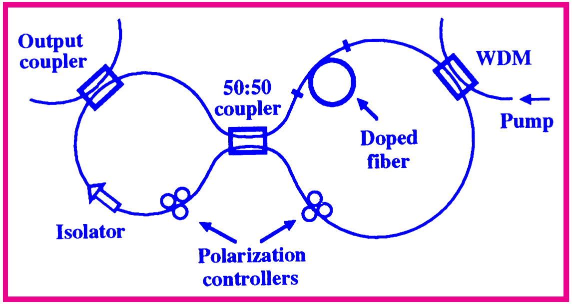

- Nonlinear amplifying-loop mirror (NALM) provides mode locking with an all-fiber ring cavity.
- NALM behaves like a saturable absorber but responds at femtosecond timescales.
- First used in 1991 and produced 290 fs pulses.
- Pulses as short as 30 fs can be obtained by compressing pulses in a dispersion-shifted fiber.

Nonlinear Polarization Rotation

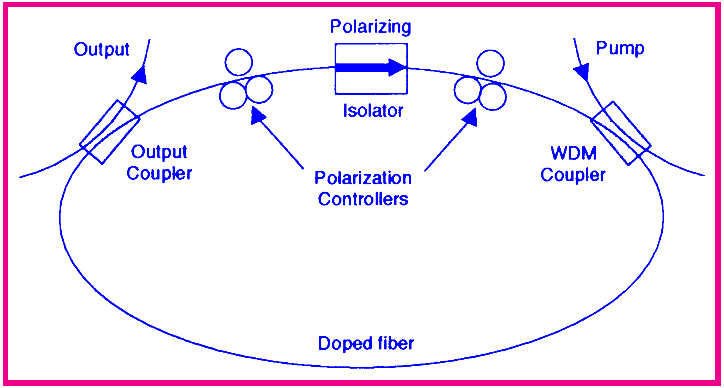

- Mode locking through intensity-dependent changes in the SOP induced by SPM and XPM.
- Mode-locking mechanism similar to that used for figure-8 lasers: orthogonally polarized components of same pulse are used.
- In a 1993 experiment, 76-fs pulses with 90-pJ energy and 1 kW of peak power generated.

Planar Waveguides

- Passive components
  - ⋆ Y and X Junctions
  - ⋆ Grating-assisted Directional Couplers
  - ⋆ Mach–Zehnder Filters
  - ⋆ Multimode Interference Couplers
  - ⋆ Star Couplers
  - ⋆ Arrayed-waveguide Gratings
- Active components
  - ⋆ Semiconductor lasers and amplifiers
  - ⋆ Optical Modulators
  - ⋆ Photodetectors

Y Junctions

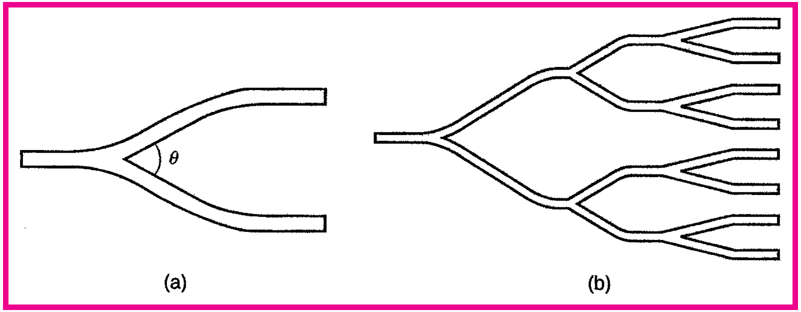

- A three-port device that acts as a power divider.
- Made by splitting a planar waveguide into two branches bifurcating at some angle θ.
- Similar to a fiber coupler except it has only three ports.
- Conceptually, it differs considerably from a fiber coupler.
- No coupling region exists in which modes of different waveguides overlap.

The Institute of OPTICS

UNIVERSITY of ROCHESTER

Y Junctions

- Functioning of Y junction can be understood as follows.
- In the junction region, waveguide is thicker and supports higher-order modes.
- Geometrical symmetry forbids excitation of asymmetric modes.
- If thickness is changed gradually in an adiabatic manner, even higher-order symmetric modes are not excited.
- As a result, power is divided into two branches.
- Sudden opening of the gap violates adiabatic condition, resulting in some insertion losses for any Y junction.
- Losses depend on branching angle θ and increase with it.
- θ should be below 1° to keep insertion losses below 1 dB.

Four-Port Couplers

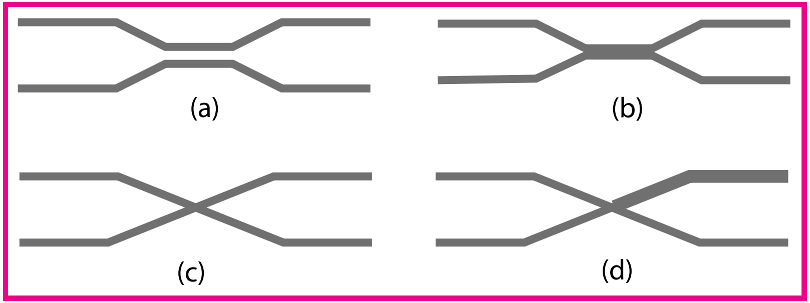

- Spacing between waveguides reduced to zero in coupled Y junctions.
- Waveguides cross in the central region in a X coupler.
- In asymmetric X couplers, two input waveguides are identical but output waveguides have different sizes.
- Power splitting depends on relative phase between two inputs.
- If inputs are equal and in phase, power is transferred to wider core; when inputs are out of phase, power is transferred to narrow core.

Grating-Assisted Directional Couplers

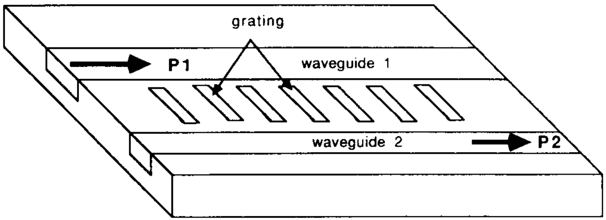

- An asymmetric directional coupler with a built-in grating.
- Little power will be transferred in the absence of grating.
- Grating helps to match propagation constants and induces power transfer for specific input wavelengths.
- Grating period $\Lambda = 2\pi/|\beta_1 - \beta_2|$.
- Typically, $\Lambda \sim 10\ \mu$m (a long-period grating).
- A short-period grating used if light is launched in opposite directions.

Mach–Zehnder Switches

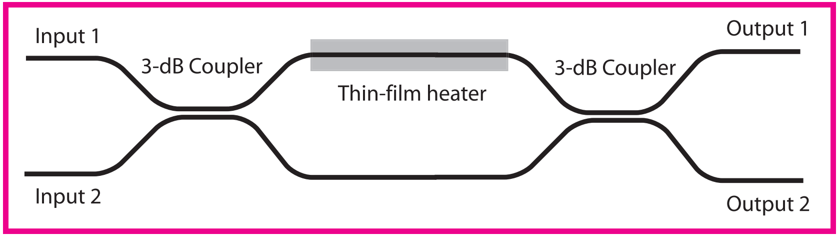

- Two arm lengths equal in a symmetric MZ interferometer.
- Such a device transfers its input power to the cross port.
- Output can be switched to bar port by inducing a π phase shift in one arm.
- Phase shift can be induced electrically using a thin-film heater (a thin layer of chromium).
- Thermo-optic effect is relatively slow.
- Much faster switching using electro-optic effect in $LiNbO_3$.

Mach–Zehnder Filters

- An asymmetric MZI acts as an optical filter.
- Its output depends on the frequency ω of incident light.
- Transfer function $H(\omega) = \sin(\omega\tau)$.
- τ is the additional delay in one arm of MZI.
- Such a filter is not sharp enough for applications.
- A cascaded chain of MZI provides narrowband optical filters.
- In a chain of N cascaded MZIs, one has the freedom of adjusting N delays and $N+1$ splitting ratios.
- This freedom can be used to synthesize optical filters with arbitrary amplitude and phase responses.

Cascaded Mach–Zehnder Filters

- Transmission through a chain of N MZIs can be calculated with the transfer-matrix approach. In matrix form

$$F_{\text{out}}(\omega) = T_{N+1} D_N T_N \cdots D_2 T_2 D_1 T_1 F_{\text{in}},$$

- T_m is the transfer matrix and D_m is a diagonal matrix

$$T_m = \begin{pmatrix} c_m & is_m \\ is_m & c_m \end{pmatrix} \qquad D_m = \begin{pmatrix} e^{i\phi_m} & 0 \\ 0 & e^{-i\phi_m} \end{pmatrix}.$$

- $c_m = \cos(\kappa_m l_m)$ and $s_m = \sin(\kappa_m l_m)$ and $2\phi_m = \omega\tau_m$.

- Simple rule: sum over all possible optical paths. A chain of two cascaded MZI has four possible paths:

$$t_b(\omega) = ic_1c_2s_3e^{i(\phi_1+\phi_2)} + ic_1s_2s_3e^{i(\phi_1-\phi_2)} + \\ i^3s_1c_2s_3e^{i(-\phi_1+\phi_2)} + is_1s_2s_3e^{-i(\phi_1+\phi_2)}$$

Back
Close

Multimode Interference Couplers

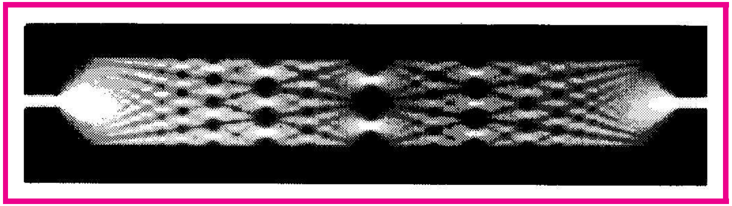

- MMI couplers are based on the Talbot effect: Self-imaging of objects in a medium exhibiting periodicity.
- Same phenomenon occurs when an input waveguides is connected to a thick central region supporting multiple modes.
- Length of central coupling region is chosen such that optical field is self-imaged and forms an array of identical images at the location of output waveguides.
- Such a device functions as an $1 \times N$ power splitter.

Multimode Interference Couplers

- Expand input field into mode $\phi_m(x)$ as $A(x,z) = \sum C_m \phi_m(x)$.
- Field at a distance z: $A(x,z) = \sum C_m \phi_m(x) \exp(i\beta_m z)$.
- Propagation constant β_m for a slab of width W_e:
  $\beta_m^2 = n_s^2 k_0^2 - p_m^2$, where $p_m = (m+1)\pi/W_e$.
- Since $p_m \ll k_0$, we can approximate β_m as

$$\beta_m \approx n_s k_0 - \frac{(m+1)^2\pi^2}{2n_s k_0 W_e^2} = \beta_0 - \frac{m(m+2)\pi}{3L_b},$$

- Beat length $L_b = \frac{\pi}{\beta_0 - \beta_1} \approx \frac{4n_s W_e^2}{3\lambda}$.
- Input field is reproduced at $z = 3L_b$.
- Multiple images of input can form for $L < 3L_b$.

Star Couplers

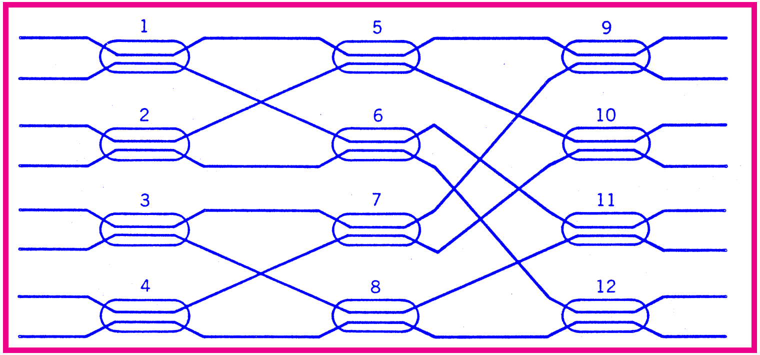

- Some applications make use of $N \times N$ couplers designed with N input and N output ports.
- Such couplers are known as star couplers.
- They can be made by combining multiple 3-dB couplers.
- A 8×8 star coupler requires twelve 3-dB couplers.
- Device design becomes too cumbersome for larger ports.

Star Couplers

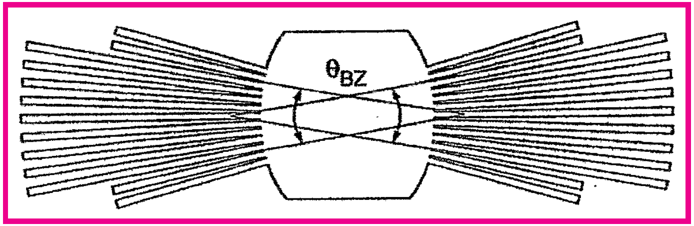

- Compact star couplers can be been made using planar waveguides.
- Input and output waveguides connected to a central region.
- Optical field diffracts freely inside central region.
- Waveguides are arranged to have a constant angular separation.
- Input and output boundaries of central slab form arcs that are centered at two focal points with a radius equal to focal distance.
- Dummy waveguides added near edges to ensure a large periodic array.

Back
Close

Theory Behind Star Couplers

- An infinite array of coupled waveguides supports supermodes in the form of Bloch functions.
- Optical field associated with a supermode:

$$\psi(x, k_x) = \sum_m F(x - ma) e^{imk_x a}.$$

- $F(x)$ is the mode profile and a is the period of array.
- k_x is restricted to the first Brillouin zone: $-\pi/a < k_x < \pi/a$.
- Light launched into one waveguide excites all supermodes within the first Brillouin zone.

Theory Behind Star Couplers

- As waveguides approach central slab, $\psi(x, k_x)$ evolves into a freely propagating wave with a curved wavefront.
- $\theta \approx k_x/\beta_s$, where β_s is the propagation constant in the slab.
- Maximum value of this angle:

$$\theta_{\mathrm{BZ}} \approx k_x^{\max}/\beta_s = \pi/(\beta_s a).$$

- Star coupler is designed such that all N waveguides are within illuminated region: $Na/R = 2\theta_{\mathrm{BZ}}$, where R is focal distance.
- With this arrangement, optical power entering from any input waveguide is divided equally among N output waveguides.
- Silica-on-silicon technology is often used for star couplers.

Arrayed-Waveguide Gratings

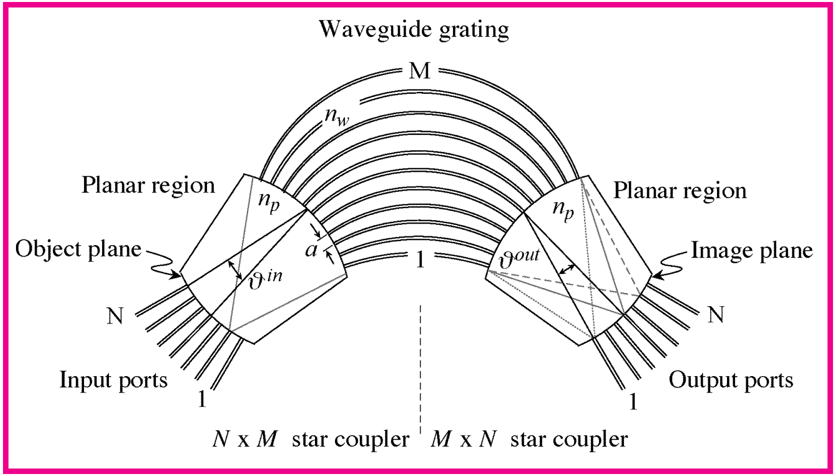

- AWG combines two $N \times M$ star couplers through an array of M curved waveguides.
- Length difference between neighboring waveguides is constant.
- Constant phase difference between neighboring waveguides produces grating-like behavior.

Theory Behind AWGs

- Consider a WDM signal launched into an input waveguides.
- First star coupler splits power into many parts and directs them into the waveguides forming the grating.
- At the output end, wavefront is tilted because of linearly varying phase shifts.
- Tilt is wavelength-dependent and it forces each channel to focus onto a different output waveguide.
- Bragg condition for an AWG:

$$k_0 n_w(\delta l) + k_0 n_p a_g(\theta_{\rm in} + \theta_{\rm out}) = 2\pi m,$$

- a_g = garting pitch, $\theta_{\rm in} = pa_i/R$, and $\theta_{\rm out} = qa_o/R$.

Back
Close

Fabrication of AWGs

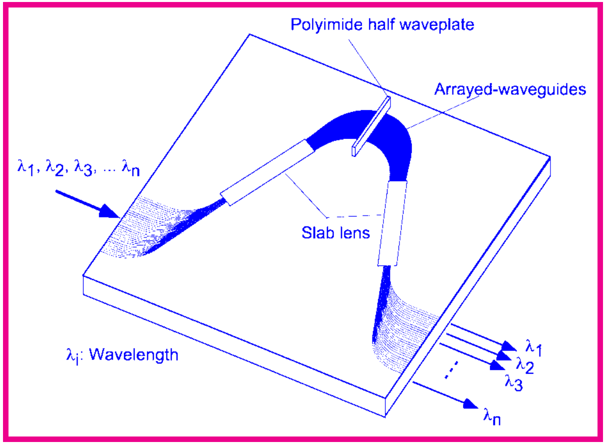

- AWGs are fabricated with silica-on-silicon technology.
- Half-wave plate helps to correct for birefringence effects.
- By 2001, 400-channel AWGs were fabricated .
- Such a device requiring fabrication of hundreds of waveguides on the same substrate.

Semiconductor Lasers and Amplifiers

- Semiconductor waveguides useful for making lasers operating in the wavelength range 400–1600 nm.
- Semiconductor lasers offer many advantages.
  - ⋆ Compact size, high efficiency, good reliability.
  - ⋆ Emissive area compatible with fibers.
  - ⋆ Electrical pumping at modest current levels.
  - ⋆ Output can be modulated at high frequencies.
- First demonstration of semiconductor lasers in 1962.
- Room-temperature operation first realized in 1970.
- Used in laser printers, CD and DVD players, and telecommunication systems.

Operating Principle

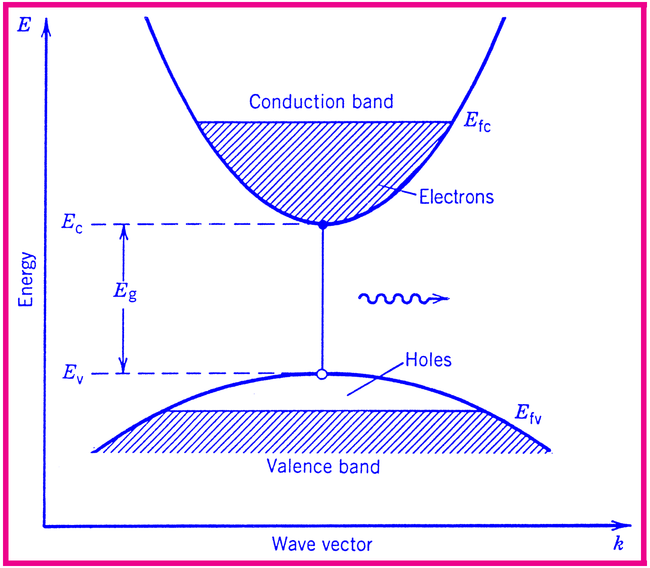

- Forward biasing of a p–n junction produces free electrons and holes.
- Electron-hole recombination in a direct-bandgap semiconductor produces light through spontaneous or stimulated emission.

Basic Structure

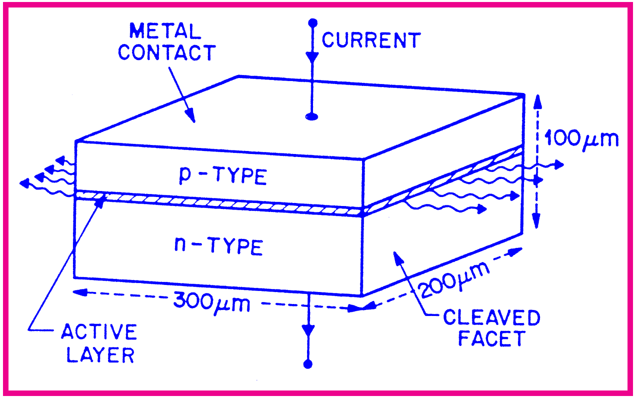

- Active layer sandwiched between p-type and n-type cladding layers.
- Their bandgap difference confines carriers to active layer.
- Active layer's larger refractive index creates a planar waveguide.
- Single-mode operation require layer thickness below 0.2 μm.
- Cladding layers are transparent to emitted light.
- Whole laser chip is typically under 1 mm in each dimension.

Advanced Laser Structures

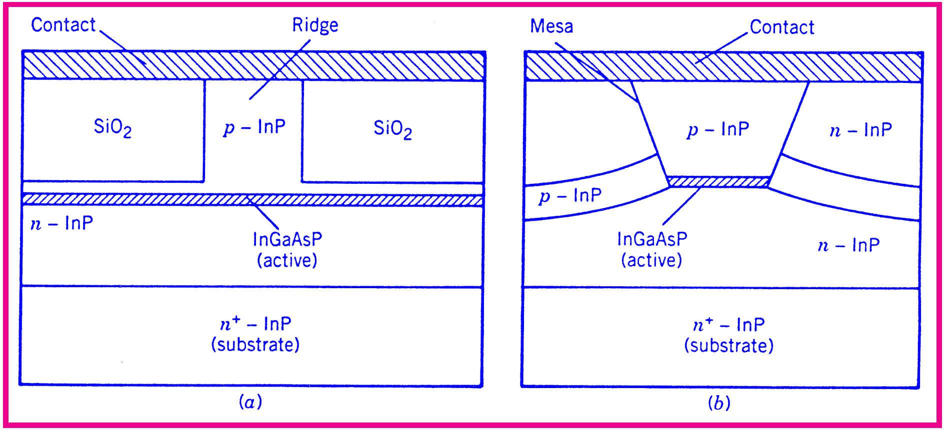

- A waveguide is also formed in the lateral direction.
- In a ridge-waveguide laser, ridge is formed by etching top cladding layer close to the active layer.
- SiO_2 ensures that current enters through the ridge.
- Effective mode index is higher under the ridge because of low refractive index of silica.

Buried Heterotructure Laser

- Active region buried on all sides by cladding layers of lower index.
- Several different structures have beeb developed.
- Known under names such as etched-mesa BH, planar BH, double-channel planar BH, and channelled substrate BH lasers.
- All of them allow a relatively large index step ($\Delta n > 0.1$) in lateral direction.
- Single-mode condition requires width to be below 2 μm.
- Laser spot size elliptical (2×1 μm^2).
- Output beam diffracts considerably as it leaves the laser.
- A spot-size converter is sometimes used to improve coupling efficiency into a fiber.

Control of Longitudinal Modes

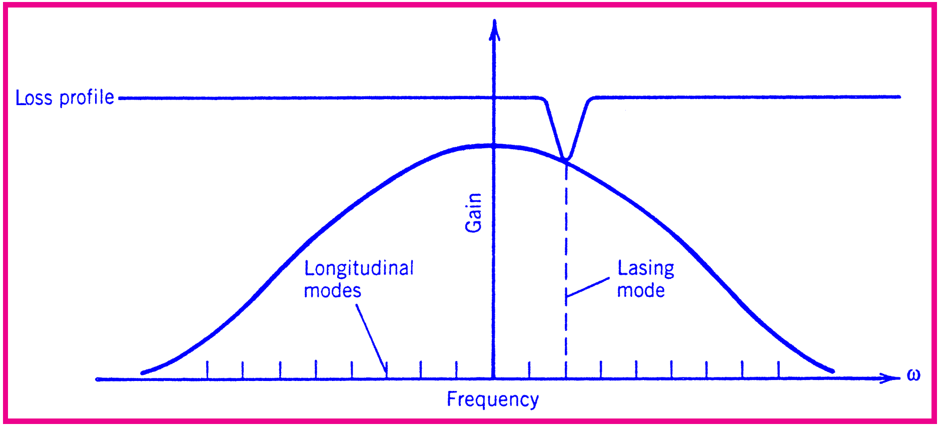

- Single-mode operation requires lowering of cavity loss for a specific longitudinal mode.
- Longitudinal mode with the smallest cavity loss reaches threshold first and becomes the dominant mode.
- Power carried by side modes is a small fraction of total power.

Distributed Feedback Lasers

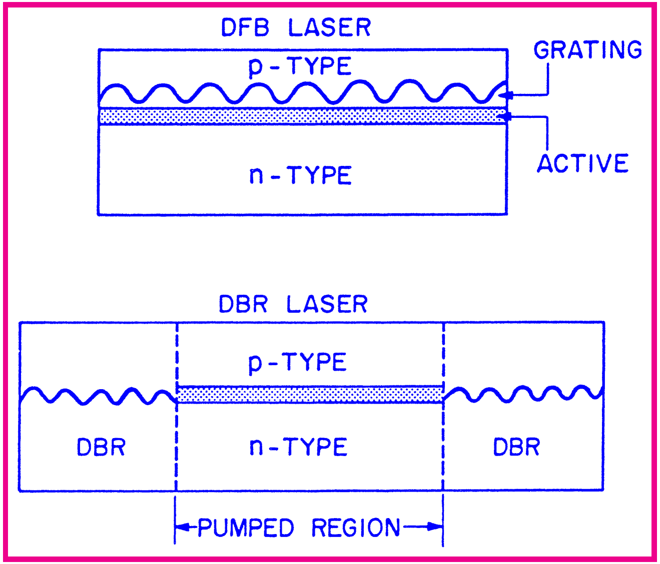

- Feedback is distributed throughout cavity length in DFB lasers.
- This is achieved through an internal built-in grating
- Bragg condition satisfied for $\lambda = 2\bar{n}\Lambda$.

Distributed Bragg reflector Lasers

- End regions of a DBR laser act as mirrors whose reflectivity is maximum for a wavelength $\lambda = 2\bar{n}\Lambda$.
- Cavity losses are reduced for this longitudinal mode compared with other longitudinal modes.
- Mode-suppression ratio is determined by gain margin.
- Gain Margin: excess gain required by dominant side mode to reach threshold.
- Gain margin of 3–5 cm^{-1} is enough for CW DFB lasers.
- Larger gain margin ($>$10 cm^{-1}) needed for pulsed DFB lasers.
- Coupling between DBR and active sections introduces losses in practice.

Back

Close

Fabrication of DFB Lasers

- Requires advanced technology with multiple epitaxial growths.
- Grating is often etched onto bottom cladding layer.
- A fringe pattern is formed first holographically on a photoresist deposited on the wafer surface.
- Chemical etching used to change cladding thickness in a periodic fashion.
- A thin layer with refractive index $n_s < n < n_a$ is deposited on the etched cladding layer, followed with active layer.
- Thickness variations translate into periodic variations of mode index $\bar{n}$ along the cavity length.
- A second epitaxial regrowth is needed to make a BH device.

Coupled-Cavity Structures

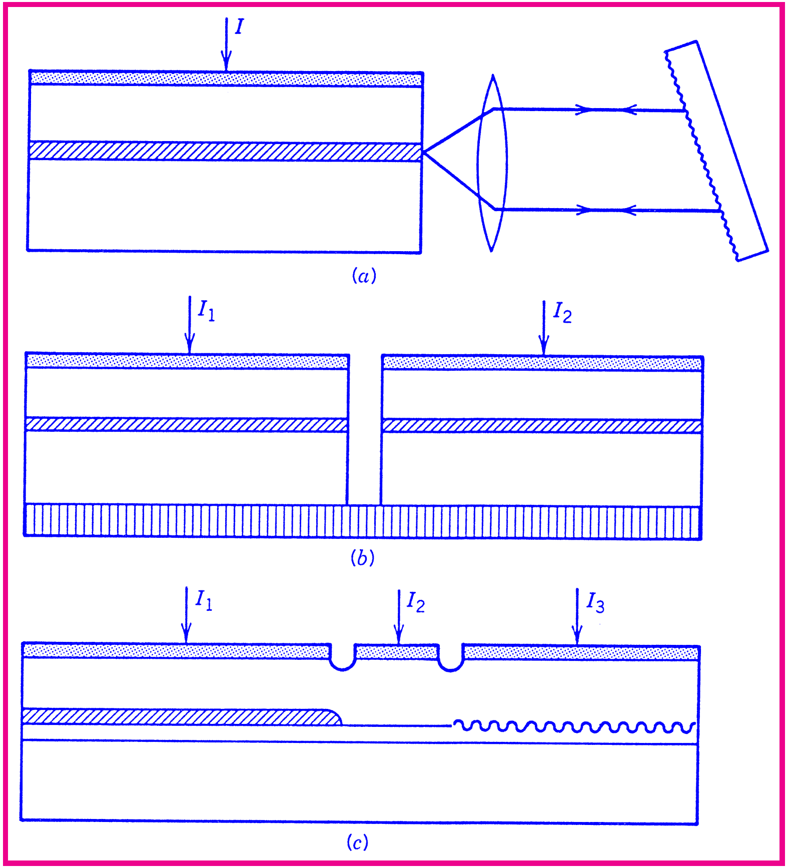

Tunable Semiconductor Lasers

- Multisection DFB and DBR lasers developed during the 1990s to meet conflicting requirements of stability and tunability.
- In a 3-section device, a phase-control section is inserted between the active and DBR sections.
- Each section can be biased independently.
- Current in the Bragg section changes Bragg wavelength through carrier-induced changes in mode index.
- Current injected into phase-control section affects phase of feedback from the DBR.
- Laser wavelength can be tuned over 10–15 nm by controlling these two currents.

Tuning with a Chirped Grating

- Several other designs of tunable DFB lasers have been developed.
- In one scheme, grating is chirped along cavity length.
- Bragg wavelength itself then changes along cavity length.
- Laser wavelength is determined by Bragg condition.
- Such a laser can be tuned over a wavelength range set by the grating chirp.
- In a simple implementation, grating period remains uniform but waveguide is bent to change $\bar{n}$.
- Such lasers can be tuned over 5–6 nm.

Tuning with a superstructure Grating

- Much wider tuning range possible using a superstructure grating.
- Reflectivity of such gratings peaks at several wavelengths.
- Laser can be tuned near each peak by controlling current in phase-control section.
- A quasi-continuous tuning range of 40 nm realized in 1995.
- Tuning range can be extended further using a 4-section device in which two DBR sections are used.
- Each DBR section supports its own comb of wavelengths but spacing in each comb is not the same.
- Coinciding wavelength in the two combs becomes the output wavelength that can be tuned widely (Vernier effect).

Tuning with a Directional Coupler

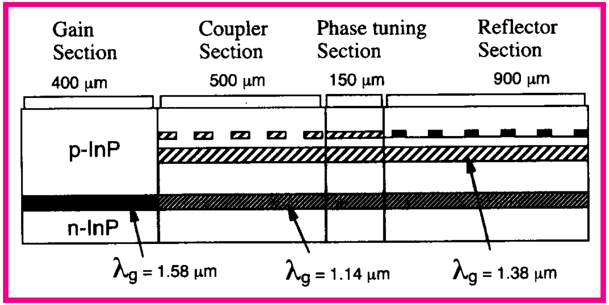

- A fourth section is added between the gain and phase sections.
- It consist of a directional coupler with a superstructure grating.
- Coupler section has two vertically separated waveguides of different thickness (asymmetric directional coupler).
- Grating selectively transfers a single wavelength to passive waveguide in the coupler section.
- A tuning range of 114 nm was produced in 1995.

Vertical-Cavity Surface-Emitting Lasers

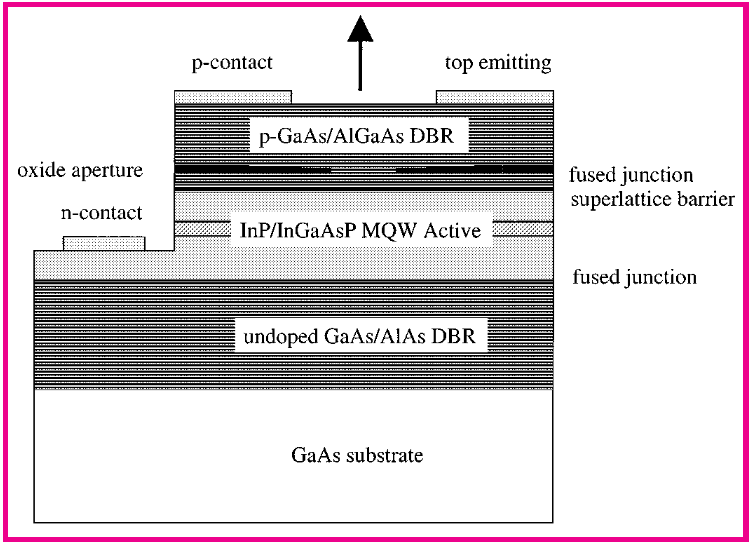

- VCSELs operate in a single longitudinal mode simply because mode spacing exceeds the gain bandwidth.
- VCSELs emit light normal to active-layer plane.
- Emitted light is in the form of a circular beam.

VCSEL Fabrication

- Fabrication of VCSELs requires growth of hundreds of layers.
- Active region in the form of one or more quantum wells.
- It is surrounded by two high-reflectivity (>99.5%) mirrors.
- Each DBR mirror is made by growing many pairs of alternating GaAs and AlAs layers, each $\lambda/4$ thick.
- A wafer-bonding technique is sometimes used for VCSELs operating in the 1.55-μm wavelength.
- Chemical etching used to form individual circular disks.
- Entire two-dimensional array of VCSELs can be tested without separating individual lasers (low cost).
- Only disadvantage is that VCSELs emit relatively low powers.

Back
Close

Semiconductor Optical Amplifiers

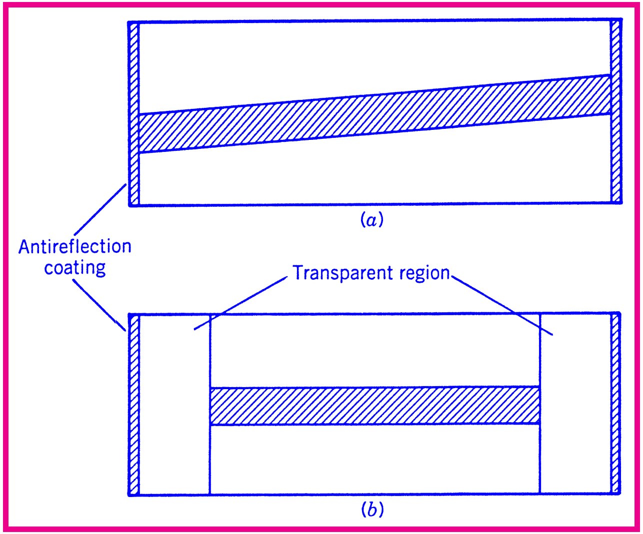

- Reflection feedback from end facets must be suppressed.
- Residual reflectivity must be $<0.1\%$ for SOAs.
- Active-region stripe tilted to realize such low feedback.
- A transparent region between active layer and facet also helps.

Gain Spectrum of SOAs

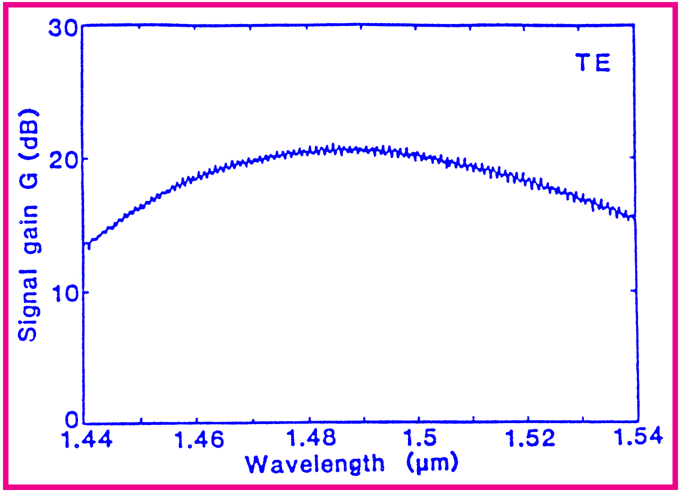

- Measured gain spectrum exhibits ripples.
- Ripples have origin in residual facet reflectivity.
- Ripples become negligible when $G\sqrt{R_1R_2} \approx 0.04$.
- Amplifier bandwidth can then exceed 50 nm.

Polarization Sensitivity of SOAs

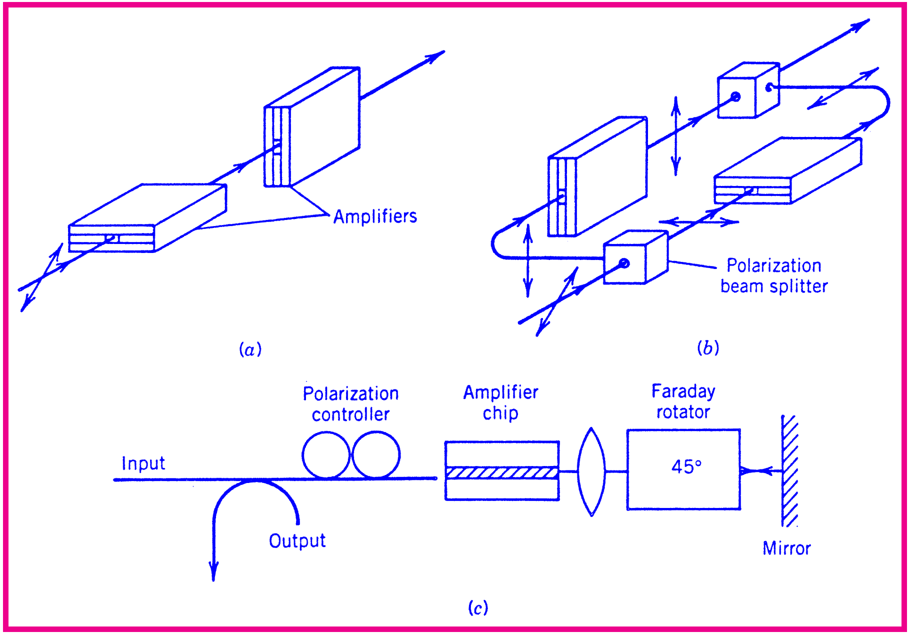

- Amplifier gain different for TE and TM modes.
- Several schemes have been devised to reduce polarization sensitivity.

SOA as a Nonlinear Device

- Nonlinear effects in SOAs can be used for switching, wavelength conversion, logic operations, and four-wave mixing.
- SOAs allow monolithic integration, fan-out and cascadability, requirements for large-scale photonic circuits.
- SOAs exhibit carrier-induced nonlinearity with $n_2 \sim 10^{-9}$ cm^2/W. Seven orders of magnitude larger than that of silica fibers.
- Nonlinearity slower than that of silica but fast enough to make devices operating at 40 Gb/s.
- Origin of nonlinearity: Gain saturation.
- Changes in carrier density modify refractive index.

Back
Close

Gain Saturation in SOAs

- Propagation of an optical pulse inside SOA is governed by

$$\frac{\partial A}{\partial z} + \frac{1}{v_g}\frac{\partial A}{\partial t} = \frac{1}{2}(1 - i\beta_c)g(t)A,$$

- Carrier-induced index changes included through β_c.
- Time dependence of $g(t)$ is governed by

$$\frac{\partial g}{\partial t} = \frac{g_0 - g}{\tau_c} - \frac{g|A|^2}{E_{\text{sat}}},$$

- For pulses shorter than τ_c, first term can be neglected.
- Saturation energy $E_{\text{sat}} = h\nu(\sigma_m/\sigma_g) \sim 1$ pJ.

Theory of Gain Saturation

- In terms of $\tau = t - z/v_g$, $A = \sqrt{P}\exp(i\phi)$, we obtain

$$\frac{\partial P}{\partial z} = g(z,\tau)P(z,\tau), \qquad \frac{\partial \phi}{\partial z} = -\tfrac{1}{2}\beta_c g(z,\tau),$$

$$\frac{\partial g}{\partial \tau} = -g(z,\tau)P(z,\tau)/E_{\text{sat}}.$$

- Solution: $P_{\text{out}}(\tau) = P_{\text{in}}(\tau)\exp[h(\tau)]$ with $h(\tau) = \int_0^L g(z,\tau)\,dz$.

$$\frac{dh}{d\tau} = -\frac{1}{E_{\text{sat}}}[P_{\text{out}}(\tau) - P_{\text{in}}(\tau)] = -\frac{P_{\text{in}}(\tau)}{E_{\text{sat}}}(e^h - 1).$$

- Amplification factor $G = \exp(h)$ is given by

$$G(\tau) = \frac{G_0}{G_0 - (G_0 - 1)\exp[-E_0(\tau)/E_{\text{sat}}]},$$

- G_0 = unsaturated amplifier gain and $E_0(\tau) = \int_{-\infty}^{\tau} P_{\text{in}}(\tau)\,d\tau$.

The Institute of OPTICS

UNIVERSITY of ROCHESTER

Chirping Induced by SOAs

- Amplifier gain is different for different parts of the pulse.
- Leading edge experiences full gain G_0 because amplifier is not yet saturated.
- Trailing edge experiences less gain because of saturation.
- Gain saturation leads to a time-dependent phase shift

$$\phi(\tau) = -\frac{1}{2}\beta_c \int_0^L g(z,\tau)\,dz = -\frac{1}{2}\beta_c h(\tau) = -\frac{1}{2}\beta_c \ln[G(\tau)].$$

- Saturation-induced frequency chirp

$$\Delta\nu_c = -\frac{1}{2\pi}\frac{d\phi}{d\tau} = \frac{\beta_c}{4\pi}\frac{dh}{d\tau} = -\frac{\beta_c P_{\rm in}(\tau)}{4\pi E_{\rm sat}}[G(\tau)-1],$$

- Spectrum of amplified pulse broadens and develops multiple peaks.

Pulse Shape and Spectrum

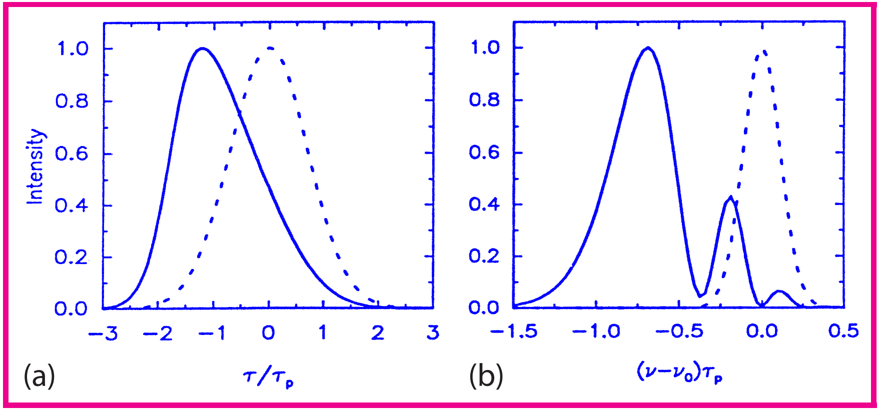

- A Gaussian pulse amplified by 30 dB. Initially $E_{\mathrm{in}}/E_{\mathrm{sat}} = 0.1$.
- Dominant spectral peak is shifted toward red side.
- It is accompanied by several satellite peaks.
- Temporal and spectral changes depend on amplifier gain.
- Amplified pulse can be compressed in a fiber with anomalous dispersion.